

Robust Post-donation Blood Screening under Limited Information

Hadi El-Amine

Dissertation submitted to the Faculty of the Virginia Polytechnic Institute and
State University in partial fulfillment of the requirements for the degree of

Doctor of Philosophy
in
Industrial and Systems Engineering

Ebru K. Bish, Chair
Douglas R. Bish
Ran Jin
Susan L. Stramer

May 3, 2016
Blacksburg, Virginia

Keywords: Blood screening, Blood safety, Pooled testing, Risk minimization, Robust solution
under uncertainty, Minmax Regret, Resource allocation, Cost-effectiveness

Copyright 2016, Hadi El-Amine

Robust Post-donation Blood Screening under Limited Information

Hadi El-Amine

(ABSTRACT)

Blood products are essential components of any healthcare system, and their safety, in terms of being free of transfusion-transmittable infections, is crucial. While the Food and Drug Administration (FDA) in the United States requires all blood donations to be tested for a set of infections, it does not dictate which particular tests should be used by blood collection centers. Multiple FDA-licensed blood screening tests are available for each infection, but all screening tests are imperfectly reliable and have different costs. In addition, infection prevalence rates and several donor characteristics are uncertain, while surveillance methods are highly resource- and time-intensive. Therefore, only limited information is available to budget-constrained blood collection centers that need to devise a post-donation blood screening scheme so as to minimize the risk of an infectious donation being released into the blood supply. Our focus is on “robust” screening schemes under limited information. Toward this goal, we consider various objectives, and characterize structural properties of the optimal solutions under each objective. This allows us to gain insight and to develop efficient algorithms. Our research shows that using the proposed optimization-based approaches provides robust solutions with significantly lower expected infection risk compared to other testing schemes that satisfy the FDA requirements. Our findings have important public policy implications.

إلى أهلي الأعزاء

To my dear family

Acknowledgments

First, I am greatly indebted to my advisors, Dr. Ebru Bish and Dr. Douglas Bish, for their support and guidance throughout my stay at Virginia Tech. I thank Ebru, my mentor, for her patience, kindness, and encouragement on both professional and personal levels. Her boundless enthusiasm, wealth of ideas, work ethics, and professionalism have made working with her an invaluable experience for me, and I am deeply grateful for that. I also thank Doug for his insightful ideas and for his clarity of thought that always steered me in the right direction.

I would also like to thank my committee members, Dr. Ran Jin and Dr. Susan Stramer, for their support and for their constructive suggestions that have improved the quality of this work.

Special thanks go to my former advisor, Dr. Bacel Maddah, for introducing me to Operations Research, providing me with the opportunity to come to the United States, and for his continued support and advice throughout the years.

I am thankful for all the friends I have had at Virginia Tech and for those living abroad for their encouragements and for making this experience enjoyable.

Finally, I am deeply thankful to my family in Lebanon for their everlasting support and unconditional love: To my parents Mohamed-Hassan and Iman, and to my siblings Nour and Hani, I dedicate this work.

Contents

1	Introduction	1
1.1	Motivation	1
1.2	Research Overview	2
2	Cost-effectiveness of Babesiosis Screening in the United States	5
2.1	Introduction	5
2.2	Materials and Methods	7
2.2.1	Screening Strategies	7
2.2.2	Model Overview	7
2.2.3	Data	8
2.2.4	Base Case	12
2.2.5	Deterministic Sensitivity Analyses	13
2.2.6	Probabilistic Sensitivity Analysis on Key Model Inputs	14
2.3	Results	14
2.3.1	Base Case	14
2.3.2	Deterministic Sensitivity Analysis on Transmission Probability Values	16
2.3.3	Deterministic Sensitivity Analysis on Prevalence Rates	17
2.3.4	Probabilistic Sensitivity Analysis on Key Model Inputs	17
2.4	Discussion	22
3	Robust Post-donation Blood Screening under Prevalence Rate Uncertainty	26
3.1	Introduction	26
3.2	The Model	29
3.2.1	Notation and Assumptions	29
3.2.2	Objective Functions	32
3.2.2.1	The Robust Problem: Maximum Regret Minimization	33
3.2.2.2	The Expected Risk Minimization Problem	34
3.3	Properties of Optimal Solutions	35
3.3.1	Structural Properties of the Optimal ERM Solution	35
3.3.2	Structural Properties of the Optimal RMM Solution	36
3.3.2.1	The Optimality Conditions for RMM	36
3.3.2.2	Further Properties of the Optimal RMM Solution	39
3.4	The Price of Robustness and the Price of Expectation-based Optimization	41
3.5	A Case Study of the United States	44
3.5.1	Case Study Data	44
3.5.2	Case Study Results	45
3.5.3	Price of Robustness Results	49

3.6	Conclusions and Future Research Directions	51
4	Optimal Pooling Strategies for Nucleic Acid Testing of Donated Blood Considering Viral Load Growth Curves and Donor Characteristics	52
4.1	Introduction	52
4.2	Notation, Assumptions, and Preliminaries	55
4.2.1	Viral Load Progression, Dilution Effect, and Testing Stochasticity	57
4.2.2	The Blood Center’s Objective	59
4.2.3	Pool Strategy Optimization	61
4.2.3.1	The Universal Testing Problem	61
4.2.3.2	The Non-universal Testing Problems	62
4.3	Structural Properties and Algorithmic Developments	63
4.3.1	Structural Properties	64
4.3.2	Algorithmic Development	66
4.4	Numerical Results	69
4.4.1	Model Calibration and Data Sources	70
4.4.2	Case Study	72
4.5	Conclusions and Suggestions for Future Research	76
5	Conclusions and Future Research Directions	78
	Bibliography	81
A	Appendix for Chapter 2	89
B	Appendix for Chapter 3	94
B.1	Summary of Notation	94
B.2	Comparative Statics Analysis	95
B.3	Discussion on Condition (C1)	96
B.4	Proofs	97
B.5	Prevalence Data and Fitting of Test Effectiveness Functions	107
B.5.1	Prevalence Data	107
B.5.2	Fitting Test Effectiveness Functions	107
C	Appendix for Chapter 4	110

List of Figures

2.1	Decision tree model used in cost-effectiveness analysis.	9
2.2	(a) $ICER_{Q_j}$ as a function of transmission probability from actively infected donors for Scenario 1-Low (donor-only scenario in which blood units from donors with resolved infection present a transmission probability of 0.3%). (b) $ICER_{Q_j}$ as a function of transmission probability from actively infected donors for Scenario 1-High (donor-only scenario in which blood units from donors with resolved infection present a transmission probability of 2.9%). (c) $ICER_{Q_j}$ as a function of the prevalence of window-period donors (donors who are Ab-negative/PCR-positive) for Scenario 1 (donor-only scenario in which blood units from donors with resolved infection present a transmission probability of 2.9% and blood units from actively infected donors present a transmission probability of 33.3%)	19
2.3	Tornado diagram showing the sensitivity of the model to prevalence values and their effect on ICER for (a) universal PCR strategy, (b) universal Ab/PCR strategy, (c) universal Ab strategy.	20
2.4	Cost-effectiveness acceptability curve showing the probability that each screening strategy is the most cost-effective at each willingness-to-pay value for (a) Scenario 1 (donor-only scenario), (b) Scenario 2 (donor-recipient scenario).	21
3.1	Total budget, B^T , vs. expected <i>Risk</i> (per 100,000 donations) for the RMM solutions and for the strategies shown in Table 3.5.	47
3.2	Joint distribution of <i>Risk</i> and <i>Regret</i> per 100,000 donations for ERM and RMM at $B^T = \$45$ and $B^T = \$60$, with FDA-compliant strategies ((a)-(b)), and without FDA-compliant strategies ((c)-(d)).	49
3.3	Π^R and its upper bound vs. B^T for the numerical study in Section 3.5.2 (a) with all five infections considered, and (b) when WNV is omitted and Condition (C1) is satisfied. (c) \mathcal{R}^L vs. B^T for the numerical study in Section 3.5.2.	50
4.1	Viral load vs. post-infection time for a typical HBV-infected individual with $\lambda = 2.6$ (value taken from [12]) and $c^0 = 6.5$ (value obtained from model calibration, see Section 4.4.1).	58
4.2	Histogram of the difference in expected number of TTI cases per 1,000,000 transfusions between the chance-constrained <i>non-universal</i> strategy (NC^{UB}) and (a) <i>current practice</i> (UT^{UB}), (b) <i>universal</i> strategy.	74
4.3	Histogram of the difference in expected TTI cost per 1,000,000 transfusions between the chance-constrained <i>non-universal</i> strategy (NC^{UB}) and (a) <i>current practice</i> (UT^{UB}), (b) <i>universal</i> strategy.	76

A.1	Deterministic sensitivity analysis on the transmission probability for actively infected donors for Scenario 2-Low.	92
A.2	Deterministic sensitivity analysis on the transmission probability for actively infected donors for Scenario 2-High.	92
B.1	The optimal budget allocation for (a) ERM and (b) RMM vs. B^T	96
B.2	Regions that satisfy Condition (C1) (shaded) for $n = 2$, $\mathbf{k} = (0.2, 0.2)$, and $B^T = 15, 25, 35$	96
B.3	Fitted exponential test effectiveness function ($k_i = 0.16$) vs. the actual test data for HBV.	109

List of Tables

2.1	Base case data and the ranges used in sensitivity analysis.	10
2.2	Comparison of assumptions and data between this study and prior studies.	12
2.3	Transmission probability sensitivity analysis data for Scenarios 1 (donor-only scenario) and 2 (donor-recipient scenario).	13
2.4	Base case results for Scenarios 1 (donor-only scenario) and 2 (donor-recipient scenario).	14
2.5	Base case detailed TTB, waste, and cost values for Scenarios 1 (donor-only scenario) and 2 (donor-recipient scenario).	15
2.6	Projected annual TTB cases averted, TTB deaths averted, total cost, testing cost, cost of positive test results, and treatment cost of TTB for implementation of the testing policies in seven endemic states for Scenarios 1 (donor-only scenario) and 2 (donor-recipient scenario) assuming approximately 2 million red cell transfusions are performed per year (ARC 2014 data).	16
3.1	Percent optimality gap for the RMM Heuristic with cardinality of Ω^h in the order of n^2 and n^3 , for $n = 10 - 18$	37
3.2	Maximum values of Π^R , $\Pi^E(\hat{\mu})$, and \mathcal{R}^L for all problem instances with $n = 2 - 10$ infections, and forecast error $r = 10\%$, 35% , and 50%	43
3.3	Mean and uncertainty sets for prevalence rates in the United States (in %).	44
3.4	Sensitivity (true positive probability) values (in %).	45
3.5	Comparison of testing solutions for various categories of screening strategies (A: Antibody/Antigen, I: ID-NAT, M: MP-NAT).	47
4.1	The expressions for functions $RR_U^b(\mathbf{S})$ and $RR_N^b(\mathbf{S}^F, \mathbf{S}^R)$, for $b \in \{LB, UB\}$	64
4.2	Prevalence rates for first-time and repeat donors (in %) and life-time treatment cost per TTI (in \$) in the United States.	70
4.3	Parameters for viral load growth models and test sensitivity functions.	70
4.4	NAT sensitivity (in %) for HBV-, HCV-, and HIV-infected window period donors for various pool sizes (from [102]).	71
4.5	Calibrated values of c_i^0 , $i \in \Psi$, and the corresponding RMSE values.	71
4.6	Pool size solutions, the resulting expected number of TTIs per 1,000,000 transfusions (with ratio of TTIs coming from first-time donors to those coming from repeat transfusions) for all strategies considered, and the worst-case ratio (\mathcal{R}).	74
4.7	Pool size solutions, the resulting expected life-time treatment cost per 1,000,000 transfusions for all strategies considered, and the worst-case ratio (\mathcal{R}).	75
A.1	Probabilistic sensitivity analysis results for Scenarios 1 (donor-only scenario) and 2 (donor-recipient scenario).	93

A.2	Probabilistic sensitivity analysis detailed TTB, waste, and cost values for Scenarios 1 (donor-only scenario) and 2 (donor-recipient scenario).	93
B.1	The notation.	94
B.2	Comparative statics results for ERM and RMM	95
B.3	Fitted parameters, k_i , and coefficients of determination (R_i^2), for $f_i(B_i) = e^{-k_i B_i}$ for HIV, HBV, HCV, babesiosis, and WNV.	109

Chapter 1

Introduction

1.1 Motivation

In both developing and developed countries, healthcare resources are limited, and demand exceeds supply. It is therefore crucial to allocate the scarce resources in the most effective and efficient way so as to improve the quality and safety of healthcare delivery. While the problem of allocating resources in healthcare systems is complex, it can greatly benefit from the logical and systematic methods and tools of Operations Research (OR).

One important decision is to select assays for screening the donated blood for transfusion-transmittable infections (TTIs). Blood units constitute an essential component of any healthcare system, and are required for patients of all age groups for a variety of treatments, including treatment of cancer patients, trauma victims, pregnant women with complications, and children with anemia; and are also needed for major surgeries. While the Food and Drug Administration (FDA) in the United States requires all blood donations to be tested for a set of TTIs, it does not dictate which particular test(s) should be used by blood centers. Multiple FDA-licensed blood screening tests are available for each infection, but all screening tests are imperfectly reliable and have different costs. To further complicate the blood screening decision, infection prevalence rates and several donor characteristics are uncertain, while surveillance methods are highly resource- and time-intensive. Therefore, only limited information is available to the budget-constrained decision-maker, who needs to devise a post-donation blood screening scheme so as to minimize the risk of an infectious donation being released into the blood supply (*Residual Risk*). This decision is of utmost importance because the consequences of transfusing infected blood are dire.

The transfusion literature studies this decision through simple cost-effectiveness (CE) studies,

which have serious limitations when used for multiple infections. These limitations have been acknowledged in the literature, including that CE relies only on the expected *Residual Risk*, it fails to account for the dependencies among the different interventions (e.g., assays), and assumes that interventions have constant return to scale [30]. Our research objective is to develop novel OR-based models and algorithms that can overcome the aforementioned limitations of CE studies in the context of the assay selection problem for donated blood. We hope that our research results will find use in industry and assist the decision-making process at blood centers. This will consequently benefit the society by providing a “safer” supply of blood with a lower TTI risk. This is especially important in developing countries where budgets are even more limited and the need for effective blood screening is even higher.

1.2 Research Overview

We first consider the assay selection problem for a single infection, babesiosis, a disease caused by the intraerythrocytic parasite *Babesia microti* (*B. microti*) [113]. This research is in collaboration with the American Red Cross, and is detailed in Chapter 2 of this dissertation. In particular, babesiosis is a TTI, and donated blood units from infected donors can lead to transfusion-transmitted babesiosis (TTB). It is the leading cause of TTIs in the US, where an estimated 21% of babesiosis cases in at-risk patients are fatal [74]. While it is thought that complicated babesiosis is more likely to occur in patients with asplenia, malignancy, human immunodeficiency virus (HIV), chronic heart, lung, and liver diseases; in patients who are taking immunosuppressive medications; or in patients with a history of organ transplantation, not all risk factors are well-understood in the medical literature [110]. On the other hand, babesiosis is endemic only in certain regions of the US: to date, 97% of confirmed babesiosis cases have occurred in the states of Connecticut, Massachusetts, Minnesota, New Jersey, New York, Rhode Island, and Wisconsin [61, 36]. Given the infection dynamics, it is difficult to accurately estimate the prevalence of *B. microti* in the US population. Hence we perform a cost-effectiveness analysis that takes into consideration this uncertainty in prevalence rates in order to determine the optimal screening strategy for babesiosis.

Chapter 3 of this research studies “robust” screening schemes for multiple infections under limited information on prevalence rates. When screening for multiple infections, traditional cost-effectiveness methodology suffers from major limitations, as it fails to account for the dependencies among the multiple assays. Consequently, we formulate the blood screening problem using a ro-

bust formulation as well as an expectation-based formulation, and obtain structural properties of their optimal solutions. Our analysis of the robust formulation also contributes to the literature on the robust nonlinear knapsack problem with continuous variables, for which we develop important structural properties. Further, we analytically characterize the *price of robustness* and the *price of expectation-based optimization*, which respectively represent the deviation, from the minimum possible expected *Residual Risk*, of the robust solution and the expectation-based solution under forecast error. Our analysis shows that the robust formulation leads to a safe blood supply under all prevalence rate possibilities, at the expense of a small increase in the expected *Residual Risk*. On the other hand, in the presence of forecast error, the expectation-based solution might deviate significantly from the true optimal solution, and may introduce unintended, but substantial, *Residual Risk* to the blood pool for various prevalence rate possibilities. Our case study of the United States confirms these findings, and also indicates that following the FDA guidelines is no guarantee of an optimal testing regime – sometimes it is better to deviate from the FDA recommendations. Indeed, our robust testing solution outperforms various testing schemes that follow the FDA guidelines, in terms of substantially reducing both the expectation and the range of *Residual Risk*. These findings have important implications on public policy.

In Chapter 4, we study screening with Nucleic Acid Testing (NAT) under uncertainty in the donor population. Unlike serological assays that screen for antibodies and antigens, NAT assays screen for genetic material, enabling them to detect the infection during the earlier stages. The higher sensitivity of NAT assays comes at higher costs. Consequently, due to limited screening budgets, blood centers resort to combining blood samples from multiple donors in pools and screening each pool once. In turn, this reduction in cost is associated with reduced screening sensitivity. In addition, the donor population is comprised of first-time and repeat donors, with quite different characteristics, including significantly lower prevalence rates in the latter group. In this setting, the budget-constrained blood center needs to devise a pooling strategy (testing pool sizes for various infections) in order to minimize the risk of TTIs. Because of these properties, it may be optimal for first-time blood donors to undergo more extensive screening than repeat donors, who donate blood frequently. Since several donor characteristics, including the proportion of repeat donors and the viral load, are uncertain, we develop a chance-constrained optimization model with the objective of minimizing the TTI risk while remaining within the testing budget with a high probability. Our findings indicate that *non-universal* NAT schemes, where first-time and repeat donors undergo different testing, can substantially reduce *Residual Risk* and the life-time treatment cost in infected

transfusion recipients. Our case study of the US indicates that non-universal NAT schemes for HBV, HCV, and HIV outperform current NAT testing practices in US blood centers.

Chapter 2

Cost-effectiveness of Babesiosis Screening in the United States

2.1 Introduction

Babesia microti is an intraerythrocytic parasite that causes babesiosis [113]. Babesiosis is associated with flu-like symptoms and can lead to death in vulnerable patients, but healthy *B. microti*-infected individuals are often asymptomatic [54, 63, 93, 110]. *B. microti* is endemic in areas of the Midwest (Minnesota and Wisconsin) and Northeast (Connecticut, Massachusetts, New Jersey, New York, and Rhode Island) [36]. In 2012, 96% (871/911) of reported babesiosis cases occurred in residents of these seven states [36]. The reported incidence of babesiosis has increased over time, likely due to enhanced awareness and geographical expansion of the disease vector; babesiosis is reportable in 18 states and became nationally notifiable in 2011 [36].

In the United States, the most common mode of transmission to humans is through the bite of an infected deer tick (*Ixodes scapularis*) [62]. However, the parasite can be transmitted to recipients of cellular blood components via asymptotically infected donors, leading to transfusion-transmitted babesiosis (TTB). Between 1979 and 2009, 162 TTB cases were reported in the US, 159 caused by *B. microti*. The reported TTB incidence appears to be increasing, as 122 (77%) of cases occurred during 2000-2009 [61]. TTB cases are likely under-recognized and under-reported.

Approximately 21% of babesiosis cases in immunocompromised patients are fatal [74]; an 18% fatality rate was noted by Herwaldt et al. [61] Traditionally, recipients at increased risk of complicated babesiosis are those with asplenia, malignancy, HIV infection, chronic heart, lung, and

liver diseases; patients taking immunosuppressive medications; or patients with a history of organ transplantation [110]. However, careful study of the medical histories of TTB patients suggests that attempting to accurately define and identify high-risk patients based on medical conditions is complex and error-prone [61].

The US Food and Drug Administration (FDA) has not licensed *B. microti* blood donor screening tests. The only intervention is a question asking donors at presentation if they have ever had babesiosis, followed by indefinite deferral of those responding “yes”. This method has low sensitivity and results in the current risk of TTB. It also leads to the deferral of donors who are no longer infectious. In 2010, the FDA’s Blood Products Advisory Committee recommended that additional strategies were needed to reduce TTB [46]. With high uncertainty around *B. microti* prevalence and its infection dynamics over time, studies are needed to determine the feasibility of *B. microti* blood donation screening.

In June 2012, the American Red Cross (ARC) began real-time screening of blood donors reporting to drives in targeted counties in CT, MA, MN, and WI [81]. The screening protocol consists of an arrayed fluorescence immunoassay (AFIA) and polymerase chain reaction (PCR) run in tandem to detect *B. microti* antibodies (Ab) and DNA, respectively, and is described in detail elsewhere [84].

The eventual availability of licensed assays leads to questions surrounding the optimal strategy to approach systematic blood donation screening, as screening all donations is unnecessary and cost-prohibitive. Potential strategies in endemic regions include: universal screening; screening only during certain months (e.g., May through October); risk-targeted screening, in which *B. microti*-tested negative units are provided only to recipients at greatest risk of clinical infection; or some combination of these strategies. While the ARC’s screening protocol includes both Ab and parasite DNA tests, using only one assay (i.e., either AFIA or PCR) is also possible. Cost-effectiveness modeling is necessary to estimate each strategy’s financial implications and TTB risk.

Comparative- and cost-effectiveness analyses published thus far have limitations. Simon et al. [99] concluded that Ab screening in endemic areas was most appropriate; this strategy avoided 3.39 cases of TTB/100,000 red blood cell (RBC) transfusions at an incremental cost-effectiveness ratio (ICER) of \$760,000 compared to a recipient-risk-targeted strategy. However, this analysis assumed that transmission probability was static, regardless of the donor’s stage of infection (i.e., Ab- versus PCR-positive), when data suggest that clinical babesiosis is more likely to occur in recipients of units from PCR-positive donors than PCR-negative/Ab-positive donors (33.3% versus 2.9%) [66].

In addition, Simon [99] did not consider the predicted amount of blood wasted; i.e., the number of *B. microti*-free blood units incorrectly discarded due to resolved infections in donors or false-positive antibody test results. Finally, the Simon analysis did not consider a PCR-only screening strategy, which remains a viable option.

More recently, Goodell et al. studied the cost-effectiveness of screening in different geographical areas using combinations of two Ab detection assays and PCR [53]. The Goodell model demonstrated that none of the screening scenarios considered was cost-effective at the implicit \$50,000 per QALY or \$1,000,000 per intervention thresholds. This could have been as a result of the lower transmission probabilities, lower probability of complicated babesiosis after transmission, different test performance characteristics, and higher testing cost estimates than used in Simon’s model.

In this analysis, we consider the comparative- and cost-effectiveness of four blood donation screening strategies for *B. microti* in endemic areas compared to the status quo (questioning the donor about history of babesiosis). Sensitivity analyses were performed to examine the effects of uncertainty in transmission probability, prevalence rates, and other key model inputs.

2.2 Materials and Methods

2.2.1 Screening Strategies

We modeled four screening strategies, including universal Ab testing, universal PCR testing, universal Ab/PCR testing in parallel, and risk-targeted-Ab/PCR screening. In this context, universal refers to screening all donors who present to blood drives in CT, MA, MN, and WI. The risk-targeted-Ab/PCR strategy was described in Simon et al. [99] and involves screening only a pre-determined portion of the blood supply, targeted for transfusion recipients identified as high-risk. In this strategy, the remainder of the blood, used for transfusion recipients identified as low-risk, comes from donors who only answered the standard questionnaire including a negative response to the babesiosis question.

2.2.2 Model Overview

We developed a decision tree model (Figure 2.1) to predict the health and economic consequences of various blood donation screening *B. microti* strategies. The model was coded and implemented in Microsoft Excel using the data reported in Table 2.1. All deterministic and probabilistic sensitivity analysis results were generated by an Excel Macro.

The decision tree model projected both health and economic outcomes. Health outcomes included the expected number of (1) complicated TTB cases, (2) uncomplicated TTB cases, (3) TTB cases averted in blood product recipients, and (4) quality-adjusted life years (QALY) per transfusion recipient. Economic outcomes included (1) each strategy’s per donation unit cost, including testing cost, cost of positive test results (blood center costs for handling and discarding Babesia-reactive units), and TTB treatment cost; and, (2) waste (the number of infection-free blood units incorrectly discarded due to false-positive test results). We also calculated a “waste index”; i.e., the ratio of the number of wasted blood units to the number of true positives.

We combined health and economic outcomes to determine the cost-effectiveness ratio (CER) and the incremental CER (ICER) of each strategy. $ICER_{Qj}$ measures the cost of the additional benefit of adopting strategy “ j ” over the status quo (questionnaire, Q), while $ICER_j$ measures that over the next most effective alternative. We used one-way deterministic sensitivity analyses to assess the individual effect of donor Ab and/or DNA prevalence and transmission probabilities on each strategy’s cost-effectiveness. In the probabilistic sensitivity analysis, we estimated the joint effect of overall input uncertainty on each strategy’s cost-effectiveness.

2.2.3 Data

We use the following notation to distinguish between donors in different infectious stages:

$Prop_W$: Proportion of Ab-negative/PCR-positive, i.e., window-period donors,

$Prop_A$: Proportion of Ab-positive/PCR-positive, i.e., actively infected donors,

$Prop_R$: Proportion of Ab-positive/PCR-negative, i.e., donors with resolved infections.

Table 2.1 provides the parameter values for the base case, ranges (lower and upper limits) for the sensitivity analyses, and for comparison, the parameter values used in Simon et al. [13] and Goodell et al [53], further summarized in Table 2.2. We assumed 100% PCR specificity based on ARC experience using investigational PCR [84]. We considered 99.5% PCR sensitivity, defined as the ability to detect DNA-positive units expected to cause babesiosis in recipients, in our base case and varied it in the probabilistic sensitivity analysis [82, 83]. For prevalence values, we used data from ongoing investigational studies conducted by the ARC including detection of eight window-period donors, 52 actively infected donors and 261 with resolved infection [83]. One-way deterministic sensitivity analysis was performed on transmission probabilities and prevalence rates, and probabilistic

sensitivity analysis was performed on all key model inputs within the sensitivity ranges provided in Table 2.1. To address the uncertainty of transmission based on the donor's stage of infection and the health state of the recipient, we considered two scenarios: a donor-only scenario (Scenario 1), in which the transmission probability from infected blood depends only on the donor's stage of infection (active versus resolved infection); and a donor-recipient scenario (Scenario 2), in which the transmission probability depends on both the donor's stage of infection and the recipient's health status (high-risk versus low-risk) (Table 2.1).

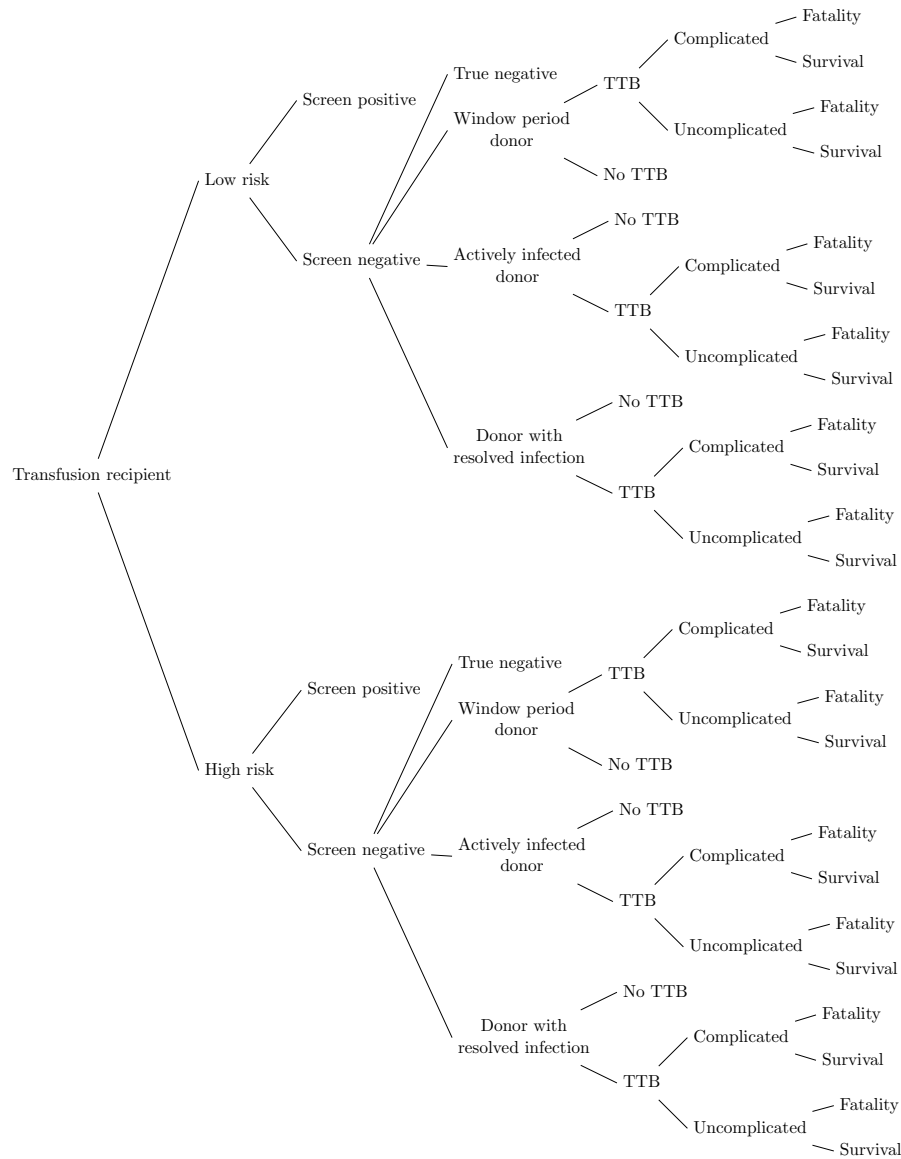


Figure 2.1: Decision tree model used in cost-effectiveness analysis.

Table 2.1: Base case data and the ranges used in sensitivity analysis.

Parameter	Base case data	Sensitivity range	References	Data and ranges used in Simon et al. [99]	Data and ranges used in Goodell et al. [53]
Screening test characteristics					
Questionnaire			[69, 120]		N/A
Sensitivity	0.125% ^a	(0.1-5%)		0.5% (0.1-5%)	
Specificity	99.97% ^a	(90-100%)		99.90% (90-100%)	
Antibody (arrayed fluorescence immunoassay)	AFIA			AFIA	Manual IFA
Sensitivity	90.4%	(85-95%)	[84]	94.0% (80-100%)	Manual IFA: 91.8% ^b (87.7-95.7%)
Specificity	99.98%	(80-100%)	[84]	97.7% (80-100%)	Manual IFA: 95% (90-100%)
PCR (polymerase chain reaction)					
Sensitivity	99.5%	(98 - 100%)	[99]	99.5%	100% ^b
Specificity	100%	(99-100%)	[84]	100%	100% (99-100%)
Antibody/PCR in parallel					
Sensitivity	100%	(90-100%)	[84]	99.9% (90-100%)	Manual IFA/PCR: 93% (90-100%)
Specificity	99.98%	(80-100%)	[84]	97.7% (80-100%)	Manual IFA/PCR: 100% (99-100%) ^d
Prevalence values ^c					
$Prop_W = \text{Ab-negative/PCR-positive}$	0.0096% (8/83,330)	(0.0050-0.0100%)	[84]	0.0360% (0.01-0.09%)	4-state ^e : 0.0204% 7-state: 0.0162% 20-state: 0.0072% 50-state: 0.0054% 4-state ^e : 0.0612% 7-state: 0.0486% 20-state: 0.0216% 50-state: 0.0162%
$Prop_A = \text{Ab-positive/PCR-positive}$	0.0624% (52/83,330)	(0.0500-0.0800%)	[84]	0.9%= $Prop_A + Prop_R$ (0.1-2.0%)	
$Prop_R = \text{Ab-positive/PCR-negative}$	0.3132% (261/83,330)	(0.2000-0.4000%)	[84]	4-state ^e : 0.5984% 7-state: 0.4752% 20-state: 0.2112% 50-state: 0.1584%	
Proportion of patient population at high-risk	29.3%	(25-75%)	[99]	29.3% (25-75%)	54%
Probability of complicated babesiosis					
High-risk patient	57%	(20-80%)	[74]	57% (20-80%)	Overall: 7% (4.8-33.0%)
Low-risk patient	32%	(10-50%)	[116]	32% (10-50%)	9.0%
Babesiosis case fatality rate (for recipients developing complicated babesiosis)					
High-risk patient	21%	(6-28%)	[57, 74, 104]	21% (6-28%)	19.2%
Low-risk patient	6%	(1-10%)	[67, 116]	6% (1-10%)	19.2%
All-cause mortality after RBC transfusion					
Year 1					
High-risk patient	38%			38% (27-49%)	
Low-risk patient	27%			27% (19-35%)	
Year 2					
High-risk patient	19%			19% (13-25%)	
Low-risk patient	11%			11% (5-15%)	
Year 3+					
High-risk patient	15%			15% (10-20%)	
Low-risk patient	8%			8% (4-12%)	
Utility values					
Baseline transfusion recipient	0.90		[1, 40]	0.90 (0.60-0.90)	0.90 (0.90-1.00)
Uncomplicated babesiosis	0.87		[78]	0.87 (0.80-0.89)	0.85 (0.83-0.93)
Complicated babesiosis	0.67		[8]	0.67 (0.40-0.80)	0.67 (0.00-0.67)

Table 2.1 continued.

Parameter	Base case data	Sensitivity range	References	Data and ranges used in Simon et al. [99]	Data and ranges used in Goodell et al. [53]
Costs					
Screening cost per donation					
Universal Ab	\$12.5 ^f		ARC internal data	\$15.0 (\$8-23)	\$21 (\$15-27)
Universal PCR	\$12.5 ^f		ARC internal data		\$22.50 (\$20-25)
Universal Ab/PCR	\$25.0 ^f		ARC internal data	\$30.0 (\$15-45)	\$43.50 (\$35-52)
Risk-targeted-Ab/PCR	\$50.0 ^{f,g}		ARC internal data	\$33.0 (\$30-39)	
Unit societal cost of a positive Ab or PCR test result	\$625 ^h	(\$417-938)	[99]	\$625 ^h (\$417-938)	\$427 ⁱ (\$213-853)
Unit societal cost of a positive questionnaire	\$103 ^j	(\$69-155)	[99]	\$103 ^j (\$69-155)	
Unit cost of symptomatic TTB case	\$22,000 ^k	(\$14,667-33,000)	[2, 99, 105]	\$22,000 ^k (\$14,667-33,000)	Moderate: \$28,707 Severe: \$72,968 ^l
Transmission probability, given that <i>Babesia</i> -infected blood is transfused to the patient				Overall: 0.4% (0.1-2.2%)	Overall: 0.98% (0.40- 12.70%) ^m
Scenario 1 (Donor-only scenario)					
Low-risk patient, actively infected donor	33.3% ⁿ		[66]	0.3%	5.1%
Low-risk patient, donor with resolved infection	2.9% ⁿ		[66]	0.3%	0.4%
High-risk patient, actively infected donor	33.3% ⁿ			0.6%	5.1%
High-risk patient, donor with resolved infection	2.9% ⁿ			0.6%	0.4%
Scenario 2 (Donor-recipient scenario)					
Low-risk patient, actively infected donor	33.3% ⁿ				
Low-risk patient, donor with resolved infection	2.9% ⁿ				
High-risk patient, actively infected donor	66.6% ⁿ				
High-risk patient, donor with resolved infection	5.8% ⁿ				

^a Based on data from Rhode Island and New York; see Appendix A for the calculations.

^b Goodell et al. [53] reports the “effective sensitivity” of Ab and PCR. For comparison, we derive the sensitivity values from Goodell’s effective sensitivity values: PCR sensitivity=12%/12%=100%; Ab sensitivity=89%/97% = 91.8%.

^c The ranges for prevalence values in the third column were calculated using the binomial 95% confidence intervals.

^d Goodell et al. [53] splits the infected donors into infection stages assuming that 3% of all infected donors are Ab-negative/PCR-positive, 9% of all infected donors are Ab-positive/PCR-positive, and 88% are Ab-positive/PCR-negative.

^e Goodell et al. [53] considers 4 variations of the universal strategy: (a) 4-state: Connecticut, Massachusetts, New York, Rhode Island; (b) 7-state: includes all states in (a) with the addition of New Jersey, Minnesota, and Wisconsin; (c) 20-state: all states in (b) with the addition of Maryland, Virginia, Vermont, New Hampshire, Maine, Delaware, Pennsylvania, California, Ohio, Florida, Texas, Michigan, and the District of Columbia; and (d) 50-state.

^f The testing cost for each strategy includes equipment, reagents, materials/consumables, direct labor, and fringe benefits.

^g For the risk-targeted strategy, unit cost is double the price of testing, based on the need to keep twice as much inventory in stock (ARC internal data).

^h Includes specimen collection, processing, donor recruitment and destruction of positive units.

ⁱ Consists of the cost of discarding a false-positive unit.

^j Lower than that for Ab and PCR assays, as screening and handling/destruction of the blood unit is not involved.

^k We use estimates that include sub-acute rehabilitation care after complicated babesiosis, medication costs [105], and hospitalization costs [2].

^l Moderate: 7 days \times \$4,101 = \$28,707. Severe: 14 days \times \$5,212 = \$72,968.

^m There is a discrepancy in the values reported in Goodell et al. [99], where this value is reported as 0.98% in the text and 9.8% in Table 1.

ⁿ Refer to Table 2.3 for the ranges used in sensitivity analysis.

Table 2.2: Comparison of assumptions and data between this study and prior studies.

		This study	Goodell et al [53]	Simon et al [99]
Strategies analyzed		Universal Ab ^a	Universal Ab ^b	Universal Ab ^c
		Universal PCR	Universal Ab/PCR	Universal Ab/PCR
		Universal Ab/PCR	Universal ELISA	Risk-targeted- Ab/PCR
		Risk-targeted- Ab/PCR Ab refers to AFIA	Universal ELISA/ PCR Universal PCR Ab refers to Manual IFA	Ab refers to AFIA
Testing costs	Ab	\$12.50	\$21.00	\$15.00
	PCR	\$12.50	\$22.50	N/A
	Ab/PCR	\$25.00	\$43.50	\$30.00
	Risk-targeted- Ab/PCR	\$50.00	N/A	\$33.00
Sensitivity	Ab	90.4%	91.8%	94.0%
	PCR	99.5%	100%	99.5%
	Ab/PCR	100%	93%	99.9%
	Questionnaire	0.125%	N/A	0.5%
Prevalence rates	Ab-negative/PCR-positive	0.0096% ^a	4-state: 0.0204% ^d	0.0360%
	Ab-positive /PCR- positive	0.0624% ^a	4-state: 0.0612% ^d	0.9000%, Ab+
	Ab-positive/PCR- negative	0.3132% ^a	4-state: 0.5984% ^d	
Transmission probability	Donor-based? (PCR-positive vs. Ab-positive/PCR-negative)	YES (33.3% vs. 2.9%)	YES (5.1% vs. 0.4%)	NO
	Recipient-based? (High-risk versus low-risk)	YES (66.6% vs. 33.3%; and 5.8% vs. 2.9%)	NO	YES Overall: 0.4% (0.6% vs. 0.3%)
Fatality rates	High-risk recipients	21%	19.2%	21%
	Low-risk recipients	6%	19.2%	6%

^a We consider screening in 4 endemic states: Minnesota, Wisconsin, Connecticut, Massachusetts. Our prevalence rates come from ongoing investigational studies conducted by the ARC in these 4 states (Appendix A).

^b Goodell et al. [53] considers 4 variations of the universal strategy: (a) 4-state: Connecticut, Massachusetts, New York, Rhode Island; (b) 7-state: includes all states in (a) with the addition of New Jersey, Minnesota, and Wisconsin; (c) 20-state: all states in (b) with the addition of Maryland, Virginia, Vermont, New Hampshire, Maine, Delaware, Pennsylvania, California, Ohio, Florida, Texas, Michigan, and the District of Columbia; and (d) 50-state.

^c Simon et al.[99] considers screening in 7 endemic states: Minnesota, Wisconsin, Connecticut, Massachusetts, New Jersey, New York, and Rhode Island.

^d Goodell et al. [53] splits the infected donors into various stages as follows: 3% of all infected donors are Ab-negative/PCR-positive, 9% of all infected donors are Ab-positive/PCR-positive, and 88% of all infected donors are Ab-positive/PCR-negative.

2.2.4 Base Case

The base case used data reported in Table 2.1, considering two variations of transmission probability: donor-only scenario (transmission probabilities are 33.3% for patients receiving blood from PCR-positive donors and 2.9% for patients receiving blood from Ab-positive/PCR-negative donors) [66] and donor-recipient scenario (the transmission probability in low-risk patients remains the same as above, but is 66.6% for high-risk patients receiving blood from PCR-positive donors and 5.8% for high-risk patients receiving blood from Ab-positive/PCR-negative donors) (Table 2.1).

2.2.5 Deterministic Sensitivity Analyses

We performed one-way deterministic sensitivity analyses on transmission probabilities and prevalence rates to study how each strategy’s effectiveness changes with possible variations in data values:

1. Deterministic sensitivity analysis on transmission probabilities: For each case in Table 2.3, we varied transmission probability within the ranges given in Table 2.3.
2. Deterministic sensitivity analysis on prevalence rates: We varied $Prop_W$, $Prop_A$, and $Prop_R$ within the ranges given in Table 2.1.

Table 2.3: Transmission probability sensitivity analysis data for Scenarios 1 (donor-only scenario) and 2 (donor- recipient scenario).

Transmission probability values	Scenario 1 (donor only scenario)		Scenario 2 (donor-recipient scenario)	
	Scenario 1-Low ^a	Scenario 1-High ^b	Scenario 2-Low ^c	Scenario 2-High ^d
Low risk patient, actively infected donor	Varied in [0.3% – 50.0%]	Varied in [2.9% – 50.0%]	Varied in [0.3% – 50.0%]	Varied in [2.9% – 50.0%]
Low risk patient, donor with resolved infection	0.3%	2.9%	0.3%	2.9%
High risk patient, actively infected donor	Varied in [0.3% – 50.0%]	Varied in [2.9% – 50.0%]	Varied in [0.6% – 50.0%]	Varied in [5.8% – 50.0%]
High risk patient, donor with resolved infection	0.3%	2.9%	0.6%	5.8%

^a Scenario 1-Low: Probability of transmission to high-risk patients is equal to the probability of transmission to low-risk patients. Blood units from donors with resolved infection present a transmission probability of 0.3%. Transmission probability for blood units from actively infected donors is varied in [0.3%-50.0%].

^b Scenario 1-High: Probability of transmission to high-risk patients is equal to the probability of transmission to low-risk patients. Blood units from donors with resolved infection present a transmission probability of 2.9%. Transmission probability for blood units from actively infected donors is varied in [2.9%-50.0%].

^c Scenario 2-Low: Probability of transmission to high-risk patients is double the probability of transmission to low-risk patients. Blood units from donors with resolved infection present a transmission probability of 0.3% for low-risk patients and 0.6% for high-risk patients. Transmission probability for blood units from actively infected donors is varied in [0.3%-50.0%] for low-risk patients, and varied in [0.6%-100.0%] for high-risk patients.

^d Scenario 2-High: Probability of transmission to high-risk patients is double the probability of transmission to low-risk patients. Blood units from donors with resolved infection present a transmission probability of 2.9% for low-risk patients and 5.8% for high-risk patients. Transmission probability for blood units from actively infected donors is varied in [2.9%-50.0%] for low-risk patients, and varied in [5.8%-100.0%] for high-risk patients.

2.2.6 Probabilistic Sensitivity Analysis on Key Model Inputs

For both donor-only and donor-recipient scenarios (Table 2.1), we performed a comprehensive probabilistic sensitivity analysis on all key model inputs to assess the impact of overall input uncertainty on each strategy’s effectiveness. As in Simon et al. [99], we assume that all variables followed triangular distributions, with ranges reported in Table 2.1 (third column), and with mode of the distribution matching the value used in the base case (Table 2.1, second column). Triangular distribution is a reasonable and commonly used approximation in the absence of information on probability distributions. We ran 10,000 replications of the Monte Carlo simulation. For each replication, we simultaneously generated a value for each variable using its probability distribution function and calculated the cost-effectiveness ratio of each strategy.

2.3 Results

2.3.1 Base Case

Table 2.4 contains the results for Scenarios 1 and 2. The lowest predicted number of TTB cases averted occurred with the questionnaire and risk-targeted screening strategies, regardless of transmission probability. The predicted number of TTB cases averted was highest for universal Ab/PCR (32.75 and 42.35/100,000 units transfused [pht, per hundred thousand units transfused], for Scenarios 1 and 2, respectively), but this strategy was also the most costly at \$27.39 unit cost/transfusion. The ICER values over the questionnaire were highest for risk-targeted-Ab/PCR (\$148,065/QALY-Scenario 1 and \$62,226/QALY-Scenario 2), and lowest for universal PCR (\$43,931/QALY-Scenario 1 and \$25,801/QALY-Scenario 2).

Table 2.4: Base case results for Scenarios 1 (donor-only scenario) and 2 (donor-recipient scenario).

Testing Strategy	TTB cases averted pht	Total unit cost (per transfusion) (\$)	Incremental cost pht (\$)	QALY per transfusion recipient	Incremental QALY pht	CER (\$/QALY)	ICER (\$/QALY)	ICER over questionnaire (\$/QALY)
Results for Scenario 1								
No Screening	0.00	7.21		5.9141637		1.22		
questionnaire (status quo)	0.02	7.23	2,694	5.9141638	0.01	1.22	201,309	
Risk-targeted Ab/PCR	9.61	20.46	1,323,058	5.9142532	8.94	3.46	148,065	148,065
Universal PCR	23.64	14.95	-23,522	5.9143396	0.80	2.53	-63,567	43,931
Universal Ab	26.74	16.15	122,129	5.9143627	2.22	2.73	51,027	44,842
Universal Ab/PCR	32.75	27.39	1,123,841	5.9144074	4.47	4.63	251,424	82,756
Results for Scenario 2								
No Screening	0.00	9.32		5.9140743		1.58		
questionnaire (status quo)	0.03	9.34	2,578	5.9140745	0.02	1.58	140,938	
Risk-targeted Ab/PCR	19.21	20.46	1,112,067	5.9142532	17.87	3.46	62,226	62,226
Universal PCR	30.57	15.54	-30,414	5.9143147	1.09	2.63	-80,968	25,801
Universal Ab	34.58	16.54	102,902	5.9143463	3.03	2.80	33,920	26,469
Universal Ab/PCR	42.35	27.39	1,085,118	5.9144074	6.11	4.63	177,602	54,206

CER = cost-effectiveness ratio.

Table 2.5 contains waste and additional cost results. The questionnaire had the most waste (99.62 units of blood wasted pht; 208.62 waste index), followed by risk-targeted-Ab/PCR (76.27 wasted units pht; 0.68 waste index). Universal PCR had a waste index of zero. The model predicted zero TTB and complicated TTB cases with the universal Ab/PCR strategy (versus 32.75 and 12.88 pht for Scenario 1, and 42.35 and 18.35 pht for Scenario 2, respectively [no screening]), but universal Ab/PCR had the highest testing cost and positive test-result cost (\$25.00+\$2.39/unit, respectively). Excluding the questionnaire (status quo), TTB cases pht (total and complicated) for the remaining strategies for Scenario 1 ranged from 6.01 and 2.36 (universal Ab) to 23.14 and 7.41 (risk-targeted-Ab/PCR), and for Scenario 2, ranged from 7.77 and 3.37 (universal Ab) to no change for the risk-targeted strategy. The remaining testing costs and positive test-result costs were \$14.65+\$0.72/unit (risk-targeted-Ab/PCR), \$12.50+\$0.45 (universal PCR), and \$12.50+\$2.33 (universal Ab).

Table 2.6 projects the annual number of TTB cases averted, number of TTB deaths averted, and total implementation cost, comprised of testing costs, costs of positive test results, and TTB treatment costs for Scenarios 1 and 2 if screening were implemented in the seven endemic US states. Assumptions include year-round donor prevalence rates in the seven states to be consistent with those reported here for four states [83], and approximately 2 million red cell transfusions in the seven states (ARC internal data). These estimates project 652-843 TTB cases and 54-77 TTB-related fatalities averted per year with universal Ab/PCR.

Table 2.5: Base case detailed TTB, waste, and cost values for Scenarios 1 (donor-only scenario) and 2 (donor-recipient scenario).

Testing Strategy	TTB cases pht	Complicated TTB cases pht	Waste (number of blood units wasted) pht	Waste index (ratio of the number of wasted blood units to the number of true positives)	Testing cost per transfusion (\$)*	Cost of positive test results per transfusion (\$)*	Treatment cost of TTB per transfusion (\$)*
Results for Scenario 1							
No Screening questionnaire (status quo)	32.75	12.88	0.00	0.00	0.00	0.00	7.21
Risk-targeted Ab/PCR	32.73	12.88	99.62	208.62	0.00	0.03	7.20
Universal PCR	23.14	7.41	76.27	0.68	14.65	0.72	5.09
Universal Ab	9.11	3.58	0.00	0.00	12.50	0.45	2.00
Universal Ab/PCR	6.01	2.36	19.92	0.06	12.50	2.33	1.32
Universal Ab/PCR	0.00	0.00	19.92	0.05	25.00	2.39	0.00
Results for Scenario 2							
No Screening questionnaire (status quo)	42.35	18.35	0.00	0.00	0.00	0.00	9.32
Risk-targeted Ab/PCR	42.32	18.34	99.62	208.62	0.00	0.03	9.31
Universal PCR	23.14	7.41	76.27	0.68	14.65	0.72	5.09
Universal Ab	11.78	5.10	0.00	0.00	12.50	0.45	2.59
Universal Ab/PCR	7.77	3.37	19.92	0.06	12.50	2.33	1.71
Universal Ab/PCR	0.00	0.00	19.92	0.05	25.00	2.39	0.00

* The sum of the last three columns equals column 3 in Table 2.4 (total unit cost per transfusion).

Table 2.6: Projected annual TTB cases averted, TTB deaths averted, total cost, testing cost, cost of positive test results, and treatment cost of TTB for implementation of the testing policies in seven endemic states for Scenarios 1 (donor-only scenario) and 2 (donor-recipient scenario) assuming approximately 2 million red cell transfusions are performed per year (ARC 2014 data).

Testing Strategy*	TTB cases averted per year	TTB deaths averted per year	Total cost per year (\$)	Testing cost per year (\$)	Cost of positive test results per year (\$)	Treatment cost of TTB per year(\$)
Scenario 1						
No Screening questionnaire (status quo)			2,885,760	0	0	2,885,760
Risk-targeted Ab/PCR	0.20	0.00	2,945,465	0	59,705	2,885,760
Universal PCR	38.41	4.60	31,524,435	29,156,122	318,429	2,049,884
Universal Ab	94.73	7.82	28,852,425	24,877,238	179,116	796,072
Universal Ab/PCR	107.27	8.82	26,349,970	24,877,238	935,384	537,348
Universal Ab/PCR	131.35	10.82	50,709,761	49,754,475	955,286	0
Scenario 2						
No Screening questionnaire (status quo)			3,741,537	0	0	3,741,537
Risk-targeted Ab/PCR	0.20	0.00	3,781,340	0	59,705	3,721,635
Universal PCR	76.82	9.19	31,524,435	29,156,122	318,429	2,049,884
Universal Ab	122.20	11.12	26,091,247	24,877,238	179,116	1,034,893
Universal Ab/PCR	138.52	12.58	26,489,282	24,877,238	935,384	676,661
Universal Ab/PCR	169.56	15.42	50,709,761	49,754,475	955,286	0

* Risk in 10 highly endemic counties of Connecticut and Massachusetts during this study was 1 confirmed TTB case per 19,500 untested donations versus 1 confirmed TTB case per 100,000 for all seven states, or approximately 5-fold lower. This 5-fold difference was used to adjust the prevalence data used for this table.

2.3.2 Deterministic Sensitivity Analysis on Transmission Probability Values

Figures 2.2(a) and 2.2(b) plot each strategy’s ICER over the questionnaire ($ICER_{Q_j}$) versus transmission probability from actively infected donors for donor-only scenarios (Scenario 1-Low and Scenario 1-High; Table 2.3). The only difference between Scenario 1-Low and Scenario 1-High is the value of transmission probability from donors with resolved infection, which is assumed 0.3% in Scenario 1-Low and 2.9% in Scenario 1-High. In particular, in each scenario, we only vary the transmission probability from actively infected donors (0.3-50% for Scenario 1-Low and 2.9-50% for Scenario 1-High), while keeping the transmission probability from donors with resolved infection constant (0.3% for Scenario 1-Low and 2.9% for Scenario 1-High).

When blood units from donors with resolved infection present a 0.3% transmission probability (Scenario 1-Low, Figure 2.2(a)) and the transmission probability from actively infected donors is above 3%, the universal PCR strategy is the most cost-effective in terms of ICER, followed by universal Ab, universal Ab/PCR, and the risk-targeted strategy. However, when units from donors with resolved infection present a transmission probability of 2.9% (Scenario 1-High, Figure 2.2(b)) and transmission probability from actively infected donors is below approximately 30%, universal Ab screening is the most cost-effective. Universal Ab and universal PCR strategies approach the

same ICER values at higher probabilities. The same patterns are observed for donor-recipient scenarios (Scenario 2-Low and Scenario 2-High), which assume transmission probabilities for high-risk patients are twice that for low-risk patients (Appendix A).

2.3.3 Deterministic Sensitivity Analysis on Prevalence Rates

Figure 2.2(c) plots each strategy's ICER over the questionnaire ($ICER_{Q_j}$) versus window-period donor prevalence (Ab-negative/PCR-positive donors) for Scenario 1, in which the transmission probabilities equal 2.9% for donors with resolved infections and 33.3% for actively infected donors. The universal PCR strategy is the most cost-effective for all window-period donor prevalence values, followed by universal Ab. The risk-targeted strategy is the least cost-effective.

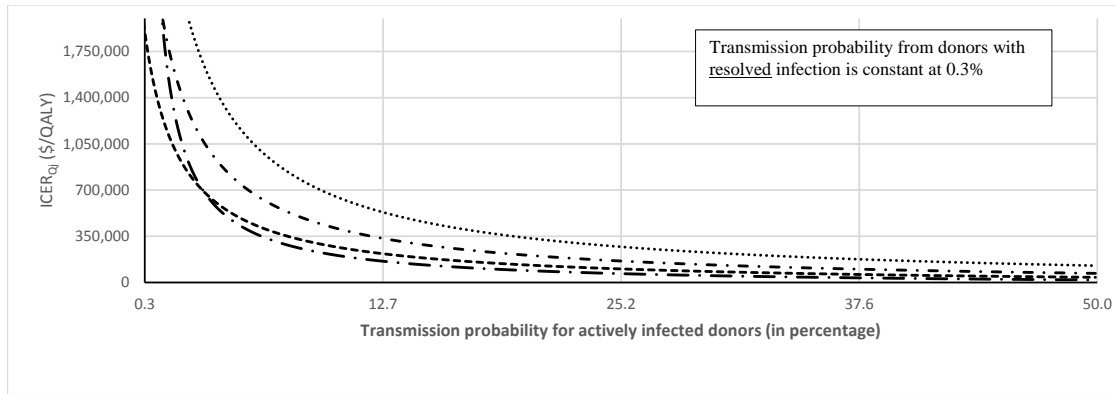
The sensitivity of ICER for universal PCR, universal Ab/PCR, and universal Ab to various prevalence values are shown in Figures 2.3(a)-(c) for Scenario 1, where the range of ICER is plotted for each strategy as the prevalence values are varied within their sensitivity ranges (Table 2.1). ICER for universal PCR and universal Ab/PCR are the least sensitive to prevalence of donors with resolved infection, while ICER for universal Ab is the least sensitive to window-period donor prevalence. Under all universal strategies, ICER is the most sensitive to the prevalence of actively infected donors, with respective ranges of [\$30,000-\$57,000/QALY], [\$90,000-\$147,000/QALY], and [\$51,000-\$96,000/QALY] for universal PCR, universal Ab/PCR, and universal Ab. For Scenario 2, not shown, the ICER ranges are respectively [\$15,000-\$36,000/QALY], [\$60,000-\$102,000/QALY], and [\$31,000-\$64,000/QALY].

2.3.4 Probabilistic Sensitivity Analysis on Key Model Inputs

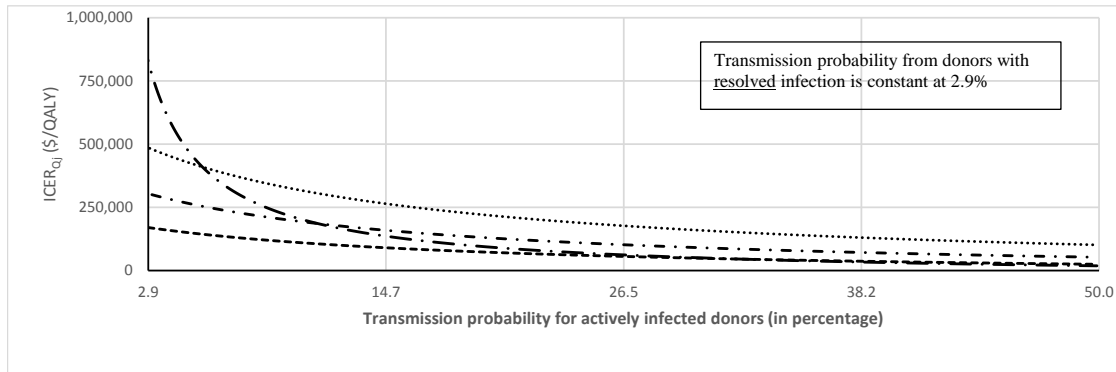
The average for each output measure over 10,000 replications shows that the expected number of TTB cases averted was highest in all cases with universal Ab/PCR, ranging from 31-41 cases pht, depending on the scenario (Appendix A). The risk-targeted strategy resulted in the fewest TTB cases averted (9-18 cases pht). The ICER over the questionnaire for both scenarios are the lowest for universal PCR, followed by universal Ab strategy. Universal PCR strategy presents lower total costs/unit transfused than universal Ab or universal Ab/PCR strategies under both scenarios.

Considering a cost-effectiveness threshold of \$1 million/QALY, the implicit threshold of society's willingness to pay for transfusion-transmitted infectious agent mitigation, Figures 2.4(a) and 2.4(b), which respectively correspond to Scenario 1 and Scenario 2, indicate that universal PCR was the preferred strategy in 85% of the 10,000 simulations, while universal Ab was preferred in the

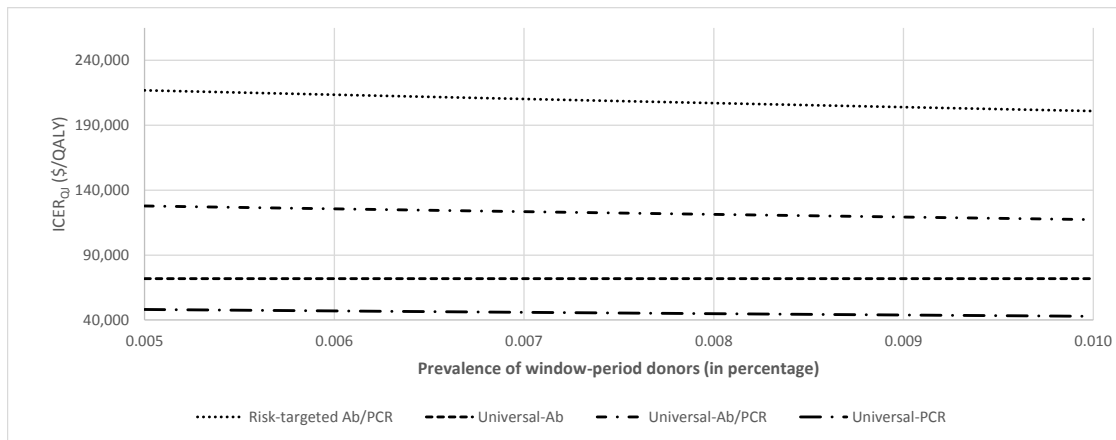
remaining 15%. The same proportions continue to hold at a threshold of \$100,000/QALY cited by Simon [99]. At a lower cost-effectiveness threshold of \$50,000/QALY cited by Goodell [53], any laboratory-based screening was preferred over the status quo in 6% of the simulations for Scenario 1 and in 98% of the simulations for Scenario 2; universal PCR in 58% of the simulations for Scenario 1 and in 83% for Scenario 2; and universal Ab in 9% of the simulations for Scenario 1 and in 15% for Scenario 2.



(a)

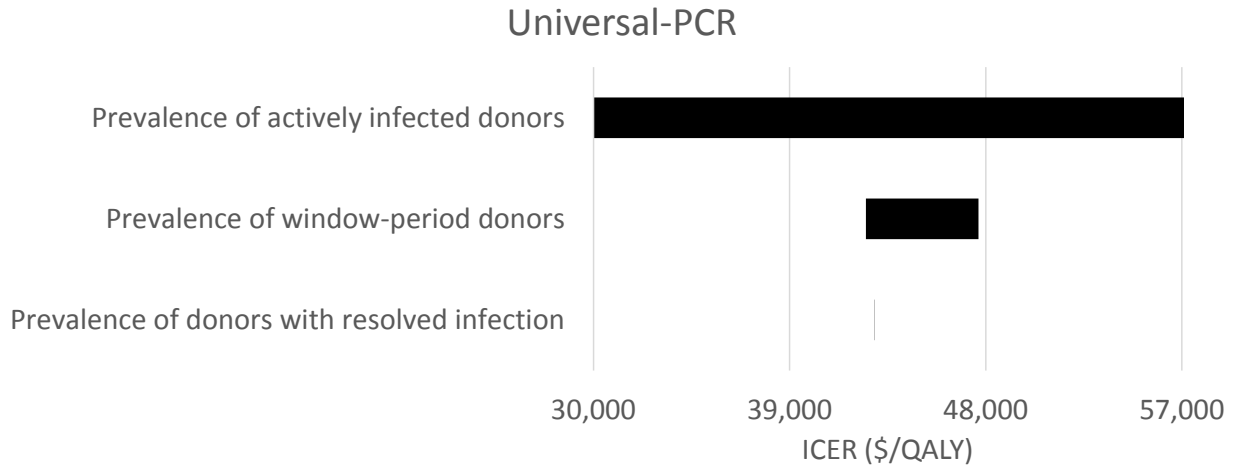


(b)

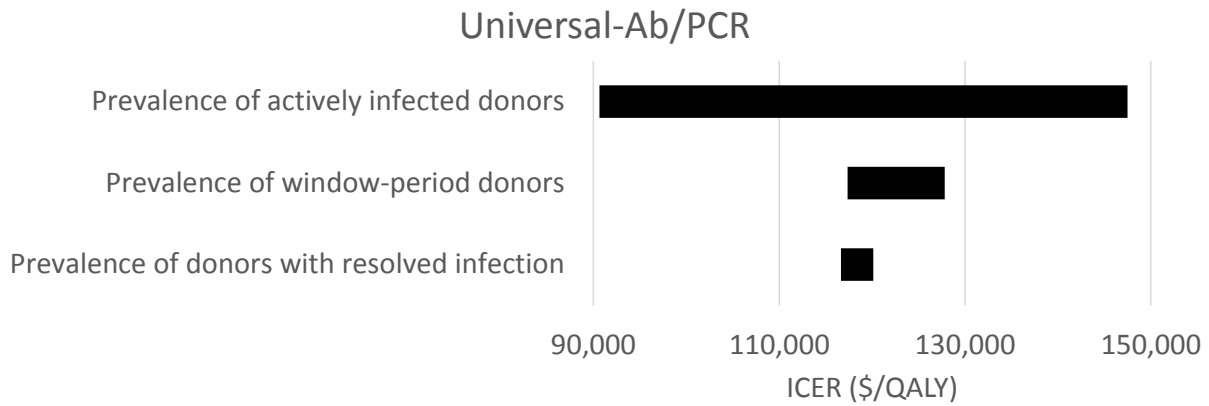


(c)

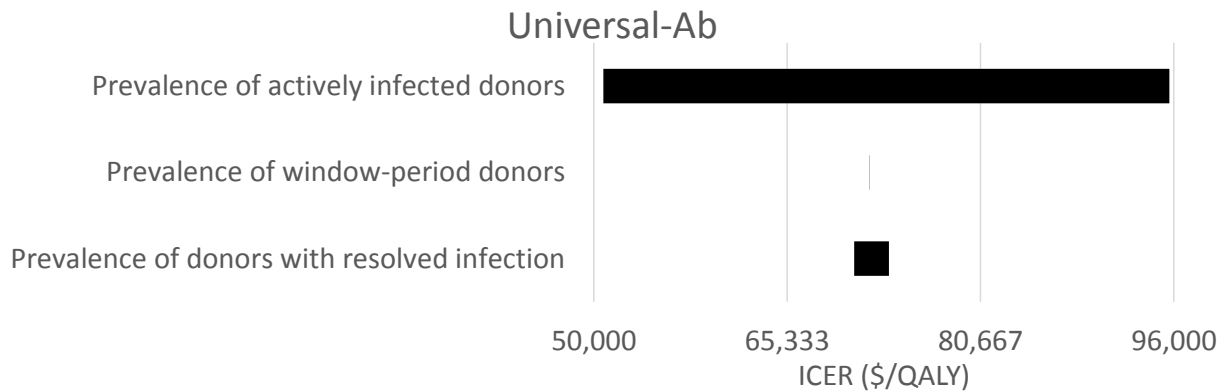
Figure 2.2: (a) $ICER_{Q_j}$ as a function of transmission probability from actively infected donors for Scenario 1-Low (donor-only scenario in which blood units from donors with resolved infection present a transmission probability of 0.3%). (b) $ICER_{Q_j}$ as a function of transmission probability from actively infected donors for Scenario 1-High (donor-only scenario in which blood units from donors with resolved infection present a transmission probability of 2.9%). (c) $ICER_{Q_j}$ as a function of the prevalence of window-period donors (donors who are Ab-negative/PCR-positive) for Scenario 1 (donor-only scenario in which blood units from donors with resolved infection present a transmission probability of 2.9% and blood units from actively infected donors present a transmission probability of 33.3%)



(a)

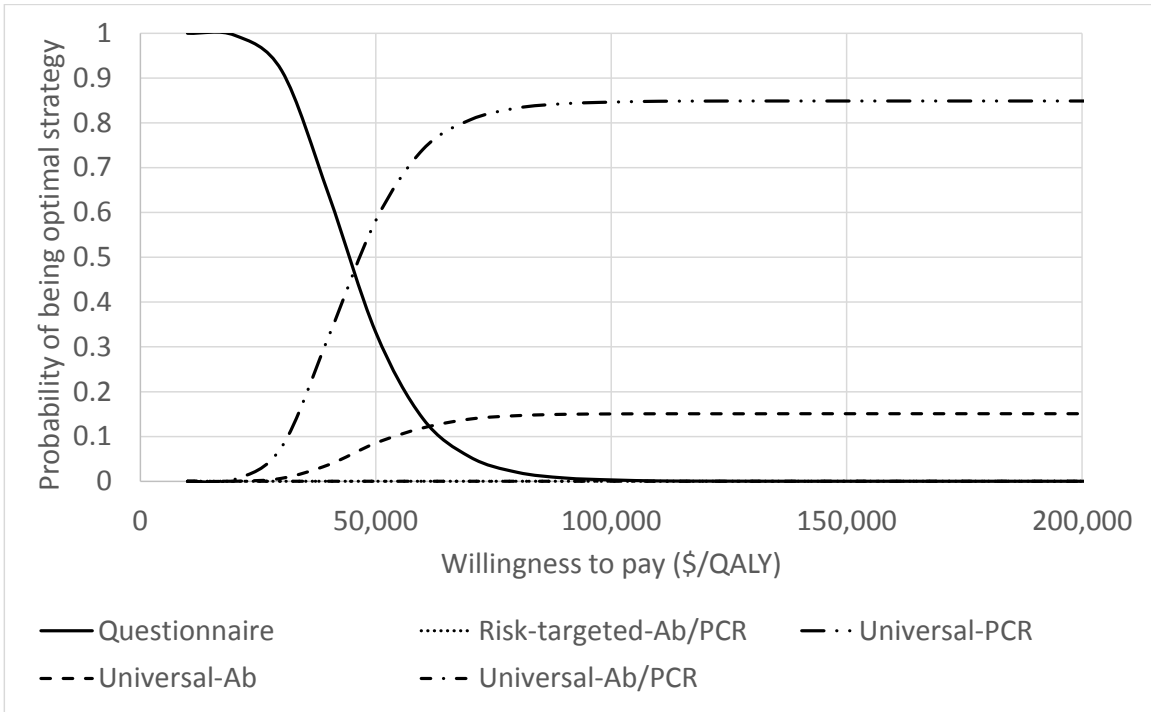


(b)

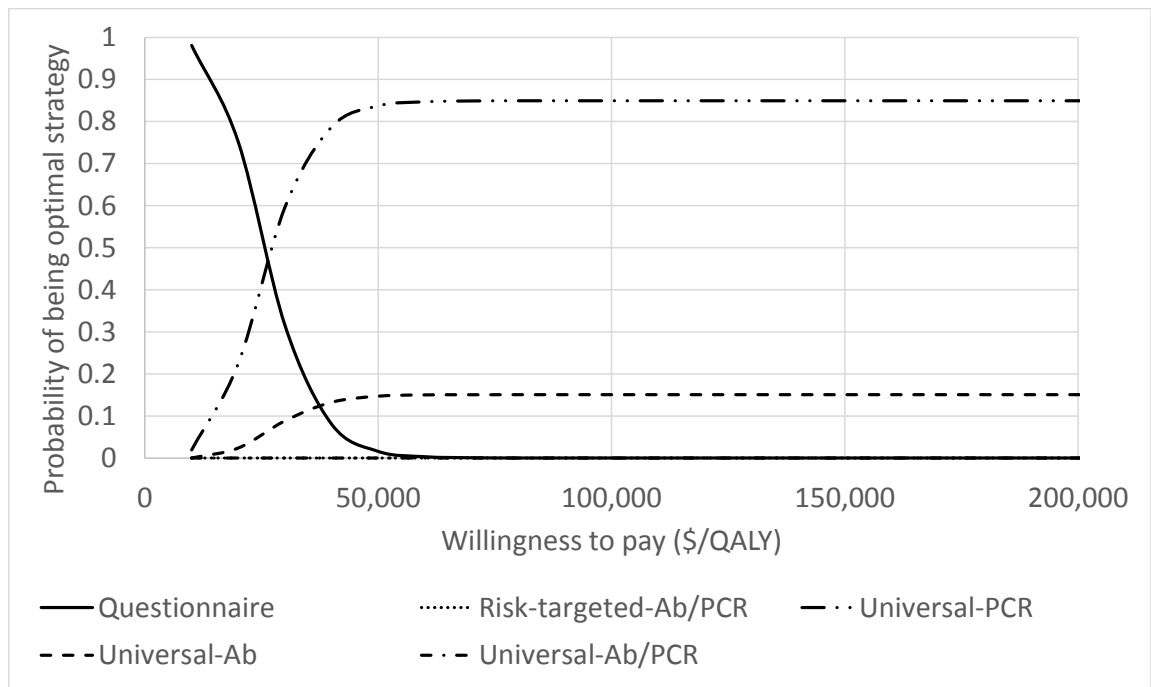


(c)

Figure 2.3: Tornado diagram showing the sensitivity of the model to prevalence values and their effect on ICER for (a) universal PCR strategy, (b) universal Ab/PCR strategy, (c) universal Ab strategy.



(a)



(b)

Figure 2.4: Cost-effectiveness acceptability curve showing the probability that each screening strategy is the most cost-effective at each willingness-to-pay value for (a) Scenario 1 (donor-only scenario), (b) Scenario 2 (donor-recipient scenario).

2.4 Discussion

B. microti is a transfusion-transmitted intraerythrocytic parasite; however, no blood donation screening requirements exist. Using prevalence and test performance data collected from ARC's investigational screening, along with published parameters, we conducted cost-effectiveness modeling on four proposed *B. microti* donation screening strategies: Ab-only, PCR-only, Ab/PCR in parallel, and recipient-risk-targeted-Ab/PCR.

The base case model determined that universal Ab/PCR is the most effective in preventing TTB. This strategy, however, was also the most costly, although ICER_{Qj} values of \$82,756/QALY-Scenario 1 and \$54,206/QALY-Scenario 2 (Table 2.4) are below the \$1 million/QALY threshold. Universal PCR was the most cost-effective: \$25,801-43,931/QALY, depending on recipient risk, and lower than the \$50,000/QALY threshold cited by Goodell [53]. The number of units wasted pht was highest with the current donor history question (99.62 pht), followed by risk-targeted-Ab/PCR (76.27 pht), with universal Ab/PCR being equal to universal Ab (19.92 pht). Universal PCR wasted zero units pht (Table 2.5).

Similar to the findings in Simon and Goodell [53, 99], our deterministic sensitivity analysis suggests that the cost-effectiveness of screening is highly sensitive to the probability of *B. microti* transmission to a recipient. When the probability of transmission to a high-risk and low-risk patient are equal and transmission probability from a donor with a resolved infection is 0.3%, universal Ab screening is most cost-effective when transmission probability from actively-infected donors is low ($\leq 3\%$). However, at higher transmission probabilities from actively-infected donors ($> 3\%$), which is more likely, the ICER (\$/QALY) drops dramatically and universal PCR is the most cost-effective (Figure 2.2(a)). However, when donors with resolved infection present a transmission probability of 2.9%, universal Ab screening is the most cost-effective until transmission probability from actively infected donors reaches $\sim 30\%$, at which point universal Ab and universal PCR achieve the same cost-effectiveness (Figure 2.2(b)).

Our model results differ from those of Simon where universal Ab screening in endemic areas was shown to avert the most TTB cases while carrying an ICER of less than \$1 million/QALY. Goodell [53] concluded that none of the screening strategies they considered was cost-effective at the \$1 million threshold, even within highly endemic areas. The lowest ICER value in their model, \$2.6 million, was for an Ab-only strategy in four endemic states.

These differences are likely due to several factors (Tables 2.1 and 2.2 compare the data and

assumptions used here versus prior studies [53, 99]). The ARC has been using investigational AFIA and PCR, not assessed in prior manuscripts. Many differences (such as different assay performance characteristics and other variables), exist that, while individually may play a small role, are unlikely the sole reason for the discrepant findings amongst the three studies. Our testing costs (\$12.50 for Ab or PCR, and \$25.00 for Ab/PCR) are lower than those used in Simon (\$15.00 for Ab and \$30.00 for Ab/PCR) and Goodell [53] (\$21.00 for manual-IFA and \$22.50 for PCR), which have a substantial impact on cost-effectiveness and make our strategies more favorable. The testing cost we used for risk-targeted-Ab/PCR (\$50.00) is higher than the \$33.00 used by Simon [99], but was validated in our prospective testing experience. It would be expected that testing costs will decrease with test licensure and greater economies of scale associated with adoption.

As noted above, all three models are sensitive to transmission probability variation. Simon did not differentiate infectivity between PCR-positive and PCR-negative units in their base case and used an overall transmission probability of 0.4% [99]. Goodell used weighted transmission probabilities (5.1% for PCR-positive and 0.4% for PCR-negative/Ab-positive donors; Tables 2.1 and 2.2) that were lower than those used in our modeling (33.3% for PCR-positive donors and 2.9% for PCR-negative/Ab-positive donors) [53]. According to hamster infectivity data collected as part of the ARC investigational study, 58% of PCR-positive donors and 6% of PCR-negative/Ab-positive donors provided donations that were infectious to hamsters [82], suggesting that transmissibility is higher than assumed in Goodell [53]. There are limitations when comparing animal models to humans; refining transmission probability estimates is necessary.

Finally, our study uses the same case fatality rates from complicated babesiosis (21% for high-risk patients and 6% for low-risk patients) as Simon, which are higher than those used by Goodell for high-risk recipients (19.2%). As with lower transmission probabilities, lower fatality rates result in lower testing cost benefits, and therefore decreased cost-effectiveness.

Screening blood units that are designated for high-risk patients (i.e., risk-targeted) has been proposed to decrease the monetary burden associated with screening [53, 99, 120]. This strategy has many limitations, including difficulty in correctly defining and identifying high-risk patients, additional resources/logistics associated with testing and maintaining two blood product inventories, and resultant increased potential for errors, as well as the liability assumed when transfusing patients who are deemed low-risk with untested, infectious units [85]. Simon considered this strategy when modeling cost-effectiveness and concluded that “risk-targeted transfusion policy for TTB prevention in endemic regions is unlikely to offer greater value compared to universal Ab screen-

ing” [99]. Our analyses likewise suggest that a risk-targeted strategy performs poorly; it resulted in the lowest number of TTB cases averted and the highest ICER values compared to the status quo, regardless of transmission probability scenario, and was never the most cost-effective strategy (Table 2.4; Figures 2.2(a)-(c)). Given the substantial limitations and poor cost-effectiveness, a risk-targeted strategy should not be considered a viable TTB intervention.

A major advantage to our model is the fact that it uses parameters based on blood donation screening data (i.e., ARC’s prospective investigational studies), rather than clinical data. Data collected in a screening environment has the advantage of using results and drawing conclusions that are more generalizable to the blood industry and removes the uncertainty present in prior publications. Our analyses also include a detailed description of waste associated with screening, accounting for the number of disposed units and positive test-result costs. Such parameters are important for assessing cost-effectiveness.

Our analysis is not without limitations. We only considered donors presenting to drives in four endemic states when building our model; using this strategy, TTB cases would continue to occur in other areas of the country, as shown by the ARC [82, 83]. The inclusion of other endemic states would have an unknown impact on cost-effectiveness, particularly due to variations in prevalence among the remaining Babesia-endemic states. Finally, as noted in both Simon and Goodell [53, 99], compared to other transfusion-transmissible agents, empirical data for *B. microti*, particularly regarding transmissibility and mortality, are lacking, thus introducing variability into any modeling effort.

Not only did we find that the cost of universal screening using any of the screening methods assessed was less than the \$1 million/QALY threshold, our analyses of waste suggest that the current method of screening by questionnaire is not only ineffective, but is also highly wasteful (i.e., the number of blood units wasted due to donor deferral pht was higher than any screening strategy). This finding serves as a reminder that improved *B. microti* mitigation strategies are needed to reduce/prevent TTB and replace ineffective policies.

In conclusion, while the lack of robust data makes cost-effectiveness modeling an inexact science and highly sensitive to variations in transmission probabilities, we suggest that universal PCR in four endemic states is an effective blood donation screening strategy. Accordingly, such a strategy would prevent 24-31 TTB cases pht at an ICER of \$26,000-44,000/QALY and a waste index of zero (Tables 2.4 and 2.5). Universal PCR offers the dual benefits of identifying and removing the most infectious blood products from the blood supply, as well as mitigating donor loss due to resolved

(Ab-positive/PCR-negative) *B. microti* infections. Using a higher cost-effectiveness threshold, the universal Ab/PCR strategy is the most effective blood donation screening strategy, as this would prevent 33-42 TTb cases pht at an ICER of \$54,000-83,000/QALY, and a waste index of 0.05.

Chapter 3

Robust Post-donation Blood Screening under Prevalence Rate Uncertainty

3.1 Introduction

Blood products are essential for a variety of medical treatments that apply to people of all ages, including organ transplants, heart surgeries, resuscitation of trauma victims; and treatment of cancer patients, premature infants, and pregnant women with complications, among others. Consequently, the availability and safety of blood is of utmost importance for a well-functioning healthcare system, hence, for the well-being of the society. Unfortunately, various infectious diseases can be transmitted through the use of blood products, including the human immunodeficiency virus (HIV), hepatitis viruses, human T-cell lymphotropic virus (HTLV), syphilis, West Nile virus (WNV), babesiosis, Chagas' disease, Dengue virus; and new infections can be expected (e.g., the Dengue virus was discovered to be transmittable through transfusion only in 2002 [68]). Consequently, post-donation screening of the blood for transfusion-transmittable infections (TTIs) is essential before the blood can be released for transfusion.

Several characteristics complicate the goal of providing safe blood: **(1)** the demand for blood products is high worldwide,¹ and blood products are highly perishable (e.g., the life-time of red

¹ It is estimated that 40-70% of the US population will need blood transfusion at some point in their lives [58]. The scarcity and safety of blood supply is a much bigger problem in certain parts of the world, e.g., sub-Saharan Africa [76].

blood cells is 21 days). Therefore, a well-functioning healthcare system requires a high and constant flow of donations, leading to a high testing cost, while healthcare resources are limited; **(2)** multiple Food and Drug Administration (FDA)-licensed blood screening tests are available for blood collection centers to choose from, and all screening tests are imperfectly reliable and come with different costs because they measure different markers in the body (e.g., antibodies, antigens, genetic material); and **(3)** the FDA requires blood collection centers to screen for a given set of infections, but remains silent on which particular tests should be used. Therefore, it is an important societal service to design an effective and efficient blood screening scheme that reduces the risk of TTIs in a resource-constrained setting.

What makes this decision even more challenging is the fact that infection prevalence rates in the donor population are highly uncertain. For emerging infections, such as babesiosis and WNV, not much is known on their dynamics and prevalence rates. Babesiosis and WNV are also highly seasonal and endemic only in certain regions, and their prevalence rates in any given year can vary significantly depending on various factors, including the climate and the intensity of the mosquito and tick populations [5, 59, 73, 84, 100]. Consequently, for such infections, it is practically very difficult to obtain accurate estimates of current prevalence rates. In addition, the uncertainty for established infections remains high even in countries with well-functioning surveillance systems (e.g., the HIV prevalence in the United States has a range of [0.5% – 1%], with a estimated mean of 0.7% [106], with the range corresponding to 71% of its mean prevalence rate). This is because surveillance methods (e.g., population-based studies, sero-prevalence surveys, sentinel surveillances) are resource- and time-extensive, and often study, due to data availability and resource limitations, sub-populations whose prevalence rates may be significantly different from the prevalence rates of the donor population [11, 34, 39, 55, 111].² Further, some infections go undiagnosed or under-reported. On the other hand, it is difficult to change the testing scheme in the short-term (e.g., on a yearly basis) due to the huge set up involved with the new testing equipment, testing protocol, and contracts with testing laboratories.

In this setting, the budget-constrained blood collection center needs to allocate its testing budget to the various infections under uncertainty on prevalence rates and with limited information (i.e., unknown prevalence distribution and moments). The objective is to determine a “robust” post-donation blood screening scheme that performs well under most prevalence rate possibilities, in

² Major blood collection centers, such as the American Red Cross, complement these surveillance studies with analysis of their own screening data of repeat donors, adjusting up the repeat donor prevalence rate by a certain factor to approximate that in first-time donors, further adding to the level of uncertainty (e.g., [65]).

terms of achieving a low TTI risk in blood cleared for transfusion (“*Residual Risk*”). This is the research problem we study in this paper.

The transfusion literature approaches this problem through simple cost-effectiveness studies, which consider only the expectation of the *Residual Risk* and fail to account for dependencies among the different infections (e.g., common resource constraints). Further, these studies rely on various restrictive assumptions, including that interventions are perfectly divisible, have constant returns to scale, and are independent [30, 40, 65, 96, 109]. In our previous research, we study the testing problem within an optimization framework that can alleviate most of these limitations, but still with the objective of minimizing the expected *Residual Risk* [24, 26, 118]. In this paper, we expand upon this earlier work to study robust post-donation blood screening schemes, explicitly accounting for the fact that prevalence rates in the donor population are uncertain and the decision-maker has limited information.

Our contributions are summarized as follows. To our knowledge, this is the first paper that models and studies the robust post-donation blood screening problem under prevalence rate uncertainty. We formulate the blood screening problem using a robust formulation as well as an expectation-based formulation, and obtain structural properties of their optimal solutions. Our analysis of the robust formulation also contributes to the literature on the robust nonlinear knapsack problem with continuous variables, for which we develop important structural properties. Further, we analytically characterize the *price of robustness* and the *price of expectation-based optimization*, which respectively represent the deviation, from the minimum possible expected *Residual Risk*, of the robust solution and the expectation-based solution under forecast error. Our analysis shows that the robust formulation leads to a safe blood supply under all prevalence rate possibilities, at the expense of a small increase in the expected *Residual Risk*. On the other hand, in the presence of forecast error, the expectation-based solution might deviate significantly from the true optimal solution, and may introduce unintended, but substantial, *Residual Risk* to the blood pool for various prevalence rate possibilities. Our case study of the United States confirms these findings, and also indicates that following the FDA guidelines is no guarantee of an optimal testing regime - sometimes it is better to deviate from the FDA recommendations. Indeed, our robust testing solution outperforms various testing schemes that follow the FDA guidelines, in terms of substantially reducing both the expectation and the range of *Residual Risk*. These findings have important implications on public policy.

The remainder of this paper is organized as follows. In Section 3.2, we introduce the notation,

decision problem, and objective functions. In Section 3.3, we study structural properties of the test selection problem under various objective functions. In Section 3.4, we analytically characterize the price of robustness and the price of expectation-based optimization. In Section 3.5, we present a case study of the United States using realistic data and discuss our findings. Finally, we conclude, in Section 3.6, with a summary of our findings and suggestions for future research. To improve the presentation, all proofs are relegated to the Appendix.

3.2 The Model

3.2.1 Notation and Assumptions

Throughout, we use boldface letters to represent vectors, and upper- and lower-case letters to respectively represent random variables and their realizations.

Let $\Psi = \{1, 2, \dots, n\}$ denote the set of infections that require (or are recommended for) screening. Let P_i , $i \in \Psi$, denote the prevalence of infection i in the donor population, which is unknown to the decision-maker. The random vector $\mathbf{P} = (P_i)_{i=1, \dots, n}$ follows an arbitrary continuous distribution with some mean $\boldsymbol{\mu} \geq \mathbf{0}$ and support (uncertainty set) $\boldsymbol{\Omega} = ([l_i, u_i])_{i=1, \dots, n}$, and may be correlated.³ We assume that the only information available to the decision-maker on \mathbf{P} is its support; neither the distribution nor the moments of \mathbf{P} are known to the decision-maker, who only has an estimate, $\hat{\boldsymbol{\mu}}$, of the mean. Indeed, it is very difficult to reliably estimate the actual distribution and mean of \mathbf{P} , especially for emerging infections. We also assume that the probability that a donor is co-infected with multiple infections in set Ψ is negligible. This assumption is common in the transfusion literature (e.g., [34, 65, 108, 115]), and is reasonable, especially in developed countries, where systematic pre-donation screening procedures make the co-infection possibility in donors extremely unlikely. The no co-infection assumption implies that $\sum_{i \in \Psi} u_i \leq 1$, which is satisfied in practice as prevalence rates of all TTIs are rather low (e.g., in the order of less than 2% in the US).

Our modeling of the uncertainty set of \mathbf{P} as a *box (interval) uncertainty set* (e.g., [17, 22]) offers several advantages in the blood screening setting. A box uncertainty set requires information only on the support of each prevalence rate; and it ensures that no prevalence realization, no matter how extreme, is discarded, thus providing a guarantee that all constraints in the robust model

³ Correlation may occur due to common risk factors for the different infections. For example, climate change may affect tick and mosquito populations in a similar way, which in turn affect prevalence of babesiosis and WNV, respectively [89, 117].

(see Section 3.2.2.1) are satisfied (see [18, 19, 20, 22] for discussion on constraint violation). This is highly desirable in blood screening, as there exist infections that can be a hit or a miss in a given year, such as the WNV, whose prevalence depends on the mosquito population. Prevalence rates of such infections may follow U-shaped distributions, with boundary points of their supports having the highest probabilities. Therefore, using uncertainty sets that discard the vertices of the box (e.g., ellipsoidal) is undesirable, as mismatches between testing schemes and actual prevalence rates lead to unnecessary infections, resulting in high social cost and suffering, and force blood centers to revise their testing schemes, leading to high set up cost. Further, we show, in Section 3.3.2, that any such adjustment to the shape of the uncertainty set is not needed in our setting, because, in the worst case, the solution to our robust model is not very conservative. Moreover, we show, in Remark 1, that utilizing a more general, *distributional uncertainty set*, which allows for known support and/or known moments [88, 97], becomes equivalent to a box uncertainty set in our setting.

The budget-constrained decision-maker needs to allocate her total testing budget per donation, of B^T , to the n infections that require screening under uncertainty on the distribution and moments of prevalence rates. Toward this end, the decision variables include B_i , $i \in \Psi$, the per-donation testing budget allocated to infection i .⁴ Let $\mathcal{F} \equiv \{\mathbf{B} : \sum_{i \in \Psi} B_i \leq B^T, B_i \geq 0, i \in \Psi\}$ denote the set of feasible allocations of the total budget B^T to the infections in set Ψ . Note that we represent a testing solution by its budget allocation vector $\mathbf{B} = (B_1, B_2, \dots, B_n)$, as the corresponding optimal test set for each infection can then be determined by solving a linear programming problem (LP) that maximizes the *sensitivity* (*true positive* probability) of the test set (see Appendix B.5). In particular, similar to [23], we consider a general class of testing schemes that we refer to as *non-universal* testing schemes, which may involve multiple test sets, each applied to a certain proportion of the donated blood units, randomly selected. That is, the decision-maker is not limited to *universal* testing schemes in which each and every unit of donated blood undergoes screening with the same test set. An example of a non-universal testing scheme is the solution to our case study (see Section 3.5): at a total budget level of \$45, \$9.4 is allocated for HIV testing per donation on average, with 90.57% of blood units (randomly selected) tested with the HIV Multi-pool Nucleic Acid Testing (MP-NAT) and the remaining 9.43% with the HIV antibody assay (Ab). Non-universal testing schemes provide the decision-maker with flexibility and have the potential to significantly

⁴ For non-universal testing schemes, B_i , $i \in \Psi$, represents the average testing budget per donation, as we discuss subsequently.

reduce the *Residual Risk*; and are equitable from a societal perspective, as blood product recipients could have blood screened by any of the test sets administered (see [23] for further discussion and examples; and Appendix B.5 for the formulation of the non-universal testing problem in our setting).

Screening tests are imperfect, and may provide inaccurate results. A major threat to blood safety comes from *false negative* testing errors, i.e., failure to detect infected blood units, which mainly occur due to donations made during the *window period*⁵ of an infection. Therefore, similar to the transfusion literature (e.g., [34, 65, 108, 115]), we assume that all testing errors come from false negative errors.⁶

Consider a random unit of donated blood. We define the following events.

Events:

- A_i+ : event that the blood unit is infected by infection i , $i \in \Psi$.
- $T_i-(B_i)$: event that the blood unit is classified as free of infection i when using a testing budget of B_i , $i \in \Psi$.

We define $T-(\mathbf{B}) \equiv \bigcap_{i \in \Psi} T_i-(B_i)$ as the event that the blood unit is classified as free of all infections in set Ψ (hence released into the blood pool reserved for transfusion). Let $f_i(B_i) \equiv Pr(T_i-(B_i)|A_i+)$ denote the false negative probability ($1 - \text{sensitivity}$) of the test set corresponding to a budget of $B_i \geq 0$ for infection $i \in \Psi$, which is decreasing in B_i . In reality, function $f_i(\cdot)$ exhibits diminishing returns to scale, as is typical of many resource allocation problems (e.g., [87]). Therefore, we make the following assumptions.

Assumption (A1). *Function $f_i(B_i) = Pr(T_i-(B_i)|A_i+)$ is strictly convex decreasing and differentiable in B_i , with $f_i(0) = 1$ and $\lim_{B_i \rightarrow +\infty} f_i(B_i) = 0$.*

Assumption (A2). *The test outcome for infection $i \in \Psi$ depends only on the prevalence of infection i in the blood unit, and not on the prevalence of other infections and/or other health conditions the donor may have.*

Note that $\lim_{B_i \rightarrow +\infty} f_i(B_i) = 0$ is a reasonable assumption, since there exists a gold-standard test, having a sensitivity of around 1, for most infections considered in this paper. Gold-standard tests, however, are used for confirmatory testing, and not for screening, due to their high costs and

⁵ The time between the development of infectious viremia and reactivity by serological or nucleic acid technology donor screening tests [34].

⁶ False positive errors, i.e., misclassification of uninfected blood units as infected, are much smaller in magnitude [47], and do not significantly impact the *Residual Risk* [26].

processing times [86, 103]. Assumption **(A2)** can be considered valid based on a number of studies that investigate the relationship between HIV and the hepatitis virus infections, and their test outcomes (e.g., [28, 92, 122]). In reality, it is extremely difficult to quantify the impact (if any) of other patient level factors on the test outcome. Hence, given the current level of medical knowledge, this assumption is considered reasonable and is commonly used in the transfusion literature.

The blood center's objective is to minimize a function of the *Residual Risk* (hereafter referred to as *Risk*) random variable, i.e., the probability that an infected blood unit is classified as infection-free by the administered test set (e.g., [26, 34, 65, 108]). The mathematical expression for *Risk* for a given budget allocation vector, $\mathbf{B} \geq \mathbf{0}$, denoted by $R(\mathbf{B})$, follows:

$$\begin{aligned}
R(\mathbf{B}) &= Pr\left(\bigcup_{i \in \Psi} A_{i+}, T-(\mathbf{B})\right) \\
&= \sum_{i \in \Psi} Pr(A_{i+}) Pr(T-(\mathbf{B}) | A_{i+}) \\
&= \sum_{i \in \Psi} P_i Pr\left(T_1-(B_1), T_2-(B_2), \dots, T_n-(B_n) | A_{1-}, \dots, A_{i+}, \dots, A_{n-}\right) \left. \vphantom{\sum_{i \in \Psi}} \right\} \begin{array}{l} \text{by the no} \\ \text{co-infection} \\ \text{assumption} \end{array} \\
&= \sum_{i \in \Psi} P_i Pr(T_i-(B_i) | A_{i+}) \prod_{\substack{j \in \Psi: \\ j \neq i}} Pr(T_j-(B_j) | A_{j-}), \quad \text{by Assumption (A2)} \\
&= \sum_{i \in \Psi} P_i f_i(B_i). \tag{3.1}
\end{aligned}$$

Thus, for a given \mathbf{B} , *Risk* can be expressed as a function of the prevalence vector, \mathbf{P} , and $f_i(B_i), i \in \Psi$, where the latter represents the reduction fraction in the original prevalence (of P_i) due to post-donation screening. Therefore, in what follows, we refer to function $f_i(\cdot)$ as the *test effectiveness function*, and denote its first-order derivative with respect to B_i as $f'_i(\cdot)$.

3.2.2 Objective Functions

The goal is to allocate the total testing budget to the infections in set Ψ so as to achieve a *robust* performance (in terms of a minimum *Risk*) under uncertainty on the prevalence vector. Toward this goal, we consider a regret-based measure commonly used for robust decision-making under uncertainty (e.g., [3, 13, 80, 88, 94, 121]), and compare its performance with the traditional objective of minimizing the expected *Risk*.

3.2.2.1 The Robust Problem: Maximum Regret Minimization

Similar to the literature, we define the *Regret* corresponding to a budget allocation vector \mathbf{B} and a prevalence vector realization \mathbf{p} as follows:

$$Regret(\mathbf{B}, \mathbf{p}) = R(\mathbf{B}, \mathbf{p}) - R(\mathbf{B}^*(\mathbf{p}), \mathbf{p}), \quad (3.2)$$

where $\mathbf{B}^*(\mathbf{p})$ is the optimal budget vector that minimizes *Risk* in the *deterministic problem* in which \mathbf{p} is given, that is, $\mathbf{B}^*(\mathbf{p}) = \underset{\mathbf{B} \in \mathcal{F}}{\operatorname{argmin}} \{R(\mathbf{B}, \mathbf{p})\}$ — the deterministic problem is a convex optimization problem that can be computed efficiently for any \mathbf{p} .

The objective is to find a feasible budget vector, \mathbf{B} , that minimizes the maximum *Regret* over all possible realizations of the random vector \mathbf{P} , that is,

$$\underset{\mathbf{B} \in \mathcal{F}}{\operatorname{minimize}} \left\{ \max_{\mathbf{p} \in \Omega} \{Regret(\mathbf{B}, \mathbf{p})\} \right\}. \quad (3.3)$$

The mathematical formulation of the *Maximum Regret Minimization Problem* follows:

Maximum Regret Minimization Problem (RMM):

$$\begin{array}{lll} \underset{\mathbf{B}, Regretmax}{\operatorname{minimize}} & Regretmax & \text{Dual variables} \\ \text{subject to} & Regret(\mathbf{B}, \mathbf{p}) \leq Regretmax, \quad \forall \mathbf{p} \in \Omega & \leftarrow \alpha_{\mathbf{p}} \end{array} \quad (3.4)$$

$$\sum_{i \in \Psi} B_i \leq B^T \quad \leftarrow \theta \quad (3.5)$$

$$B_i \geq 0, \quad \forall i \in \Psi. \quad \leftarrow \delta_i \quad (3.6)$$

Denote the optimal budget solution to **RMM** as \mathbf{B}^{*R} , with $I^{*R} = \{i \in \Psi : B_i^{*R} > 0\}$ denoting the set of infections that are allocated non-zero budget (the *allocation set*) and $Regretmax^* = \max_{\mathbf{p} \in \Omega} \{Regret(\mathbf{B}^{*R}, \mathbf{p})\}$. Let $\alpha_{\mathbf{p}}$, $\mathbf{p} \in \Omega$, θ , and δ_i , $i \in \Psi$, denote the dual variables respectively corresponding to Constraints (3.4)-(3.6) in **RMM**.

Because \mathbf{P} is a continuous random vector, the number of constraints in (3.4) is uncountable. Therefore, **RMM**, i.e., the minmax *Regret* version of a nonlinear knapsack problem with continuous variables, is a semi-infinite programming problem with a linear objective function and an uncountable number of constraints, each of which is jointly convex in the decision variable vector \mathbf{B} . Hence, in its current form, **RMM** is intractable. In general, the minmax *Regret* version of most polynomially solvable problems is NP-hard (e.g., [3, 14, 80]).

The minmax *Regret* criterion has been used for decision problems under uncertainty (e.g., [13,

50, 90, 124]), including the newsvendor problem (e.g., [88, 107]). In particular, Perakis et al. [88] study the minmax *Regret* version of the newsvendor problem under a distributional uncertainty set, which is a convex set of distributions that satisfy a number of known moments and/or support. A similar, distributionally robust, minmax *Regret* formulation in our setting becomes equivalent to the original **RMM** (i.e., with interval uncertainty), as we discuss in Remark 1. In addition, the results in [88] are specific to the newsvendor problem with a single-dimensional decision variable (the order quantity), and the analysis crucially depends on the closed-form expression for the optimal order quantity. As opposed to this, **RMM** is the *Regret* version of a nonlinear knapsack problem with a multi-dimensional decision variable vector; and hence, in general its optimal solution cannot be expressed in closed-form. Therefore, our problem necessitates new analysis that is tailored to the blood screening setting, as we discuss subsequently.

In general, robust optimization problems are solved by developing their computationally tractable counter-parts. Such robust counter-parts have been developed for certain classes of problems, including LP, quadratic programming, and semi-definite programming problems, considering specific types of uncertainty sets (e.g., [18, 19, 20, 21, 22]). Finding a computationally tractable, equivalent formulation of **RMM** critically depends on studying structural properties of the deterministic *Risk* minimization problem and of **RMM**. This involves studying how Constraint set (3.4) behaves in \mathbf{p} so that an equivalent **RMM** formulation can be constructed, and we pursue this avenue in Section 3.3.2.

3.2.2.2 The Expected Risk Minimization Problem

For an estimate, $\hat{\boldsymbol{\mu}}$, of the mean prevalence vector, the mathematical formulation of the *Expected Risk Minimization Problem* follows:

Expected Risk Minimization Problem (ERM):

$$\begin{array}{lll}
 \underset{\mathbf{B}}{\text{minimize}} & E[R(\mathbf{B}, \hat{\boldsymbol{\mu}})] = \sum_{i \in \Psi} \hat{\mu}_i f_i(B_i) & \text{Dual variables} \\
 \text{subject to} & (3.5) & \leftarrow \lambda \\
 & (3.6). & \leftarrow \gamma_i
 \end{array}$$

Let $\mathbf{B}^{*E}(\hat{\boldsymbol{\mu}})$ and $I^{*E}(\hat{\boldsymbol{\mu}}) = \{i \in \Psi : B_i^{*E}(\hat{\boldsymbol{\mu}}) > 0\}$ respectively denote the optimal budget allocation vector and the allocation set for **ERM** with a prevalence vector estimate, $\hat{\boldsymbol{\mu}}$. Also, let λ

and $\gamma_i, i \in \Psi$, denote the dual variables respectively corresponding to Constraints (3.5) and (3.6) in **ERM**. Note that the deterministic *Risk* minimization problem with a given $\mathbf{p} \in \Omega$ (see Section 3.2.2.1) corresponds to **ERM**, with $\hat{\boldsymbol{\mu}}$ replaced by \mathbf{p} .

3.3 Properties of Optimal Solutions

We provide important structural properties of **ERM** and **RMM** optimal solutions in Sections 3.3.1 and 3.3.2, respectively.

3.3.1 Structural Properties of the Optimal ERM Solution

Lemma 1. *For any $\hat{\boldsymbol{\mu}} \geq \mathbf{0}$, **ERM** objective function, $E[R(\mathbf{B}, \hat{\boldsymbol{\mu}})]$, is strictly jointly convex in \mathbf{B} . Then, a feasible budget allocation vector $\mathbf{B} \in \mathcal{F}$ is optimal for **ERM** if and only if there exist non-negative KKT multipliers λ and $\gamma_i, i \in \Psi$, such that:*

$$\hat{\mu}_i f'_i(B_i) + \lambda - \gamma_i = 0, \quad i \in \Psi \quad (3.7)$$

$$\gamma_i B_i = 0, \quad i \in \Psi. \quad (3.8)$$

Lemma 1 allows us to establish important structural properties of an optimal **ERM** solution. For this purpose, we order the infections in set Ψ in non-decreasing order of $\hat{\mu}_i f'_i(0)$ and relabel such that:

$$\hat{\mu}_1 f'_1(0) \leq \hat{\mu}_2 f'_2(0) \leq \dots \leq \hat{\mu}_n f'_n(0). \quad (3.9)$$

That is, infections are ordered according to their highest initial “return” to scale, i.e., noting that $f'_i(\cdot) < 0, i \in \Psi$, when no budget is allocated to any infection, an initial allocation to infection 1 will result in the highest reduction in the expected *Risk*, followed by infection 2, and so on. This is similar to the concept of cost-effectiveness (see, for example, [30]). In order to simplify the subsequent presentation, throughout this section we adopt the notation that infections are relabeled such that $\{1, 2, \dots, n\}$ is an ordered set following (3.9).

Theorem 1. *The optimal allocation set, $I^{*E}(\hat{\boldsymbol{\mu}})$, follows a threshold policy, that is, infections enter set $I^{*E}(\hat{\boldsymbol{\mu}})$ in the order given by (3.9) as B^T increases:*

$$I^{*E}(\hat{\boldsymbol{\mu}}) = \begin{cases} \{1, \dots, i\}, & \text{if } TH^i \leq B^T < TH^{i+1}, \text{ for } i = 1, \dots, n-1 \\ \{1, \dots, n\}, & \text{if } B^T \geq TH^n, \end{cases} \quad (3.10)$$

where $TH^1 = 0, TH^i = \sum_{j=1}^{i-1} \tilde{B}_j^i, i = 2, \dots, n$, and $\tilde{B}_j^i, j = 1, \dots, i-1$, is the solution to:

$\widehat{\mu}_j f'_j(\widehat{B}_j^i) = \widehat{\mu}_i f'_i(0)$. Further, the optimal budget allocation vector, $\mathbf{B}^{*E}(\widehat{\boldsymbol{\mu}})$, is the unique solution to:

$$\begin{aligned} \frac{f'_i(B_i^{*E}(\widehat{\boldsymbol{\mu}}))}{f'_j(B_j^{*E}(\widehat{\boldsymbol{\mu}}))} &= \frac{\widehat{\mu}_j}{\widehat{\mu}_i}, \quad \forall i, j \in I^{*E}(\widehat{\boldsymbol{\mu}}) \\ B_i^{*E}(\widehat{\boldsymbol{\mu}}) &= 0, \quad i \in \Psi \setminus I^{*E}(\widehat{\boldsymbol{\mu}}). \end{aligned} \quad (3.11)$$

Thus, finding an optimal solution to **ERM** is simple: Once set $I^{*E}(\widehat{\boldsymbol{\mu}})$ is identified for a budget level B^T , $\mathbf{B}^{*E}(\widehat{\boldsymbol{\mu}})$ is the solution to a set of nonlinear equations. The optimality condition in (3.11) indicates that the optimal non-zero budget allocation for infections in set $I^{*E}(\widehat{\boldsymbol{\mu}})$ is the one for which the incremental benefit of additional screening is equal for all infections. Similarly, the thresholds, TH^1, \dots, TH^n , in (3.10) imply that infection $i \in \Psi$ enters the allocation set $I^{*E}(\widehat{\boldsymbol{\mu}})$ only when the incremental benefit of screening for infection i equals the incremental benefit of additional screening for every infection that is already in $I^{*E}(\widehat{\boldsymbol{\mu}})$. Further, Theorem 1 indicates that the optimal **ERM** allocation set does not fluctuate much as the total testing budget, B^T , changes over time, which occurs commonly in practice. For example, if B^T increases over time, infections that are already in the allocation set will continue to be screened for, with possible addition of new infections to the allocation set. This stability is a desirable property of the optimal allocation set.

3.3.2 Structural Properties of the Optimal RMM Solution

We first derive the optimality conditions for **RMM** in Section 3.3.2.1. Then, in Section 3.3.2.2, we analyze the structural properties of the optimal **RMM** solution.

3.3.2.1 The Optimality Conditions for RMM

Recall that **RMM**, in its current form, is intractable because the number of constraints in (3.4) is uncountable. In what follows, we first reduce, without loss of optimality, the number of constraints in (3.4) to a countable set.

Definition 1. A prevalence vector realization \mathbf{p} is a boundary vector if for each $i \in \Psi$, either $p_i = l_i$ or $p_i = u_i$. Let $\Omega^b \equiv \{\mathbf{p} \in \Omega : p_i = l_i \text{ or } p_i = u_i, \forall i \in \Psi\}$.

Theorem 2. For any given $\mathbf{B} \geq \mathbf{0}$, the maximum Regret occurs at a boundary vector in set Ω^b , that is,

$$\max_{\mathbf{p} \in \Omega} \{\text{Regret}(\mathbf{B}, \mathbf{p})\} = \max_{\mathbf{p} \in \Omega^b} \{\text{Regret}(\mathbf{B}, \mathbf{p})\}.$$

Then, an equivalent **RMM** formulation follows by replacing Constraint (3.4) with (2.4’):

$$Regret(\mathbf{B}, \mathbf{p}) \leq Regretmax, \forall \mathbf{p} \in \Omega^b. \quad (2.4')$$

Thus, to solve **RMM** to optimality, it is sufficient to consider a finite set of 2^n boundary vectors. We will use this equivalent formulation of **RMM** in the remainder of the paper. In practice, the number of infections that require screening is less than ten [23]; hence, the number of constraints in (2.4’) is computationally manageable in our setting. However, from a theoretical perspective, we also discuss below the effectiveness of a polynomial-time heuristic for **RMM**.

Our numerical study of **RMM** leads to the following interesting observation: when prevalence vectors in Ω^b are arranged in non-decreasing order of their *Regret* values at the optimal **RMM** solution, \mathbf{B}^{*R} , those with the highest *Regret* values are “balanced,” with almost half of the components of \mathbf{p} at their upper bound and the remainder at their lower bound. We use this observation to develop a polynomial-time heuristic for **RMM**, which involves selecting, out of 2^n vectors in Ω^b , a subset, Ω^h , with polynomial cardinality, and solving **RMM** with Ω^b in (2.4’) replaced with Ω^h . Specifically, the **RMM** Heuristic randomly selects n^d , $d \in \mathbb{Z}_+$, vectors from the set of balanced vectors defined as $\{\mathbf{p} \in \Omega^b : \lfloor n/2 \rfloor - 1 \leq \sum_{i \in \Psi} \mathcal{I}_{(p_i = u_i)} \leq \lfloor n/2 \rfloor + 1\}$, where \mathcal{I}_{cond} denotes the indicator variable, which equals 1 if *cond* is satisfied, and 0 otherwise. Note that the total number of balanced vectors in Ω^b is $\frac{n!}{\left[\left(\frac{n-1}{2}\right)!\right]^2} \binom{4}{n+1}$ if n is odd, and $\frac{n!}{\left[\left(\frac{n}{2}\right)!\right]^2} \binom{3n+2}{n+2}$ if n is even.

To study the effectiveness of the **RMM** Heuristic, we consider two variations of it comprised of n^2 and n^3 vectors in set Ω^h , respectively. For a given n , we randomly generate 400 problem instances, comprised of $\Omega = ([l_i, u_i])_{i \in \Psi}$, \mathbf{k} , and B^T , and determine the average (over 400 instances) optimality gap between the optimal **RMM** solution and the **RMM** Heuristic solution, i.e., $\frac{Regretmax^* - Regretmax^H(n^d)}{Regretmax^*}$, see Table 3.1.

Table 3.1: Percent optimality gap for the **RMM** Heuristic with cardinality of Ω^h in the order of n^2 and n^3 , for $n = 10 - 18$.

Order	n	10	11	12	13	14	15	16	17	18
$\mathcal{O}(n^2)$		0.44	0.64	0.42	0.80	0.45	1.02	0.57	0.97	0.56
$\mathcal{O}(n^3)$		0.03	0.42	0.08	0.65	0.17	0.90	0.33	0.86	0.35

For $n = 10 - 18$, the **RMM** Heuristic results in optimality gaps that are less than 1.02% and 0.90%, respectively for $\mathcal{O}(n^2)$ and $\mathcal{O}(n^3)$. Thus, the **RMM** Heuristic performs well in our setting. Moreover, its performance can be further improved through, for example, a Benders-type

decomposition scheme in which a slave problem is solved to generate the violated constraints in the master problem, which, in turn, is solved again with augmented constraints, and so on (see, for example, [50]). In addition, the subsequent Theorem 3 provides another effective way to solve **RMM** under certain conditions.

We next provide insights on the optimal **RMM** solution under a more general form of the uncertainty set.

Remark 1. *The distributionally robust version of **RMM** is defined as (similar to [41, 88, 97]):*

$$\text{minimize } \left\{ \max_{\mathbf{B} \in \mathcal{F}} \text{Regret}(\mathbf{B}, D) = \left\{ E_D [R(\mathbf{B})] - \min_{\mathbf{Z} \in \mathcal{F}} E_D [R(\mathbf{Z})] \right\} \right\}, \quad (3.12)$$

where the random vector \mathbf{P} follows an unknown distribution that belongs to a convex set of distributions \mathcal{D} , each satisfying a set of known moments and/or support. Hence, the objective is to find a feasible budget allocation vector that minimizes the maximum Regret over all distributions in set \mathcal{D} .⁷

- (i) *If only the first moment (mean, $\boldsymbol{\mu}$) of \mathbf{P} is known, then all distributions in \mathcal{D} have the same $\boldsymbol{\mu}$ and (3.12) reduces to **ERM**, that is, $\mathbf{B}^{*R}(\boldsymbol{\mu}) = \mathbf{B}^{*E}(\boldsymbol{\mu})$.*
- (ii) *If only the support ($\boldsymbol{\Omega}$) of \mathbf{P} is known, then (3.12) reduces to **RMM**, with $R(\mathbf{B}, \mathbf{p})$ replaced by $E_D[R(\mathbf{B})]$ (see (2.4')-(3.6)), and the distribution that yields the maximum Regret is a two-point distribution with weights on the boundaries of its support, l_i and u_i , $i \in \Psi$. (This result can be proven in a similar way to Theorem 2.)*

To obtain further properties of **RMM**, note that for any given $\boldsymbol{\mu}$, we can represent, without loss of generality, the uncertainty set of P_i as $[l_i, u_i] = [\mu_i(1 - a_i^l), \mu_i(1 + a_i^u)]$, $i \in \Psi$, by finding appropriate vectors $\mathbf{a}^l = (a_i^l)_{i=1, \dots, n}$ and $\mathbf{a}^u = (a_i^u)_{i=1, \dots, n}$, for some $0 \leq a_i^l, a_i^u \leq 1$, $i = 1, \dots, n$. We refer to \mathbf{a}^l and \mathbf{a}^u as *support multiplier vectors*. Since this can be done for any $\boldsymbol{\mu}$, we do not require *a-priori* knowledge of the true mean $\boldsymbol{\mu}$, but only knowledge of the uncertainty set $\boldsymbol{\Omega}$. As it will become clear later, we choose to represent the uncertainty set $\boldsymbol{\Omega}$ using the $(\boldsymbol{\mu}, \mathbf{a}^l, \mathbf{a}^u)$ notation, as this will allow us to study structural properties of **RMM** and subsequently characterize its price of robustness in Section 3.4.

⁷ Observe that, as opposed to the definition of *Regret* in (3.2), which is defined as a function of the realizations in $\boldsymbol{\Omega}$, *Regret* is defined in (3.12) as a function of the distributions in \mathcal{D} , and hence, as a function of the expected *Risk*, as is common in literature; see for e.g., [41, 88, 97].

We label the prevalence vectors in Ω^b as $\Omega^b = \{\mathbf{p}_1, \dots, \mathbf{p}_{|\Omega^b|}\}$, where $|\Omega^b| = 2^n$, and let $\mathcal{Z} = \{1, \dots, 2^n\}$ denote the index set. Let $U_i = \{z : \mathbf{p}_z \in \Omega^b \text{ and } (\mathbf{p}_z)_i = u_i\}$, for $i \in \Psi$, that is, U_i is the index set of \mathbf{p} vectors in Ω^b for which the i^{th} component, p_i , equals its upper bound, u_i . Let $A_i \equiv 1 + a_i^u \sum_{z \in U_i} \alpha_z - a_i^l \sum_{z \in \mathcal{Z} \setminus U_i} \alpha_z$, $\forall i \in \Psi$, where α_z , $z \in \mathcal{Z}$, are the dual variables corresponding to Constraint (2.4').

Lemma 2. *A feasible budget allocation vector $\mathbf{B} \in \mathcal{F}$ and a Regretmax value are optimal for RMM if and only if there exist non-negative KKT multipliers θ , δ_i , $i \in \Psi$, and α_z , $z \in \mathcal{Z}$, such that:*

$$\mu_i f'_i(B_i) A_i - \delta_i + \theta = 0, \quad i \in \Psi \quad (3.13)$$

$$\alpha_z [\text{Regret}(\mathbf{B}, \mathbf{p}_z) - \text{Regretmax}] = 0, \quad z \in \mathcal{Z} \quad (3.14)$$

$$\delta_i B_i = 0, \quad i \in \Psi \quad (3.15)$$

$$\sum_{z \in \mathcal{Z}} \alpha_z = 1. \quad (3.16)$$

3.3.2.2 Further Properties of the Optimal RMM Solution

In order to obtain closed-form expressions for the optimal budget vector in the deterministic *Risk* minimization problem, we next impose the following assumption, which is motivated by the efficacy data for all FDA-licensed blood screening tests. In particular, we find that test effectiveness functions can be approximated reasonably well by exponential functions, resulting in coefficients of determination of $R^2 \geq 0.94$ for all infections considered in the case study (see Appendix B.5).

Assumption (A3). *The test effectiveness function, $f_i(\cdot)$, $i \in \Psi$, is exponential, i.e., $f_i(B_i) = e^{-k_i B_i}$, with some $k_i > 0$, for $B_i \geq 0$, $i \in \Psi$.*

Let $S(I) \equiv \sum_{i \in I} \frac{1}{k_i}$, for $I \subseteq \Psi$, and denote $S(\Psi)$ simply by S . We also let $c_i \equiv \frac{1/k_i}{S}$, $i \in \Psi$; then $\sum_{i \in \Psi} c_i = 1$.

Definition 2. *For any given n and \mathbf{k} , all problem instances that share common support multiplier vectors, $\mathbf{a}^l = (a_i^l)_{i=1, \dots, n}$ and $\mathbf{a}^u = (a_i^u)_{i=1, \dots, n}$, are said to be in the same “family.”*

For any given n and \mathbf{k} , we represent a problem instance by \mathbf{a}^l , \mathbf{a}^u , $\boldsymbol{\mu}$, and B^T . In the following, we are able to show that all problem instances within the same family share common properties, which we exploit in detail in the remainder of Sections 3.3.2.2 and 3.4. These properties allow us to: (i) utilize **ERM**, an easier problem to solve, to determine the optimal **RMM** solution for all

instances of the family, given the optimal **RMM** solution for any one instance of the family; and (ii) derive analytical expressions on the price of robustness ratio and the price of expectation-based optimization ratio.

To facilitate the subsequent analysis, in the remainder of Sections 3.3.2.2 and 3.4, we impose the following technical condition, which ensures that each infection is allocated some budget in the optimal solution to the deterministic *Risk* minimization problem for each $\mathbf{p} \in \Omega^b$.

Condition (C1): $B_i^*(\mathbf{p}) > 0, \forall i \in \Psi, \forall \mathbf{p} \in \Omega^b$.

We note that Condition **(C1)**, under Assumption **(A3)**, is almost always satisfied when the total testing budget, B^T , is not unrealistically low (see Section 3.5 for discussion on real data), and becomes less restrictive for higher values of \mathbf{k} (see Appendix B.3). All subsequent results of this section and Section 3.4 rely on Assumption **(A3)** and Condition **(C1)**.

Lemma 3. *For **RMM**, the optimal dual variable vector, α , corresponding to Constraint (2.4') is solely a function of the support multiplier vectors, \mathbf{a}^l and \mathbf{a}^u , and is independent of μ and B^T .*

Interestingly, Lemma 3 states that the dual variable vector α , which indicates the set of prevalence vectors that achieve the maximum *Regret* value, remains the same for the entire family of problem instances.

Theorem 3. *Consider any family of problem instances. The optimal **RMM** solution can be found by either:*

(i) *Solving a modified **ERM**, with the mean prevalence vector modified as $\mu * \mathbf{A}$, that is $\mathbf{B}^{*R}(\mu) = \mathbf{B}^{*E}(\mu * \mathbf{A})$, where $*$ denotes the component-wise vector product operator; or*

(ii) *Solving a regular **ERM**, where*

$$\mathbf{B}^{*R}(\mu) = \mathbf{B}^{*E}(\mu) + \Delta_{\mathbf{b}}^*(\mathbf{a}^l, \mathbf{a}^u), \quad (3.17)$$

where $\Delta_{\mathbf{b}}^*(\mathbf{a}^l, \mathbf{a}^u)$ is the optimal solution to:

$$\begin{aligned} & \underset{\Delta_{\mathbf{b}}}{\text{minimize}} && \sum_{i \in \Psi} \frac{A_i}{k_i} e^{-k_i \Delta_{bi}} \\ & \text{subject to} && \sum_{i \in \Psi} \Delta_{bi} = 0. \end{aligned} \quad (3.18)$$

The second part of Theorem 3 indicates that for the entire family of problem instances, their corresponding **ERM** and **RMM** optimal solutions differ by a constant vector $\Delta_{\mathbf{b}}^*(\mathbf{a}^l, \mathbf{a}^u)$, which solely depends on the support multiplier vectors, \mathbf{a}^l and \mathbf{a}^u . Note that the determination of

$\Delta_b^*(\mathbf{a}^l, \mathbf{a}^u)$ requires the knowledge of \mathbf{A} (equivalently, of $\boldsymbol{\alpha}$) for any one instance in the family. Consequently, determining the optimal **RMM** solution for all problem instances in one family (which, without Theorem 3, would require solving 2^n deterministic *Risk* minimization problems for all $\mathbf{p} \in \Omega^b$ and an additional **RMM** for each problem instance) now reduces to solving **RMM** for any one instance in the family and using **ERM** to find the optimal **RMM** solution for all other instances in the family. Finally, Theorem 9, presented in Appendix B.4, characterizes how *Regret* functions, and hence the maximum *Regret* value, shift as parameters $\boldsymbol{\mu}$ and B^T are perturbed, greatly facilitating sensitivity analyses.

3.4 The Price of Robustness and the Price of Expectation-based Optimization

RMM provides a robust solution that may be sub-optimal for minimizing the expected *Risk*. On the other hand, the **ERM** solution, by relying on an estimate, $\hat{\boldsymbol{\mu}}$, of the mean prevalence vector, $\boldsymbol{\mu}$, may also deviate from the expected *Risk* minimizing solution, $\mathbf{B}^{*E}(\boldsymbol{\mu})$. Then, an important question is whether the decision-maker would be better off using the robust formulation, **RMM**, or the expected risk minimizing formulation, **ERM**, with the estimated $\hat{\boldsymbol{\mu}}$ vector? To answer this question, we quantify the loss of optimality in the expected *Risk* coming from the **RMM** and **ERM** solutions, as well as the robustness of the **ERM** solution.

Definition 3. *The price of robustness ratio, Π^R ([18]), the price of expectation-based optimization ratio, $\Pi^E(\hat{\boldsymbol{\mu}})$, and the **ERM** Regret deviation, \mathcal{R} , are respectively defined as:*

$$\Pi^R = \frac{E[R(\mathbf{B}^{*R}, \boldsymbol{\mu})]}{E[R(\mathbf{B}^{*E}(\boldsymbol{\mu}), \boldsymbol{\mu})]}, \quad \Pi^E(\hat{\boldsymbol{\mu}}) = \frac{E[R(\mathbf{B}^{*E}(\hat{\boldsymbol{\mu}}), \boldsymbol{\mu})]}{E[R(\mathbf{B}^{*E}(\boldsymbol{\mu}), \boldsymbol{\mu})]}, \quad \text{and} \quad \mathcal{R} = \max_{\mathbf{p} \in \Omega} \left\{ \frac{\text{Regret}(\mathbf{B}^{*E}(\boldsymbol{\mu}), \mathbf{p})}{\text{Regret}(\mathbf{B}^{*R}, \mathbf{p})} \right\}.$$

Thus, higher values of Π^R and $\Pi^E(\hat{\boldsymbol{\mu}})$ respectively indicate that **RMM** and **ERM** solutions deviate further from the minimum possible expected *Risk*, while a higher value of \mathcal{R} indicates that the **ERM** solution deviates further in *Regret* from the optimal **RMM** solution. In order to study the robustness of the **ERM** solution due to prevalence uncertainty only (and not due to forecast error), we express \mathcal{R} as a function of the true mean, $\boldsymbol{\mu}$.

In the remainder of this section, we restrict our attention to cases where Condition **(C1)** and Assumption **(A3)** are satisfied. Recall that Theorem 3 indicates that in these cases the optimal **ERM** and **RMM** solutions are linked with an additive expression, which involves function

$\Delta_b^*(\mathbf{a}^l, \mathbf{a}^u)$ that remains constant within each family. Thus, Theorem 3 allows us to express $E[R(\mathbf{B}^{*R}, \boldsymbol{\mu})]$ as a function of $\mathbf{B}^{*E}(\boldsymbol{\mu})$, leading to exact expressions on Π^R and $\Pi^E(\hat{\boldsymbol{\mu}})$.

Theorem 4. *We have:*

$$\Pi^R = \sum_{i \in \Psi} c_i e^{-k_i \Delta_{bi}^*} = \frac{\sum_{i \in \Psi} c_i / A_i}{\prod_{i \in \Psi} (1/A_i)^{c_i}} \quad \text{and} \quad \Pi^E(\hat{\boldsymbol{\mu}}) = \frac{\sum_{i \in \Psi} c_i (\mu_i / \hat{\mu}_i)}{\prod_{i \in \Psi} (\mu_i / \hat{\mu}_i)^{c_i}},$$

where $\Delta_b^*(\mathbf{a}^l, \mathbf{a}^u)$ and $\mathbf{A}(\mathbf{a}^l, \mathbf{a}^u)$ are as defined in (3.18). Further,

$$\mathcal{R} \geq \mathcal{R}^L \equiv \max_{\mathbf{p} \in \Omega^b} \left\{ \frac{\sum_{i \in \Psi} c_i h_i(\mathbf{p}) - \prod_{i \in \Psi} (h_i(\mathbf{p}))^{c_i}}{\sum_{i \in \Psi} c_i h_i(\mathbf{p}) e^{-k_i \Delta_{bi}^*} - \prod_{i \in \Psi} (h_i(\mathbf{p}))^{c_i}} \right\},$$

$$\text{where, for } \mathbf{p} \in \Omega^b, h_i(\mathbf{p}) \equiv \begin{cases} 1 - a_i^l, & \text{if } p_i = l_i \\ 1 + a_i^u, & \text{if } p_i = u_i \end{cases}, \quad \forall i \in \Psi.$$

Interestingly, both Π^R and $\Pi^E(\hat{\boldsymbol{\mu}})$ can be expressed as ratios of the weighted arithmetic mean to the weighted geometric mean, with weights \mathbf{c} , of $1/A_i$, and $\mu_i/\hat{\mu}_i$, $i \in \Psi$, respectively. This follows due to the equivalence between **ERM** and **RMM** solutions, stated in Theorem 3.

Corollary 1. Π^R and \mathcal{R}^L remain constant for all problem instances of the same family.

Lemma 4. *If the mean prevalence estimate, $\hat{\boldsymbol{\mu}}$, has a forecast error $(\mathbf{r}^l, \mathbf{r}^u)$, i.e., $\mu_i \in [\hat{\mu}_i(1 - r_i^l), \hat{\mu}_i(1 + r_i^u)]$, $i \in \Psi$, then $\Pi^E(\hat{\boldsymbol{\mu}})$ is maximized when $\mu_i = \hat{\mu}_i(1 - r_i^l)$ or $\mu_i = \hat{\mu}_i(1 + r_i^u)$, for all $i \in \Psi$.*

As Theorem 4 and Lemma 4 show, the price of robustness ratio, Π^R , and the lower bound on the **ERM Regret** deviation, \mathcal{R}^L , are independent of the mean prevalence vector, $\boldsymbol{\mu}$, and the total budget, B^T , and only depend on the support multiplier vectors, \mathbf{a}^l and \mathbf{a}^u , while $\Pi^E(\hat{\boldsymbol{\mu}})$ only depends on the magnitude of the forecast error, \mathbf{r}^l and \mathbf{r}^u . These results greatly facilitate the derivation of the maximum values of Π^R , $\Pi^E(\hat{\boldsymbol{\mu}})$, and \mathcal{R}^L by reducing the search over \mathbf{k} , $\boldsymbol{\mu}$, B^T , \mathbf{a}^l , \mathbf{a}^u , and \mathbf{r} to a search over \mathbf{k} , \mathbf{a}^l , \mathbf{a}^u , and \mathbf{r} only.

We next utilize Theorem 4 and Lemma 4 to compute Π^R , $\Pi^E(\hat{\boldsymbol{\mu}})$, and \mathcal{R}^L for problem instances having $n = 2 - 10$ infections, see Table 3.2. Specifically, we discretize \mathbf{k} , \mathbf{a}^l , and \mathbf{a}^u , and perform an exhaustive search in $a_i^l \in [0, 0.75]$ and $a_i^u \in [0, 2.00]$, $i \in \Psi$,⁸ to determine the maximum values of Π^R and \mathcal{R}^L for each n . We also determine the maximum value of $\Pi^E(\hat{\boldsymbol{\mu}})$ at various levels of

⁸ The maximum allowable value for a_i^l is 1 since $\mu_i(1 - a_i^l) \geq 0$, while a_i^u can take values higher than 1 if $\mu_i < 0.5$.

forecast error, considering $r_i^l = r_i^u = r$, $i \in \Psi$, with $r = 10\%$, 35% , and 50% . Table 3.2 indicates that the expected *Risk* of all **RMM** solutions deviates by no more than 6.64% from the minimum possible expected *Risk* (i.e., **ERM** solution with known μ). On the other hand, **ERM** solutions may deviate significantly (by more than 105.39%) from the minimum possible *Regret* value. Further, under forecast error, **ERM** expected *Risk* may deviate from the minimum possible expected *Risk* by around 0.50%, 6%, and 15% for all n values, for $r = 10\%$, 35% , and 50% , respectively.

The estimation of the mean prevalence vector is resource- and time-consuming, and in practice, r can be higher than 50% [6], resulting in $\Pi^E(\hat{\mu})$ values that are significantly higher than Π^R . This has important implications: For realistic values of the forecast error, r , **RMM** outperforms **ERM** not only in terms of the *Regret* objective, but also in terms of the expected *Risk*, suggesting that **RMM** would be a safer approach to use. In addition, for all values of r , **ERM** exhibits significantly higher *Regret* values, further emphasizing the importance of using a robust approach. Finally, the values of Π^R , $\Pi^E(\hat{\mu})$, and \mathcal{R}^L , do not fluctuate significantly with n , indicating that **RMM** outperforms **ERM** independently of the number of infections.

From a theoretical perspective, the next question is whether there exists a family of problem instances for which the price of robustness ratio equals one.

Corollary 2. *Under Condition (C1) and Assumption (A3), $\Pi^R = 1$, equivalently, $\mathbf{B}^{*R} = \mathbf{B}^{*E}(\mu)$, for any family of problem instances with identical test effectiveness functions, symmetric uncertainty sets, and identical support multiplier vectors, i.e., $\mathbf{k} = (k, \dots, k)$ for some $k > 0$, and $\mathbf{a}^l = \mathbf{a}^u = (a, \dots, a)$, for some $a \in [0, 1]$.*

Table 3.2: Maximum values of Π^R , $\Pi^E(\hat{\mu})$, and \mathcal{R}^L for all problem instances with $n = 2 - 10$ infections, and forecast error $r = 10\%$, 35% , and 50% .

n	$\Pi^E(\hat{\mu})$			Π^R	\mathcal{R}^L
	$r = 10\%$	$r = 35\%$	$r = 50\%$		
2	0.48%	6.55%	15.32%	6.64%	105.39%
3	0.48%	6.72%	15.79%	6.49%	146.78%
4	0.50%	6.72%	15.79%	6.32%	140.62%
5	0.50%	6.83%	15.92%	6.24%	150.02%
6	0.50%	6.82%	15.92%	6.17%	148.90%
7	0.50%	6.84%	15.97%	6.19%	152.77%
8	0.50%	6.84%	15.98%	6.16%	155.00%
9	0.50%	6.85%	15.98%	6.16%	158.61%
10	0.50%	6.85%	15.99%	6.16%	163.25%

3.5 A Case Study of the United States

In this section, we perform a case study for the United States. Our objectives are three-fold: (i) to compare the optimization-based testing schemes with FDA-compliant schemes; (ii) to compare **ERM** and **RMM** testing schemes; and (iii) to derive the price of robustness ratio for **RMM**.

The FDA requires screening of donated blood for HIV, hepatitis viruses B and C (HBV and HCV), HTLV, and syphilis; recommends testing for WNV; and neither requires nor recommends testing for babesiosis [47]. In our case study, we consider HIV, HBV, HCV, WNV, and babesiosis. (Syphilis and HTLV are omitted due to a lack of reliable data.)

3.5.1 Case Study Data

Table 3.3 presents the prevalence in the United States for the infections considered in our study. The uncertainty sets were constructed from published lower and upper bounds on prevalence rates. Additional information on the data is provided in Appendix B.5.1. In order to focus on the robustness of **ERM** and not on the forecast error, we assume that the mean prevalence rates presented in Table 3.3 are the true means.

Table 3.3: Mean and uncertainty sets for prevalence rates in the United States (in %).

<i>Infection</i>	<i>Mean (%)</i>	<i>Uncertainty set(%)</i>	<i>Source</i>
HIV	0.7	(0.5, 1.0)	[106]
HBV	0.345	(0.250, 0.440)	[38]
HCV	1.6	(1.3, 1.9)	[10]
Babesiosis	0.385	(0.255, 0.490)	[25, 84]
WNV	0.0495	(0.0044, 0.1500)	[33, 100]

Screening tests typically look for an infection specific bio-marker. In blood screening, tests are either serological, which look for antibody (Ab) or antigen (Ag) bio-markers, or genetic nucleic acids tests (NAT), which look for infection specific nucleic acids. NAT offers higher efficacy than serological tests because the nucleic acid bio-markers directly measure the infection (e.g., viral load) and thus are at a detectable concentration earlier than antibodies or antigens, which are based on the immune response (thus NAT has a shorter window period). NAT also has pooling flexibility, thus it can be performed on individual donations (ID-NAT), or on mini-pools (MP-NAT) of samples from multiple donations, but, due to dilution, pooling reduces the test’s efficacy [16, 65, 101, 115]. Depending on the infection, pairing an antibody or an antigen test with an NAT increases the

overall sensitivity. Therefore, we consider both individual and paired tests in our study.

Specifically, FDA-licensed tests include ID-NAT, MP-NAT, and Ab/Ag for each of HIV, HBV, and HCV; and ID-NAT and MP-NAT for WNV. Currently there are no FDA-licensed tests for babesiosis, but an Ab test and an ID-NAT test are undergoing the FDA approval process and are currently used by the American Red Cross in a pilot study [84]. Therefore, we also consider the Ab and ID-NAT tests for babesiosis in our case study. Table 3.4 reports test sensitivity values, which come from published or publicly available data when available; when not available, they are derived using the methodology described in [26]. Unit testing costs are \$4 for each of HIV Ab, HCV Ab, and HBV Ag tests [65]; and \$15 and \$10 respectively for ID-NAT and MP-NAT per infection [26, 65].

Table 3.4: Sensitivity (true positive probability) values (in %).

<i>Infection</i>	<i>Single Tests</i>			<i>Paired Tests</i>	
	<i>ID-NAT</i>	<i>MP-NAT^a</i>	<i>Ab/Ag^b</i>	<i>ID-NAT+Ab/Ag</i>	<i>MP-NAT+Ab/Ag</i>
HIV	99.90 [102]	99.70 [102]	70.96	99.97 ^c	99.91 ^c
HBV	93.30 [47]	82.90 [47]	45.00 ^d	96.32 ^e	90.60 ^e
HCV	97.74 [47]	81.31 [47]	16.70 ^d	98.12 ^c	84.43 ^c
Babesiosis [25]	99.50	–	90.40	100.00 ^c	–
WNV [45]	99.98	97.50	–	–	–

^a Pool size of 16 for HIV, HBV, and HCV, and 6 for WNV.

^b Derived using the methodology in [26].

^c NAT+Ab paired test.

^d The sensitivity values are low as these tests do not perform well when used individually (e.g., [64]).

^e NAT+Ag paired test.

Given the FDA requirements and recommendations, blood centers need to devise a FDA-compliant testing scheme. For example, the American Red Cross routinely screens for HIV (MP-NAT&Ab), HBV (MP-NAT&Ag), HCV (MP-NAT&Ab), and WNV (MP-NAT) [6]. This testing scheme corresponds to a total testing budget of \$52 using the cost data given above.

3.5.2 Case Study Results

We compare our optimization results with seven FDA-compliant testing schemes. The schemes belong to one of three categories: (i) *FDA-required*, which only screens for HIV, HBV, and HCV; (ii) *FDA-required and -recommended*, which additionally screens for WNV; and (iii) *FDA-required and -recommended with babesiosis*, which screens for all five infections considered. For each of these categories, we consider the following two methods for test selection: (1) *min-cost*, which chooses

the lowest cost test for each infection, and (2) *min-risk*, which chooses the most sensitive test for each infection. Additionally, we consider another FDA-required and -recommended test scheme currently employed by some blood centers [6], which we refer to as *current*, which screens for HIV, HBV, and HCV with MP-NAT&Ab/Ag; and for WNV with MP-NAT. For each of these schemes, we evaluate the testing cost, which we use to set the various budget-levels for the optimization. We do not restrict the optimization models to FDA-compliant solutions and always allow the model to choose from screening tests for all five infections.

Table 3.5 reports the testing solution for each of the FDA-compliant schemes, along with the total budget required, the corresponding **ERM** and **RMM** solutions at that budget level, and the resulting $E[R]$ and *Regretmax* values per 100,000 donations for each solution (we assume that each donor supplies blood to a single transfusion recipient). Notice that the optimization-based solutions (**ERM** and **RMM**) perform better in terms of the expected *Risk* and *Regretmax* compared to the seven FDA-compliant schemes. For example, at $B^T = \$45$ (*FDA-required, min-risk*), **ERM** reduces the expected *Risk* from 673 to 310 TTIs per 100,000 donations, while **RMM** reduces *Regretmax** from 487 to 21, a 25-fold reduction. The fact that these significant reductions come not from a higher budget but from a better allocation of the total budget is important to note. Specifically, out of the 673 TTIs per 100,000 donations, 31 are due to HBV while 642 are due to HIV, HCV, babesiosis, and WNV combined; on the other hand, with **RMM** there are 315 TTIs per 100,000 donations, of which 87 are due to HBV (corresponding to an increase of 56), and 228 are due to HIV, HCV, babesiosis, and WNV combined (corresponding to a decrease of 414). Figure 3.1 provides a comparison between each strategy in Table 3.5 and the solution of **RMM** for budget levels between \$1 and \$75. The vertical (horizontal) distance between each point and the curve represents the reduction in cost (expected *Risk*) achieved by using **RMM**. For example, for the \$52 budget of the *current* strategy, **RMM** solution provides a 65% reduction in expected *Risk* (from 669 to 236 TTIs per 100,000 donations). Alternatively, **RMM** solution achieves the same expected *Risk* as the *current* strategy using a significantly 46% lower budget (\$28 vs. \$52). It is important to note that all the optimization-based solutions (**ERM** and **RMM**) are FDA-compliant except for $B^T = \$12$, where, due to the very limited testing budget, **RMM** and **ERM** substitute screening for HBV with screening with Babesiosis, resulting in a 16% reduction in expected *Risk* (from 1759 to 1474 TTIs per 100,000 donations).

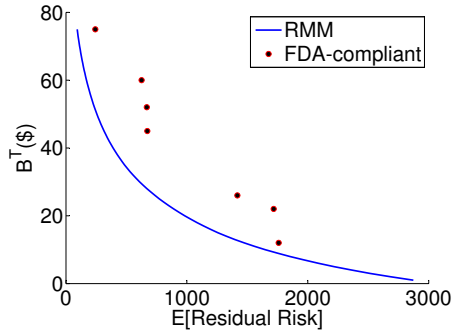


Figure 3.1: Total budget, B^T , vs. expected *Risk* (per 100,000 donations) for the **RMM** solutions and for the strategies shown in Table 3.5.

Table 3.5: Comparison of testing solutions for various categories of screening strategies (A: Antibody/Antigen, I: ID-NAT, M: MP-NAT).

Policy	B^T	Tests Selected					Objective Function Values (per 100,000 donations)			
		HIV	HBV	HCV	Babesiosis	WNV	$E[R]$	$Regret_{max}$	Π^R	\mathcal{R}^L
FDA-required										
min-cost	12	A-100%	A-100%	A-100%	-	-	1,759	413		
RMM		A-78.9%	-	M-73.8%	A-36.7%	-	1,474	32	0.01%	58.30%
ERM		A-79%	-	M-72.8%	A-39%	-	1,474	36		
min-risk	45	I-100%	I-100%	I-100%	-	-	673	487		
RMM		M-90.6%, A-9.43%	M-76.6%, A-23.4%	I-100%, A-100%	I-18.8%, A-81.2%	M-9.44%	315	21	1.62%	86.82%
ERM		M-93.5%, A-6.48%	M-81.7%, A-18.3%	I-100%, A-100%	I-21%, A-79%	-	310	34		
FDA-required and -recommended										
min-cost	22	A-100%	A-100%	A-100%	-	M-100%	1,718	1,039		
RMM		M-24.1%, A-75.9%	A-39.2%	I-37.1%, M-62.9%	A-78.2%	-	892	28	0.01%	34.89%
ERM		M-23.7%, A-76.3%	A-39.1%	I-35.8%, M-64.2%	A-80.6%	-	892	30		
current	52	M-100%, A-100%	M-100%, A-100%	M-100%, A-100%	-	M-100%	669	583		
RMM		M-100%, A-14%	I-11.4%, M-88.6%	I-100%, A-100%	I-26.5%, A-73.5%	M-17.7%	236	23	1.72%	167.35%
ERM		M-100%, A-22.2%	I-22.6%, M-77.4%	I-100%, A-100%	I-29.6%, A-70.4%	-	232	49		
min-risk	60	I-100%	I-100%	I-100%	-	I-100%	626	613		
RMM		M-100%, A-44.6%	I-57%, M-43%	I-100%, A-100%	I-34.6%, A-65.4%	M-28.8%	170	23	0.60%	99.97%
ERM		M-100%, A-51.4%	I-63.6%, M-36.4%	I-100%, A-100%	I-37.4%, A-62.6%	M-15.8%	169	40		
FDA-required and -recommended with babesiosis										
min-cost	26	A-100%	A-100%	A-100%	A-100%	M-100%	1,418	856		
RMM		M-36.3%, A-63.7%	A-71.1%	I-66.3%, M-33.7%	A-91.6%	-	736	23	0.01%	32.29%
ERM		M-35.8%, A-64.2%	A-71%	I-65%, M-35%	A-94%	-	736	24		
min-risk	75	I-100%	I-100%	I-100%	I-100%	I-100%	243	211		
RMM		I-3.34%, M-96.7%, A-100%	I-100%, A-46.4%	I-100%, A-100%	I-50.9%, A-49.1%	M-52.7%	93	19	0.06%	20.06%
ERM		I-3.73%, M-96.3%, A-100%	I-100%, A-47.7%	I-100%, A-100%	I-51.7%, A-58.3%	M-49%	93	22		

In order to further examine the various solutions, we randomly generate 10,000 realizations of the prevalence vector and evaluate, at each realization, the *Risk* and *Regret* incurred by **ERM** and **RMM** solutions at the same budget levels presented in Table 3.5. We assume, in a similar fashion to [25], that the prevalence rates of HIV, HBV, HCV, and babesiosis, each follow an independent triangular distribution with the upper bound, lower bound, and mean given in Table 3.3. We also assume that the prevalence of WNV follows a scaled and shifted U-Shaped beta distribution

with range and means presented in Table 3.3. Figure 3.2 presents *Risk* versus *Regret* (both per 100,000 donations) for total budget levels of \$45 (*FDA-required, min-risk*) and \$60 (*FDA-required, min-risk*). Notice that for all budget levels, **ERM** and **RMM** significantly outperform the FDA-compliant strategies, where the *Risk* and *Regret* values and ranges are orders of magnitude smaller. For example, from Figure 3.2(a), which corresponds to a total testing budget of \$45, the *Risk* range for the optimization-based strategies is between [200, 450] per 100,000 donations, while this range is between [500, 900] per 100,000 donations for the *FDA min-risk* policy.

Next, we focus on the differences between **ERM** and **RMM** solutions. First, it is important to note that **ERM** and **RMM** solutions differ mostly for moderate to high budget levels (\$45 to \$60 in Table 3.5). This is because when B^T is low, the number of feasible test sets are limited due to the extremely tight budget. In reality testing budgets are moderate in the United States, and it is for this case that **ERM** and **RMM** solutions differ. To give an idea on how these solutions generally differ, consider a budget level of \$45: **ERM** does not screen for WNV, while **RMM** screens 9.44% of blood units for WNV, and screens for HIV, HBV, and babesiosis with the NAT test (MP- or ID-NAT) on a lower proportion of blood units, and with the Ab/Ag test on a higher proportion of blood units than **ERM**. Thus, unlike the **ERM** solution that screens for only four infections, **RMM** screens for five infections, increasing the robustness of the solution significantly by decreasing the *Regretmax* (34 vs 21 corresponding to a 38% decrease), and at a minuscule increase in expected *Risk* (315 vs 310, corresponding to a 1.62% increase). Note that, among the budget levels presented in Table 3.5, the highest price of robustness ratio, Π^R , is 1.72%, which is incurred at a budget level of \$45. For all budget levels between \$12 and \$59, the minimum, maximum, and average values of Π^R are given by 0.0004%, 1.8150%, and 0.5504%, respectively.

In order to further study the differences between **ERM** and **RMM** solutions, we omit the FDA data points from Figures 3.2(a) and 3.2(b), and present Figures 3.2(c) and 3.2(d) for total budget levels of \$45 and \$60, respectively. Notice that for both **ERM** and **RMM**, *Risk* is bi-modal, as it takes values in either [225, 325] or [375, 450] for $B^T = \$45$ (Figure 3.2(c)) and [112, 166] or [197, 261] for $B^T = \$60$ (Figure 3.2(d)). For both budget levels, **RMM** generates *Regret* values that are less variable when compared to **ERM**, which generates *Regret* values that are significantly higher when the *Risk* values are high. Also note that the maximum *Regret* values that are incurred by **ERM** are significantly higher than **RMM**. Therefore, we see that **RMM** yields a more robust solution that: (1) generates a smaller maximum *Regret* value, and (2) a more balanced *Regret* that does not fluctuate and that is significantly lower than that of **ERM** when the *Risk* values are high. This

increase in robustness over **ERM** comes at a negligible price, where the increase in expected *Risk* is respectively 1.62% and 0.60% for \$45 and \$60, corresponding to an increase of 5 (315 vs. 310) and 1 (170 vs. 169) TTIs per 100,000 donations, respectively.

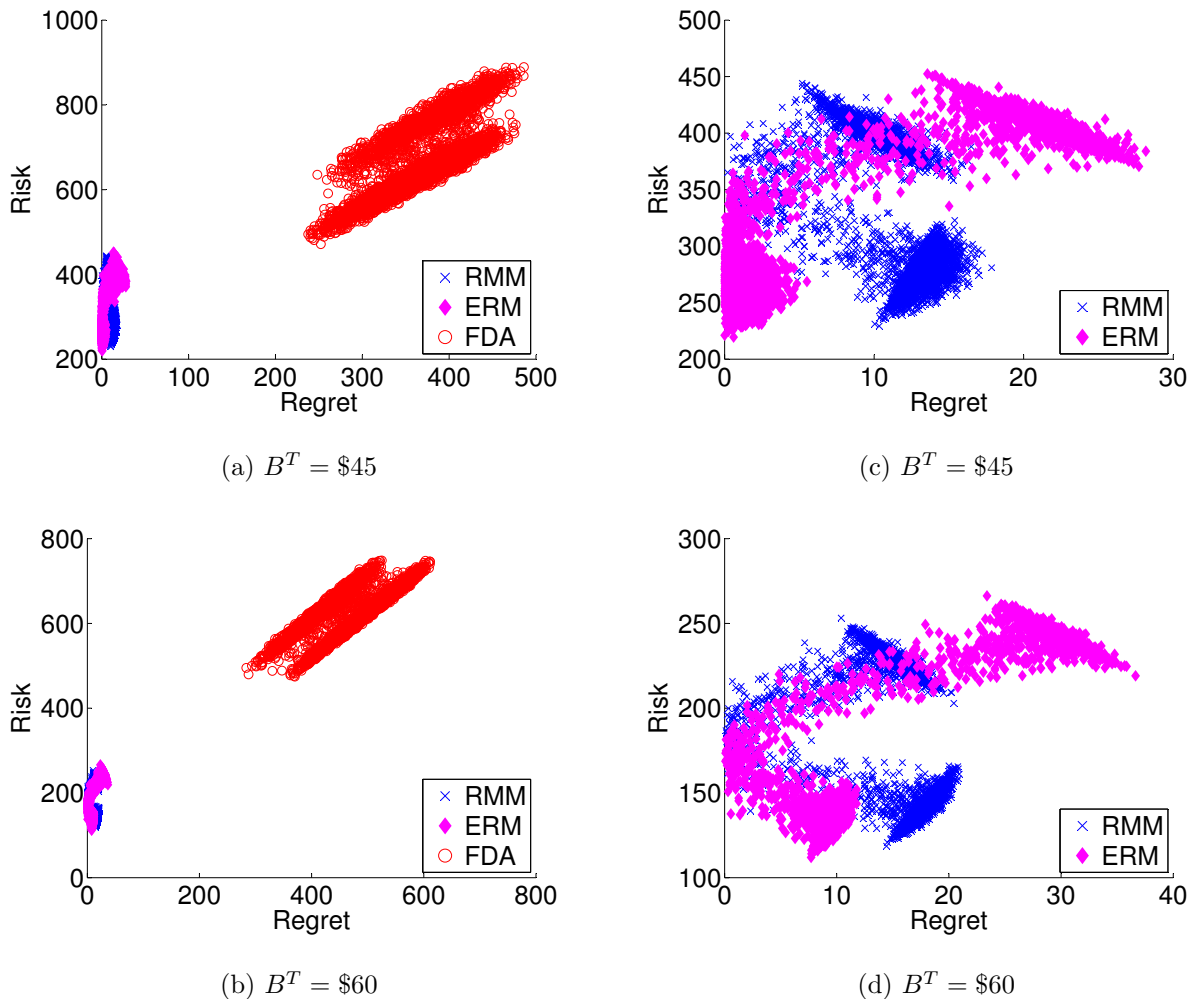


Figure 3.2: Joint distribution of *Risk* and *Regret* per 100,000 donations for **ERM** and **RMM** at $B^T = \$45$ and $B^T = \$60$, with FDA-compliant strategies ((a)-(b)), and without FDA-compliant strategies ((c)-(d)).

3.5.3 Price of Robustness Results

First, we provide an upper bound on Π^R that does not require Condition **(C1)** and Assumption **(A3)**.

Theorem 5. For any problem instance, an upper bound on Π^R is given by:

$$\Pi^R \leq 1 + \frac{\max_{\mathbf{p} \in \Omega^b} \{R(\mathbf{B}, \mathbf{p}) - R(\mathbf{B}^*(\mathbf{p}), \mathbf{p})\}}{R(\mathbf{B}^{*E}, \boldsymbol{\mu})}, \quad \forall \mathbf{B} \in \mathcal{F}.$$

Thus, any feasible budget vector, $\mathbf{B} \in \mathcal{F}$, can be used to generate the upper bound on Π^R . Figure 3.3(a) plots the price of robustness ratio, Π^R , as a function of B^T for the case study. An upper bound on Π^R is constructed using Theorem 5 with $\mathbf{B} = \frac{1}{|\Omega^b|} \sum_{\mathbf{p} \in \Omega^b} \mathbf{B}^*(\mathbf{p})$. Notice that the upper bound on Π^R is less than 13% in general, and less than 10% for $B^T \leq \$52$. Furthermore, for the data in our case study, the maximum Π^R value is around 1.8% for $B^T = \$48$, translating into an increase in expected *Risk* of 5 (278 vs. 273) TTIs per 100,000 donations.

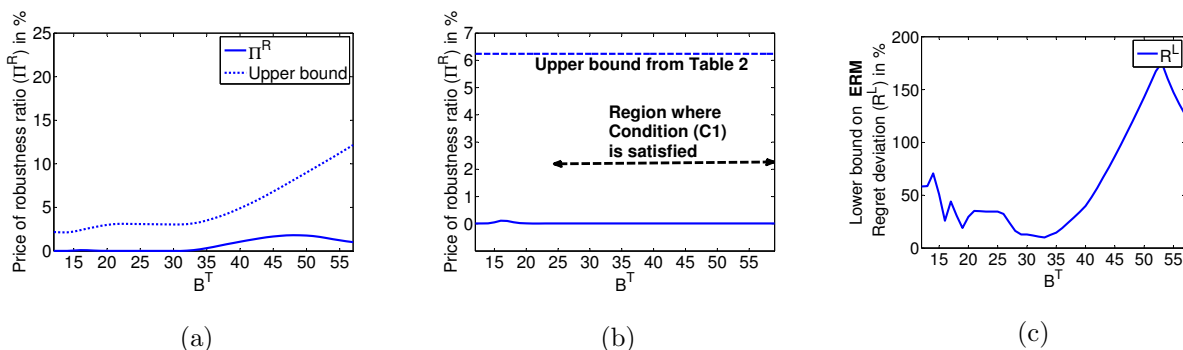


Figure 3.3: Π^R and its upper bound vs. B^T for the numerical study in Section 3.5.2 (a) with all five infections considered, and (b) when WNV is omitted and Condition (C1) is satisfied. (c) \mathcal{R}^L vs. B^T for the numerical study in Section 3.5.2.

Next, we consider a case where we omit screening for WNV due to its high seasonality, as its prevalence can be either low or high with non-zero probabilities. That is, we only consider screening for HIV, HBV, HCV, and babesiosis; solve **ERM** and **RMM** for total budget levels ranging from \$12 to \$57; and evaluate the corresponding price of robustness ratio, Π^R . In Figure 3.3(b), we plot Π^R vs B^T and show that for $B^T \geq \$21$, Condition (C1) holds, which implies, by Theorem 4, that Π^R remains constant, and that the bounds computed in Table 3.2 apply.

Figure 3.3(c) plots the **ERM** *Regret* deviation lower bound, \mathcal{R}^L , as a function of B^T for this case study. Notice that \mathcal{R}^L is greater than 10% in general, and reaches a maximum value of 175.4% for $B^T = \$53$, corresponding to an increase in *Regret* increase of at least 23 (36 vs. 13) TTIs per 100,000 donations.

3.6 Conclusions and Future Research Directions

The decision of how to allocate the testing budget to each TTI is of utmost importance for blood collection centers, and in turn, for the society, as poorly designed post-donation testing schemes may lead to a high number of TTIs. All infections considered in this study can lead to serious health outcomes, resulting in high healthcare costs and significant reduction in quality of life and even fatality in patients.

We show that the expected *Risk* minimizing testing solution that is based only on point prevalence rate estimates can lead to sub-optimal testing schemes that may introduce significant, and unintended, *Risk* to the blood pool. Further, under forecast error, the robust testing solution outperforms the expected *Risk* minimizing solution not only in terms of *Regret*, but also in terms of the expected *Risk*. Our case study of the United States suggests that robust testing solutions can significantly reduce the maximum *Regret* values at a very low price of robustness. We also find that following the FDA guidelines is no guarantee of an optimal testing regime - sometimes it is better to deviate from the FDA recommendations. Indeed, our robust testing solution outperforms several policies that follow the FDA guidelines.

Various extensions of this work are worthy of future research. It is important to expand our models to the case where forecast error is a function of the budget or effort allocated by the blood collection center to forecasting efforts. Other important directions include considering a dynamic, multi-period version of this problem, where infection dynamics change stochastically over time; and expanding our models to increase model realism, such as considering the different societal cost of each infection. We hope that our study, which shows that robust blood screening strategies can offer significant safety benefits to the society, motivates the research community and practitioners to study and consider robust testing schemes, because the consequences of transferring infected blood are dire, while prevalence rates are highly uncertain.

Chapter 4

Optimal Pooling Strategies for Nucleic Acid Testing of Donated Blood Considering Viral Load Growth Curves and Donor Characteristics

4.1 Introduction

Blood products are essential for a variety of medical procedures, including heart surgeries, cancer treatments, organ transplantations, and resuscitation of trauma victims. Unfortunately, there exist many transfusion-transmittable infections (TTIs), including the human immunodeficiency virus (HIV), hepatitis B and C viruses (HBV and HCV), West Nile virus (WNV), babesiosis, Chagas disease, and Dengue virus. Consequently, the screening of donated blood for TTIs is crucial before it is released for transfusion.

Nucleic Acid Testing (NAT) technology for HIV, HBV, HCV, and WNV screening in donated blood has been recently licensed in the United States (US) by the Food and Drug Administration (FDA)¹. Unlike serological assays that rely on antibodies and antigens, NAT assays screen for genetic material (DNA or RNA) from the infectious agent, enabling the detection of the infection during its earlier stages, when serological screening may fail due to low levels of antibodies and/or antigens. The much higher sensitivity (true positive probability) of NAT comes at a higher cost

¹ Respectively in 2005, 2001, 1999, and 2005 [47].

than serological screening. Consequently, due to limited testing budgets, it is common practice for blood centers to perform NAT (if any) on *pools* of samples from multiple donors [7, 9, 114, 115]. Due to the low prevalence rates of TTIs, pooled testing substantially reduces the number of tests required, hence the testing cost. However, pooling results in a *dilution effect*, i.e., as the number of blood units in the pool increases, the viral concentration (load) in an infected blood unit is diluted by the infection-free units in the pool to the point that it may no longer be detectable by the pooled NAT [112, 114, 115]. Thus, pooling reduces the sensitivity of the NAT, and in turn, increases the *Residual Risk* of TTIs, i.e., the probability of releasing an infected blood unit into the blood supply. Therefore, the NAT pool size for each infection should be carefully selected considering the infection dynamics (i.e., how the viral load varies over time following an infection), dilution effect, and prevalence rates within the donor population. Indeed, TTI prevalence rates of first-time donors and repeat donors, i.e., donors who donate frequently, differ, and sometimes substantially. For example, a study of around six million donations collected by the American Red Cross in the year 2008 indicates that HBV, HCV, and HIV prevalence rates among repeat donors are respectively 112-, 35-, and 7-fold lower than those for first-time donors [125].

The current practice in US blood centers is to use NAT to screen for each of HBV, HCV, and HIV in pools of 16 for all donors [6]; this corresponds to a “universal” testing scheme, which does not differentiate between first-time and repeat donors, and hence utilizes common pool sizes for both donor groups. Currently, the use of donor group-specific (“non-universal”) testing strategies in US blood centers is limited to antibody testing for Chagas disease, which is administered only to first-time donors [7]. Thus, a natural question that arises is whether it would be beneficial to extend donor group-based differentiation to NAT testing for HBV, HCV, and HIV. Consequently, our research goal is to study the benefits of infection-specific universal testing schemes, and of donor group- and infection-specific non-universal testing schemes, considering HBV, HCV, and HIV testing. The objective is to derive NAT pooling schemes (universal and non-universal) that may reduce the current *Residual Risk* (or related treatment cost) of TTIs, while maintaining or reducing the current testing cost. Along the same lines as Chagas testing, in order to keep the logistics manageable, we restrict donor-based differentiation to first-time and repeat donor groups only, as this has been feasible to implement for Chagas testing. We also note that under the current testing processes in the US, multiple blood samples, extracted from each donated blood unit, simultaneously undergo testing for the different infections. Hence, infection-specific testing (with different pool sizes) remains a viable strategy.

The split between first-time and repeat donors varies from year to year (first-time donors constitute between 10% to 30% of all US donors in a given year [42, 65]). As a result, any non-universal strategy that screens the two donor groups with different NAT pool sizes will incur a random testing cost that varies with the proportion of first-time donors in a given year, making its implementation somewhat challenging for the blood center with respect to their testing budget constraint. Due to the set up involved with establishing new testing protocols and contracts with testing laboratories, it is difficult for blood centers to alter their testing scheme in the short-term (e.g., on a yearly basis). Hence, this uncertainty in the total testing cost needs to be taken into account while devising donor group-specific pool sizes.

In this setting, the budget-constrained decision-maker needs to allocate the testing budget among the various TTIs. The objective is to determine optimal infection- and/or donor group-specific (i.e., first-time vs. repeat donor) NAT pool sizes so as to minimize the risk (or life-time treatment cost of transfusion recipients) of TTIs, while ensuring that the testing budget remains feasible with a given probability. We also aim to quantify the benefits of donor group-based (non-universal) NAT testing schemes over universal schemes and over the current practice.

Our research provides a bridge between the transfusion literature and the statistics literature. In particular, transfusion researchers develop and utilize post-infection viral load growth models in order to estimate the impact of pool size and dilution effect on the *Residual Risk* [31, 49, 52, 114, 115]. Statisticians, on the other hand, derive expressions for the relevant metrics in pooled testing, including *Residual Risk* and expected number of tests, considering various pooling structures that apply in various contexts [4, 9, 43, 56, 70]. However, none of these studies consider pool size optimization nor non-universal pooled testing as we do in this paper. Wein and Zenios [112] is a notable exception that studies the dilution effect for various pool sizes, but for a single infection (HIV) and considering universal testing schemes for serological screening only. As such, their study does not consider viral load models that apply to NAT. Our contribution is to formulate and solve novel pool size optimization models for both universal and non-universal NAT testing schemes that consider viral load growth characteristics for the different infections and the dilution effect of pooling, under uncertainty on the proportion of first-time donors. Our findings indicate that non-universal NAT schemes can substantially reduce *Residual Risk* and the life-time treatment cost in infected transfusion recipients. For example, our case study of the US indicates that non-universal NAT schemes for HBV, HCV, and HIV infections may lead to a reduction of around 5.8 expected TTI cases per 1,000,000 transfusions, and around a 1.7-fold reduction in the treatment cost for

infected recipients over current NAT testing practices in US blood centers.

The remainder of this paper is organized as follows. In Section 4.2, we introduce the notation and assumptions, and provide some preliminaries. In Section 4.3, we study universal and non-universal pool size optimization models, characterize their structural properties, and develop effective solution methodologies. In Section 4.4, we present a case study of the US using published or publicly available data. Finally, we conclude, in Section 4.5, with a summary of our findings and suggestions for future research.

4.2 Notation, Assumptions, and Preliminaries

We use bold-face letters to represent vectors, and upper- and lower-case letters to respectively represent random variables and their realizations. We respectively denote by $F_Y(\cdot)$, $F_Y^{-1}(\cdot)$, and $f_Y(\cdot)$ the cumulative distribution function (CDF), inverse of CDF, and probability density function (pdf) of random variable Y . We also respectively denote by $\Phi(\cdot)$ and $\phi(\cdot)$ the CDF and pdf of the standard normal distribution.

Let $\Psi = \{1, 2, \dots, n\}$ denote the set of TTIs to which NAT is to be administered², and let p_i^F and p_i^R respectively denote the prevalence rate of infection i , $i \in \Psi$, for first-time and repeat donor populations. We let Γ (with support in $[0, 1]$) denote the random proportion of first-time donors among all donors in a given year,³ with mean μ_Γ and standard deviation σ_Γ . The transfusion literature provides estimates on μ_Γ and σ_Γ (e.g., [42, 65, 125]), which we use to calibrate our model in Section 4.4.1. Let $\mu_{p_i} \equiv \mu_\Gamma p_i^F + (1 - \mu_\Gamma) p_i^R$, $i \in \Psi$. We assume that the probability that a blood donor is co-infected with multiple infections in set Ψ is negligible. This assumption is common in the transfusion literature (e.g., [34, 44, 65, 108, 115, 118]), and is reasonable, especially in developed countries where systematic pre-donation questionnaires and health screening procedures are highly effective in deferring co-infected donors, who are likely to be symptomatic.

For each infection i , $i \in \Psi$, the decision-maker (blood center) needs to determine the NAT pool size of S_i ($\in \{1, \dots, S_i^{max}\}$), where S_i^{max} denotes the maximum NAT pool size possible for infection i (due, for example, to technology availability or FDA regulations [47]) and $S_i = 1$ represents individual NAT testing (i.e., NAT administered separately to each blood unit). The transfusion

² We consider that NAT is to be administered for all infections in set Ψ ; this applies when set Ψ contains infections for which post-donation NAT screening has been shown to be cost-effective over serological testing (e.g., HBV, HCV, and HIV) (e.g., [37, 79]).

³ *Residual Risk* is a weighted average of the *Residual Risk* from first-time donors (with weight Γ) and repeat donors (with weight $1 - \Gamma$). Hence, only the randomness in the split between donor groups, and not the total number of donors, is relevant for our derivations; see Section 4.2.2.

literature studies pooled NAT tests of up to 24 units in the US (e.g., [101]), and hence, we use $S_i^{max} = 24, \forall i \in \Psi$.

The decision-maker's objective is to determine an optimal pooling strategy, which we represent by $\mathbf{S} = (S_i)_{i \in \Psi}$, that minimizes the *Residual Risk* (or life-time treatment cost of infected transfusion recipients) for the TTIs in set Ψ , subject to a per-donation testing budget constraint, of B . In universal testing schemes, the decision-maker needs to select a common pool size vector, \mathbf{S} , that applies to all donors, while in non-universal testing schemes, the decision-maker has the flexibility to choose different pool size vectors, \mathbf{S}^F and \mathbf{S}^R , which respectively apply to first-time and repeat donors.

Let $C(\mathbf{S})$ denote the per-donation testing cost of pooling strategy \mathbf{S} . We consider a general cost function $C(\cdot)$ that is strictly, jointly convex decreasing in \mathbf{S} , i.e., as the pool size increases, the testing cost per unit reduces, but at a diminishing rate. This type of a cost function applies not only in the context of blood screening (e.g., [26, 65]), but for many resource allocation problems in general (e.g., [30]). Tests provide binary outcomes, with a negative result indicating that all units in the pool are infection-free, and a positive result indicating otherwise.

We define the following events.

Events:

- $I_i+(S_i)$: event that a blood unit, randomly chosen from a pool of size S_i , is infected by infection i , $S_i \in \mathbb{Z}_+$, $i \in \Psi$ (with complement $I_i-(S_i)$)
- $T_i-(S_i)$: event that the pooled test outcome for a random pool of size S_i is negative for infection i , indicating that all units in the pool are free of infection i , $S_i \in \mathbb{Z}_+$, $i \in \Psi$ (with complement $T_i+(S_i)$).

We also define $A_i+(S_i)$ as the event that a random pool of size S_i contains at least one blood unit with infection i , $S_i \in \mathbb{Z}_+$, $i \in \Psi$ (with complement $A_i-(S_i)$), that is $\{I_i+(S_i)\} \Rightarrow \{A_i+(S_i)\}$, and define $T-(\mathbf{S}) \equiv \cap_{i \in \Psi} T_i-(S_i)$ as the event that a random blood unit is classified as free of all infections in set Ψ based on pooling strategy \mathbf{S} (hence released for transfusion). Let $\beta_i(S_i) \equiv \Pr(T_i-(S_i)|A_i+(S_i))$ denote the false negative probability (1– sensitivity) of the test for infection i when it is administered to a pool of size S_i , for $S_i \in \mathbb{Z}_+$, $i \in \Psi$.

Assumption (A4). (i) Any pool of size $S_i \in \{1, \dots, S_i^{max}\}$ contains at most one unit with infection i , $i \in \Psi$. (ii) For universal testing schemes, $\Pr(A_i+(S_i)) \approx S_i \mu_{p_i}$; and for non-universal testing schemes, $\Pr(A_i+(S_i)) \approx S_i p_i^F (S_i p_i^R)$ for pools comprised of units from first-time (repeat) donors

only, for $S_i \in \{1, \dots, S_i^{max}\}$, $i \in \Psi$.

The first part of Assumption (A4) is common in the transfusion literature [34, 65, 108, 114, 115], and is reasonable due to the low TTI prevalence rates and small NAT pool sizes (of at most 24 units). To motivate the second part of (A4), let $N_i(S_i)$ denote the random number of blood units with infection i , $i \in \Psi$, in a pool of size S_i , $S_i \in \mathbb{Z}_+$. Then, for universal testing schemes, the conditional random variable, $N_i(S_i)|\Gamma$, is binomial with parameters (S_i, p_i^{inf}) , where $p_i^{inf} \equiv \Gamma p_i^F + (1 - \Gamma) p_i^R$. In order not to substantially alter the prevalence rates with Assumption (A4), we re-distribute the expected number of infections of type i , $i \in \Psi$, among all the pools so that each pool receives at most one infection of type i , that is, considering a total of k pools, each with size S_i , for some $k \in \mathbb{Z}_+$, we write:

$$\begin{aligned} \Pr(A_i+(S_i)|\Gamma) &\approx \frac{E[N_i(kS_i)|\Gamma]}{k} = S_i p_i^{inf} \\ \Rightarrow \Pr(A_i+(S_i)) &= \int_0^1 \Pr(A_i+(S_i)|\Gamma = \gamma) f_\Gamma(\gamma) d\gamma \approx S_i \mu_{p_i}. \end{aligned}$$

Similarly, for non-universal testing, where pools contain units only from the same donor group, the probability of event $\{A_i+(S_i)\}$ is approximated by $S_i p_i^F$ for pools from first-time donors and by $S_i p_i^R$ for pools from repeat donors.

In the next section, we discuss our modeling of infection progression (in terms of variations in viral load) in an infected individual, the dilution effect in pooled testing, and the stochasticity in test outcomes.

4.2.1 Viral Load Progression, Dilution Effect, and Testing Stochasticity

NAT measures the viral load in the blood unit, which is then classified as infected or infection-free based on comparison of its viral load with a pre-determined threshold value. Therefore, an accurate modeling of post-infection viral load progression is crucial for deriving the test's sensitivity for different pool sizes, which will be input to the optimization models in Section 4.2.3. For this purpose, we define TD_i as the donation time, from time of infection, of a random donor with infection i , $i \in \Psi$. Similar to the transfusion literature, we model TD_i as a uniform random variable in $[0, \tau]$, where τ denotes the minimum allowable inter-donation period (i.e., minimum time between two successive donations of a repeat donor) [34, 108, 114, 119]⁴. We denote by t_i^w the window period of infection i , $i \in \Psi$ [34, 114, 115], i.e., the time needed for the viral load of

⁴ In the US, the minimum allowable inter-donation time for whole blood is 56 days [48].

an infected individual to reach a level that is detectable with a high probability (a probability of 0.999 is typically used in the literature to determine the window period). For all the infections considered in the case study, $t_i^w \leq \tau$, $i \in \Psi$ (see Section 4.4.1).

The viral load growth for an infected individual during the ramp-up phase, which covers the window period, is commonly modeled in the transfusion and infectious disease literature using the *doubling time viral load model*, characterized by a doubling time, λ , i.e., the number of days it typically takes the viral load (number of viral copies per one mL of blood) to double (e.g., [31, 114, 115]); this model is validated by clinical data from HBV-, HCV-, and HIV-infected individuals [27, 49, 51, 60]. According to this model, the viral load of an individual with infection i , $i \in \Psi$, at time t post-infection, denoted by $v_i(t)$, is given by $v_i(t) = c_i^0 2^{t/\lambda_i}$, $t \in [0, t_i^w]$, where c_i^0 denotes the starting viral load at time of infection; see Figure 4.1 for an illustration of the typical viral load growth for an HBV-infected donor within the window period.

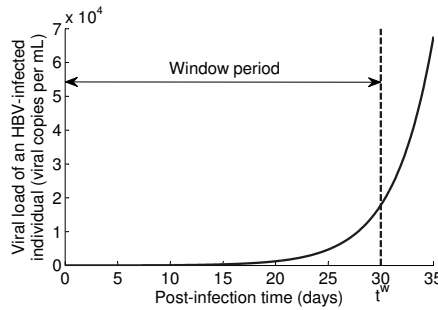


Figure 4.1: Viral load vs. post-infection time for a typical HBV-infected individual with $\lambda = 2.6$ (value taken from [12]) and $c^0 = 6.5$ (value obtained from model calibration, see Section 4.4.1).

We also model the dilution effect of pooling and the stochasticity in test outcomes (i.e., within sample variability), where the latter refers to the possibility that the same test may stochastically produce different outcomes when used repetitively on the same unit due to measurement errors (e.g., [112, 123]). In particular, in order to capture these aspects of testing, we model the test's sensitivity using a probit model, adopted from the transfusion literature (e.g., [114, 115]). Then, the conditional probability that a pool of size S_i tests positive for infection i , indicating that the pool contains an infected unit, given that it actually contains an infected unit from a donor with donation time t , follows:

$$\Pr\left(T_i + (S_i) | A_i + (S_i), TD_i = t\right) = \Phi\left(g_i(S_i) + t \frac{b_i}{\lambda_i} \log 2\right), \quad (4.1)$$

where $g_i(S_i) \equiv a_i + b_i \log\left(\frac{c_i^0}{S_i}\right)$, $a_i \equiv -\frac{z \log(x_i^1)}{\log(x_i^2/x_i^1)}$, $b_i \equiv \frac{z}{\log(x_i^2/x_i^1)}$, x_i^1 and x_i^2 are parameters reported in the literature for NAT for infection i , $i \in \Psi$, and $z = \Phi^{-1}(0.95)$.

Assumption (A5). *Each test has perfect sensitivity outside of the infected donor's window period, and has perfect specificity (true negative probability).*

Assumption (A5) follows by definition of the window period, which indicates that infected units outside of the window period have a viral load sufficient for a probability of detection of at least 0.999. Further, the literature suggests that false positive testing errors, i.e., misclassification of infection-free blood units as infected, are very small in magnitude (e.g., [26, 34, 108]), and do not substantially impact the *Residual Risk* [26, 34, 65, 108, 115].

With this background, we are ready to derive the test's (unconditional) sensitivity for any pool size.

Lemma 5. *For a given pool size S_i , $S_i \in \mathbb{Z}_+$, the false negative probability (1-sensitivity) of NAT for infection i , $i \in \Psi$, follows:*

$$\beta_i(S_i) = \Pr(T_i - (S_i) | A_i + (S_i)) \approx \frac{t_i^w}{\tau} + \frac{\lambda_i}{\tau b_i \log 2} \left[H(g_i(S_i)) - g_i(S_i) - t_i^w \frac{b_i}{\lambda_i} \log 2 \right],$$

where $H(x) \equiv x\Phi(x) + \phi(x)$.

Proof. Using the conditional sensitivity given in Eq. (4.1), the test's sensitivity as a function of pool size follows:

$$\begin{aligned} 1 - \beta_i(S_i) &= \Pr\left(T_i + (S_i) | A_i + (S_i)\right) = \int_0^\tau \Pr\left(T_i + (S_i) | A_i + (S_i), TD_i = t\right) \frac{1}{\tau} dt, \quad \text{since } TD_i \sim U[0, \tau] \\ &= \frac{1}{\tau} \int_0^{t_i^w} \Pr\left(T_i + (S_i) | A_i + (S_i), TD_i = t\right) dt + \frac{1}{\tau} \int_{t_i^w}^\tau 1 dt, \quad \text{by Assumption (A5)} \\ &= 1 - \frac{t_i^w}{\tau} + \frac{\lambda_i}{\tau b_i \log 2} \left[H(\mathcal{K}_i(S_i)) - H(g_i(S_i)) \right], \end{aligned}$$

where $\mathcal{K}_i(S_i) \equiv g_i(S_i) + t_i^w \frac{b_i}{\lambda_i} \log 2$. Then, the approximation in the lemma follows since $\Phi(\mathcal{K}_i(S_i)) \geq 0.999$ and $\phi(\mathcal{K}_i(S_i)) \approx 0$, leading to $H(\mathcal{K}_i(S_i)) \approx \mathcal{K}_i(S_i)$. ■

Note that $\lim_{S_i \rightarrow +\infty} \beta_i(S_i) = 1$, that is, screening with an extremely large pool size becomes equivalent to no screening.

4.2.2 The Blood Center's Objective

The blood center's objective is to minimize the expectation of the *Residual Risk* random variable, i.e., the probability of releasing an infected blood unit into the blood supply, which is a commonly

used measure in the transfusion literature (e.g., [26, 34, 65, 71, 75, 95, 108]).

Lemma 6. *The Residual Risk for universal and non-universal testing schemes, respectively denoted by RR_U and RR_N , follows:*

(i) *For a universal testing scheme with a pool size vector \mathbf{S} , $RR_U(\mathbf{S}) \equiv \sum_{i \in \Psi} \mu_{p_i} \beta_i(S_i) \delta_i^U(\mathbf{S})$,*

$$\text{where } \delta_i^U(\mathbf{S}) \equiv \int_0^1 \prod_{j \in \Psi \setminus \{i\}} \left[1 - (S_j - 1) (\gamma p_i^F + (1 - \gamma) p_i^R) (1 - \beta_j(S_j)) \right] f_\Gamma(\gamma) d\gamma, \quad i \in \Psi.$$

(ii) *For a non-universal testing scheme with pool size vectors \mathbf{S}^F and \mathbf{S}^R , which respectively apply to first-time donors and repeat donors,*

$$RR_N(\mathbf{S}^F, \mathbf{S}^R) \equiv \Gamma \sum_{i \in \Psi} p_i^F \beta_i(S_i^F) \delta_i^F(\mathbf{S}^F) + (1 - \Gamma) \sum_{i \in \Psi} p_i^R \beta_i(S_i^R) \delta_i^R(\mathbf{S}^R),$$

$$\text{where } \delta_i^X(\mathbf{S}^X) \equiv \prod_{j \in \Psi \setminus \{i\}} \left[1 - (S_j - 1) p_i^X (1 - \beta_j(S_j)) \right], \text{ for } X \in \{F, R\}, \quad i \in \Psi.$$

Proof. By definition, *Residual Risk* is the probability that an infected blood unit will not be detected. Then, for universal testing schemes, we can write:

$$\begin{aligned} RR_U(\mathbf{S}) &= \Pr \left(T - (\mathbf{S}), \bigcup_{i \in \Psi} I_i + (S_i) \right) = \Pr \left(\bigcup_{i \in \Psi} \left(T - (\mathbf{S}), I_i + (S_i) \right) \right) \\ &= \sum_{i \in \Psi} \Pr \left(T - (\mathbf{S}) \mid I_i + (S_i) \right) \Pr \left(I_i + (S_i) \right), \text{ by no co-infection assumption} \\ &= \sum_{i \in \Psi} \Pr \left(T - (\mathbf{S}) \mid I_i + (S_i) \right) \left(\underbrace{\Pr \left(I_i + (S_i) \mid A_i + (S_i) \right) \Pr \left(A_i + (S_i) \right)}_{=0 \text{ (by (A5))}} + \Pr \left(I_i + (S_i) \mid A_i - (S_i) \right) \Pr \left(A_i - (S_i) \right) \right) \\ &= \sum_{i \in \Psi} \Pr \left(T_1 - (S_1), \dots, T_n - (S_n) \mid \underbrace{I_1 - (S_1), \dots, I_i + (S_i), \dots, I_n - (S_n)}_{\text{by no co-infection assumption}} \right) \underbrace{\frac{1}{S_i} S_i \mu_{p_i}}_{\text{by (A4)}} \\ &= \sum_{i \in \Psi} \mu_{p_i} \Pr \left(T_i - (S_i) \mid I_i + (S_i) \right) \underbrace{\int_0^1 \prod_{j \in \Psi \setminus \{i\}} \Pr \left(T_j - (S_j) \mid I_j - (S_j), \Gamma = \gamma \right) f_\Gamma(\gamma) d\gamma}_{\equiv \delta_i^U(\mathbf{S})} \\ &= \sum_{i \in \Psi} \mu_{p_i} \beta_i(S_i) \delta_i^U(\mathbf{S}). \end{aligned} \tag{4.2}$$

The event, $\{T_j - (S_j) \mid I_j - (S_j)\}$, $j \in \Psi \setminus \{i\}$, in the expression of $\delta_i^U(\mathbf{S})$ in Eq. (4.2), is the event that pool S_j , which contains the particular blood unit not infected with infection j , tests negative for infection j , which further depends on the presence or absence of infection j within the remaining $S_j - 1$ units in the pool. Then,

$$\begin{aligned}
\Pr(T_j - (S_j) | I_j - (S_j), \Gamma) &= \Pr(T_j - (S_j) | I_j - (S_j), A_j - (S_j), \Gamma) \Pr(A_j - (S_j) | I_j - (S_j), \Gamma) \\
&\quad + \Pr(T_j - (S_j) | I_j - (S_j), A_j + (S_j), \Gamma) \Pr(A_j + (S_j) | I_j - (S_j), \Gamma) \\
&= \underbrace{1}_{\text{by (A5)}} \times \Pr(A_j - (S_j - 1) | \Gamma) + \beta_j(S_j) \Pr(A_j + (S_j - 1) | \Gamma) \\
&= 1 - (S_j - 1) p_j^{inf} (1 - \beta_j(S_j)), \tag{4.3}
\end{aligned}$$

and substituting (4.3) in the expression for $\delta_i^U(\mathbf{S})$, $i \in \Psi$, completes the proof of part (i).

For part (ii), the *Residual Risk* expression in the lemma follows because $RR_N(\mathbf{S}^F, \mathbf{S}^R) = \Gamma RR_U(\mathbf{S}^F, \mathbf{p}^F) + (1 - \Gamma) RR_U(\mathbf{S}^R, \mathbf{p}^R)$, where $RR_U(\mathbf{S}^F, \mathbf{p}^F)$ and $RR_U(\mathbf{S}^R, \mathbf{p}^R)$ can be obtained by replacing μ_{p_i} , $\forall i \in \Psi$, by p_i^F and p_i^R , respectively, in the expression of $RR_U(\cdot)$ in Eq. (4.2). ■

Remark 2. Using Lemma 6, the life-time TTI treatment cost of infected transfusion recipients, which we denote by *C-RR*, follows:

$$\text{Universal schemes: } C\text{-}RR_U(\mathbf{S}) \equiv \sum_{i \in \Psi} w_i \mu_{p_i} \beta_i(S_i) \delta_i^U(\mathbf{S}),$$

Non-universal schemes:

$$C\text{-}RR_N(\mathbf{S}^F, \mathbf{S}^R) \equiv \Gamma \sum_{i \in \Psi} w_i p_i^F \beta_i(S_i^F) \delta_i^F(\mathbf{S}^F) + (1 - \Gamma) \sum_{i \in \Psi} w_i p_i^R \beta_i(S_i^R) \delta_i^R(\mathbf{S}^R),$$

where w_i , $i \in \Psi$, represents the life-time hospitalization and medication cost for infection i , and $\delta_i^U(\mathbf{S})$ and $\delta_i^X(\mathbf{S})$, $X \in \{F, R\}$, are as defined in Lemma 6.

4.2.3 Pool Strategy Optimization

We provide the formulations for the universal and non-universal testing problems respectively in Sections 4.2.3.1 and 4.2.3.2, considering the objective of minimizing the expected *Residual Risk*. The corresponding formulations that minimize the life-time TTI treatment cost can be obtained by simply replacing $RR(\cdot)$ with $C\text{-}RR(\cdot)$ in the objective function (see Remark 2); and we consider both objective functions in the case study of Section 4.4.

4.2.3.1 The Universal Testing Problem

In universal testing schemes, blood from all donors is screened using a common pool size vector, \mathbf{S} . The current practice in US blood centers, which typically use a pool size of 16 for each of HBV, HCV, and HIV [6], is an example of a universal testing scheme. The mathematical formulation of the *Universal Testing Problem (UT)* follows:

Universal Testing Problem (UT):

$$\begin{aligned}
 & \underset{\mathbf{S}}{\text{minimize}} && E[RR_U(\mathbf{S})] = \sum_{i \in \Psi} \mu_{p_i} \beta_i(S_i) \delta_i^U(\mathbf{S}) \\
 & \text{subject to} && C(\mathbf{S}) \leq B \tag{4.4} \\
 & && \mathbf{1} \leq \mathbf{S} \leq \mathbf{S}^{max} \tag{4.5} \\
 & && \mathbf{S} \text{ integer,} \tag{4.6}
 \end{aligned}$$

where $\delta_i^U(\mathbf{S}) = \int_0^1 \prod_{j \in \Psi \setminus \{i\}} [1 - (S_j - 1)(\gamma p_i^F + (1 - \gamma) p_i^R)(1 - \beta_j(S_j))] f_\Gamma(\gamma) d\gamma$, $i \in \Psi$, as defined in Lemma 6, and $C(\cdot)$ is a jointly, strictly convex decreasing function in \mathbf{S} . Note that since the universal testing *Residual Risk* function does not depend on random variable Γ , we have $E[RR_U(\mathbf{S})] = RR_U(\mathbf{S})$, but we keep the expectation of *Residual Risk* in the formulation for **UT** in order to be consistent with the formulation of the non-universal testing problem, and to simplify the presentation in Section 4.3.

4.2.3.2 The Non-universal Testing Problems

In non-universal testing schemes, the goal is to determine a flexible pooling strategy, which may involve different pool sizes for first-time and repeat donors, respectively denoted by \mathbf{S}^F and \mathbf{S}^R , so as to minimize the expected risk (or the life-time treatment cost) of TTIs. For non-universal strategies, the total testing cost incurred by the blood center is given by $\Gamma C(\mathbf{S}^F) + (1 - \Gamma) C(\mathbf{S}^R)$, which is a random variable. Consequently, the average testing budget, of B per donation, may be exceeded depending on the realization of Γ , i.e., the proportion of first-time donors in a given year. As discussed in Section 4.1, it may be difficult for blood centers to alter their testing scheme in the short-term (e.g., on a yearly basis). Therefore, it is important for the decision-maker to have some control over the proportion of time the testing budget is exceeded in a given year. For this purpose, we formulate the blood center’s problem as a *chance-constrained* problem (see, for example, [98]), with the objective of finding an optimal non-universal pooling scheme for which the testing budget remains feasible with a probability of at least α , for some given α . The mathematical formulation of the *Chance-constrained Non-universal Testing Problem (NC)* follows:

Chance-constrained Non-universal Testing Problem (NC):

$$\begin{aligned}
& \underset{\mathbf{S}^F, \mathbf{S}^R}{\text{minimize}} && E [RR_N(\mathbf{S}^F, \mathbf{S}^R)] = \mu_\Gamma \sum_{i \in \Psi} p_i^F \beta_i(S_i^F) \delta_i^F(\mathbf{S}^F) + (1 - \mu_\Gamma) \sum_{i \in \Psi} p_i^R \beta_i(S_i^R) \delta_i^R(\mathbf{S}^R) \\
& \text{subject to} && \Pr \left(\Gamma C(\mathbf{S}^F) + (1 - \Gamma) C(\mathbf{S}^R) \leq B \right) \geq \alpha && \text{(CC}(\alpha)\text{)} \\
& && \mathbf{1} \leq \mathbf{S}^F, \mathbf{S}^R \leq \mathbf{S}^{max} && \text{(4.7)} \\
& && \mathbf{S}^F, \mathbf{S}^R \text{ integer,} && \text{(4.8)}
\end{aligned}$$

where $\delta_i^X(\mathbf{S}^X) \equiv \prod_{j \in \Psi \setminus \{i\}} \left[1 - (S_j - 1) p_i^X (1 - \beta_j(S_j)) \right]$, for $X \in \{F, R\}$, $i \in \Psi$, as defined in Lemma 6. Constraint (CC(α)) ensures that the per-donation budget constraint remains feasible with a probability of at least α .

For comparison purposes, we also study a non-universal strategy obtained by ensuring compliance to the testing budget only on average, i.e., with no probabilistic guarantee in general. This is done by replacing Γ in the budget constraint by its mean value, μ_Γ (see Constraint (4.9)). Then, when Γ follows a symmetric distribution, for example, the budget constraint in (4.9) will be feasible with a probability of only 0.5. The resulting problem, which we refer to as the *Expectation-based Non-universal Testing Problem (ERM)*, reflects the behavior of a decision-maker who considers only the expected values of the random variables.

Expectation-based Non-universal Testing Problem (NE):

$$\begin{aligned}
& \underset{\mathbf{S}^F, \mathbf{S}^R}{\text{minimize}} && E [RR_N(\mathbf{S}^F, \mathbf{S}^R)] = \mu_\Gamma \sum_{i \in \Psi} p_i^F \beta_i(S_i^F) \delta_i^F(\mathbf{S}^F) + (1 - \mu_\Gamma) \sum_{i \in \Psi} p_i^R \beta_i(S_i^R) \delta_i^R(\mathbf{S}^R) \\
& \text{subject to} && \mu_\Gamma C(\mathbf{S}^F) + (1 - \mu_\Gamma) C(\mathbf{S}^R) \leq B && \text{(4.9)} \\
& && \text{(4.7), (4.8).}
\end{aligned}$$

In the following, we respectively denote the optimal solutions to **UT**, **NC**, and **ERM** as \mathbf{S}^{*U} , $(\mathbf{S}^F, \mathbf{S}^R)^{*C}$, and $(\mathbf{S}^F, \mathbf{S}^R)^{*E}$.

4.3 Structural Properties and Algorithmic Developments

Problems **UT**, **NC**, and **ERM** are integer programming problems with non-convex and non-separable objective functions (see Lemma 6), and are difficult to solve in their current form. Therefore, in this section we study structural properties of these problems and derive tight lower and

upper bounds on their objective functions in order to facilitate the solution procedure. This allows us to perform a change of variable that ensures the convexity of the derived lower and upper bounds. We then show that under this change of variable, the feasible regions of **UT**, **NC**, and **ERM** remain convex for a large family of testing cost functions, which include functions of practical interest. These results enable us to develop an efficient and effective solution procedure with a worst-case performance guarantee, in terms of the maximum ratio of the *Residual Risk* generated by the heuristic to the optimal *Residual Risk*.

4.3.1 Structural Properties

To bound the *Residual Risk*, we first introduce some new notation. For universal strategies, $RR_U^{LB}(\mathbf{S})$ and $RR_U^{UB}(\mathbf{S})$ correspond to $RR_U(\mathbf{S})$ (see Lemma 6), with $\delta_i^U(\cdot)$, $i \in \Psi$, replaced by $\delta_i^{min,U}$ and 1, respectively, where $\delta_i^{min,U} \equiv \delta_i^U(\mathbf{S}^{max})$. For non-universal strategies, similar definitions apply for $RR_N^{LB}(\mathbf{S}^F, \mathbf{S}^R)$ and $RR_N^{UB}(\mathbf{S}^F, \mathbf{S}^R)$, with $\delta_i^{min,X} \equiv \delta_i^X(\mathbf{S}^{max})$, $X \in \{F, R\}$; see Table 4.1.

Table 4.1: The expressions for functions $RR_U^b(\mathbf{S})$ and $RR_N^b(\mathbf{S}^F, \mathbf{S}^R)$, for $b \in \{LB, UB\}$.

Bound (b)	Lower Bound (LB)	Upper Bound (UB)
$RR_U^b(\mathbf{S})$	$\sum_{i \in \Psi} \delta_i^{min,U} \mu_{p_i} \beta_i(S_i)$	$\sum_{i \in \Psi} \mu_{p_i} \beta_i(S_i)$
$RR_N^b(\mathbf{S}^F, \mathbf{S}^R)$	$\Gamma \sum_{i \in \Psi} \delta_i^{min,F} p_i^F \beta_i(S_i^F) + (1 - \Gamma) \sum_{i \in \Psi} \delta_i^{min,R} p_i^R \beta_i(S_i^R)$	$\Gamma \sum_{i \in \Psi} p_i^F \beta_i(S_i^F) + (1 - \Gamma) \sum_{i \in \Psi} p_i^R \beta_i(S_i^R)$

Lemma 7. *The Residual Risk can be bounded as follows:*

(i) *For a universal testing scheme with a pool size vector \mathbf{S} ,*

$$RR_U^{LB}(\mathbf{S}) \leq RR_U(\mathbf{S}) \leq RR_U^{UB}(\mathbf{S}).$$

(ii) *For a non-universal testing scheme with pool size vectors \mathbf{S}^F and \mathbf{S}^R , which respectively apply to first-time donors and repeat donors,*

$$RR_N^{LB}(\mathbf{S}^F, \mathbf{S}^R) \leq RR_N(\mathbf{S}^F, \mathbf{S}^R) \leq RR_N^{UB}(\mathbf{S}^F, \mathbf{S}^R).$$

Proof. We only prove part (i), as the proof of part (ii) is similar. For universal schemes, using $\delta_i^U(\mathbf{S}) = \int_0^1 \prod_{j \in \Psi \setminus \{i\}} [1 - (S_j - 1)(\gamma p_i^F + (1 - \gamma) p_i^R)(1 - \beta_j(S_j))] f_\Gamma(\gamma) d\gamma$, $i \in \Psi$ (see Lemma 6, part (i)), we derive $\frac{\partial \delta_i^U(\mathbf{S})}{\partial S_i} = 0$, $i \in \Psi$, and

$$\frac{\partial \delta_i^U(\mathbf{S})}{\partial S_j} = \int_0^1 \mathcal{P}_j \mathcal{Q}_{ij} f_\Gamma(\gamma) d\gamma \leq 0, \quad j \in \Psi \setminus \{i\},$$

where $\mathcal{P}_j \equiv -(\gamma p_j^F + (1 - \gamma) p_j^R) (1 - \beta_j(S_j) - (S_j - 1)\beta_j'(S_j)) \leq 0$, and

$$\mathcal{Q}_{ij} \equiv \prod_{k \in \Psi \setminus \{i,j\}} \left[1 - (S_k - 1) (\gamma p_k^F + (1 - \gamma) p_k^R) (1 - \beta_k(S_k)) \right] \geq 0.$$

Hence, $\delta_i^{min,U}$, the minimum of $\delta_i^U(\cdot)$, is achieved at $\mathbf{S} = \mathbf{S}^{max}$. Hence, $0 \leq \delta_i^{min,U} \leq \delta_i(\mathbf{S}) \leq 1$, $i \in \Psi$, and the result follows. ■

Lemma 7 proves to be useful in developing an effective heuristic for Problems **UT**, **NC**, and **ERM**, and in establishing a performance guarantee for the heuristic. In particular, for each problem, the heuristic, which we refer to as the ‘‘Upper Bound Heuristic’’ (**UBH**), solves an approximate problem, which is derived from its counter-part by substituting $RR_U(\mathbf{S})$ or $RR_N(\mathbf{S}^F, \mathbf{S}^R)$ in their objective function by $RR_U^{UB}(\mathbf{S})$ or $RR_N^{UB}(\mathbf{S}^F, \mathbf{S}^R)$. Further, in order to derive the worst-case performance ratio of the heuristic solution with respect to the optimal solution (\mathcal{R}), we solve another approximate problem by substituting $RR_U(\mathbf{S})$ or $RR_N(\mathbf{S}^F, \mathbf{S}^R)$ in the corresponding objective function by $RR_U^{LB}(\mathbf{S})$ or $RR_N^{LB}(\mathbf{S}^F, \mathbf{S}^R)$. We refer to the corresponding upper and lower bound problems as Problems **UT^b**, **NC^b**, and **NE^b**, for $b \in \{LB, UB\}$. All subsequent results in this section hold for all problems, **UT**, **NC**, and **ERM**. Therefore, in the remainder of this section, we drop the problem index and simply denote the optimal pool vector (i.e., minimizer of the exact *Residual Risk* expression in the corresponding problem) as \mathbf{S}^* , and the minimizer of the corresponding upper or lower bound problem as \mathbf{S}^{*b} , $b \in \{LB, UB\}$.

We first bound the loss in optimality in the expected *Residual Risk* obtained by the upper bound problem, and then develop a solution methodology for exactly solving the upper and lower bound problems.

Theorem 6. *For each Problem, **UT**, **NC**, and **ERM**, the worst-case ratio of the expected Residual Risk obtained by respectively solving **UT^{UB}**, **NC^{UB}**, and **NE^{UB}** to the optimal expected Residual Risk is bounded from above by \mathcal{R} :*

$$\frac{E[RR(\mathbf{S}^{*UB})]}{E[RR(\mathbf{S}^*)]} \leq \frac{E[RR^{UB}(\mathbf{S}^{*UB})]}{E[RR^{LB}(\mathbf{S}^{*LB})]} \equiv \mathcal{R} \leq \frac{1}{\delta^{min}},$$

$$\text{where } \delta^{min} \equiv \begin{cases} \min_{i \in \Psi} \{ \delta_i^{min,U} \}, & \text{for Problem } \mathbf{UT} \\ \min_{i \in \Psi, X \in \{F,R\}} \{ \delta_i^{min,X} \}, & \text{for Problems } \mathbf{NC} \text{ and } \mathbf{ERM} \end{cases}.$$

Proof. We can write, $E[RR(\mathbf{S}^*)] \geq E[RR^{LB}(\mathbf{S}^*)] \geq E[RR^{LB}(\mathbf{S}^{*LB})]$, where the first inequality follows by Lemma 7 and the second inequality follows by definition of \mathbf{S}^{*LB} . Further,

by Lemma 7, we have $E[RR(\mathbf{S}^{*UB})] \leq E[RR^{UB}(\mathbf{S}^{*UB})]$, and hence \mathcal{R} is an upper bound on the worst-case performance ratio of the **UBH**. Next, to prove that $\mathcal{R} \leq \frac{1}{\delta^{min}}$, by definition of δ^{min} , we can write, $\sum_{i \in \Psi} \delta^{min} \mu_{p_i} \beta_i(S_i) \leq \sum_{i \in \Psi} \delta_i^{min,U} \mu_{p_i} \beta_i(S_i)$ for universal testing schemes; and $\Gamma \sum_{i \in \Psi} \delta^{min} p_i^F \beta_i(S_i^F) + (1-\Gamma) \sum_{i \in \Psi} \delta^{min} p_i^R \beta_i(S_i^R) \leq \Gamma \sum_{i \in \Psi} \delta_i^{min,F} p_i^F \beta_i(S_i^F) + (1-\Gamma) \sum_{i \in \Psi} \delta_i^{min,R} p_i^R \beta_i(S_i^R)$ for non-universal testing schemes. Hence, $E[RR^{LB}(\mathbf{S}^{*LB})] \geq \delta^{min} E[RR^{UB}(\mathbf{S}^{*LB})] \geq \delta^{min} E[RR^{UB}(\mathbf{S}^{*UB})]$, where the second inequality follows by definition of \mathbf{S}^{*UB} , and the proof follows. ■

Note that in order to determine \mathcal{R} , one needs to solve both the upper bound and lower bound problems; hence Theorem 6 also provides an upper bound on \mathcal{R} , which depends only on problem parameters.

4.3.2 Algorithmic Development

Next, we develop a solution methodology for efficiently finding the optimal solutions to the upper and lower bound problems, **UT^b**, **NC^b**, and **NE^b**, $b \in \{LB, UB\}$. In the remainder of the paper, we restrict our attention to a family of cost functions that satisfy the following technical condition:

Condition (C2): The testing cost function, $C(\mathbf{S})$, is separable in $S_i, i \in \Psi$, and satisfies:

$$S_i \frac{\partial^2 C(\mathbf{S})}{\partial S_i^2} + \frac{\partial C(\mathbf{S})}{\partial S_i} > 0, \quad \forall i \in \Psi.$$

Condition **(C2)** ensures that function $C(\mathbf{S})$, which is strictly, jointly convex in \mathbf{S} , remains strictly, jointly convex in $\log(\mathbf{S})$. Many cost functions that are practically relevant in the blood screening setting satisfy Condition **(C2)**, e.g., $C(\mathbf{S}) = \sum_{i \in \Psi} \left(K_i + \frac{c_i}{S_i} \right)$, for $K_i, c_i > 0, i \in \Psi$, which considers a fixed preparation cost per blood unit (K_i) and a variable cost (c_i/S_i) that depends on the size of the pool. In what follows, we let $L_i \equiv \log(S_i), i \in \Psi$.

Lemma 8.

- (i) Function $E[RR^b(\mathbf{S})]$, $b \in \{LB, UB\}$, is strictly, jointly convex in $\log(\mathbf{S})$, for $\mathbf{S} \geq \mathbf{1}$.
- (ii) All cost functions, $C(\mathbf{S})$, that satisfy Condition **(C2)**, are strictly, jointly convex in $\log(\mathbf{S})$, for $\mathbf{S} \geq \mathbf{1}$.

Proof. For the first part, we present the proof for universal schemes and for the upper bound problem, as the proof for non-universal schemes and the lower bound problem is similar (see Lemma 7 for the objective functions of the upper and lower bound problems). Recall that for universal schemes, $E[RR^{UB}(\mathbf{S})] = \sum_{i \in \Psi} \mu_{p_i} \beta_i(S_i)$. Function $\beta_i(S_i)$ is convex if and only if $\left[H(g_i(S_i)) - \right.$

$g_i(S_i) - t_i^w \frac{b_i}{\lambda_i} \log 2$ is convex (see Lemma 5). For all $i \in \Psi$, function $g(S_i) = a_i + b_i \log(c_i^0) - b_i L_i$ is affine in L_i . Furthermore, function $H(x)$ is strictly convex in x , since $H''(x) = \phi(x) > 0$. Therefore, $H(g_i(S_i))$, the composition of a strictly convex function with an affine function, is strictly convex in L_i [29]. Since the summation of strictly convex and affine functions remains strictly convex [29], $H(g_i(S_i)) - g(S_i)$ is strictly convex in L_i , which, in turn, implies that function $\beta_i(S_i)$ is strictly convex in L_i . Then, the proof of the first part follows by noting that $E[RR_U^{UB}(\mathbf{S})]$ is separable in S_i , $i \in \Psi$ (equivalently, in L_i , $i \in \Psi$), and is a weighted sum of strictly convex functions with positive weights $(\mu_{p_i}, i \in \Psi)$, and hence is strictly, jointly convex in $\mathbf{L} = \log(\mathbf{S})$.

To prove the second part, note that:

$$\frac{\partial C(\mathbf{S})}{\partial L_i} = \sum_{j \in \Psi} \frac{\partial C(\mathbf{S})}{\partial S_j} \frac{\partial S_j}{\partial L_i} = \frac{\partial C(\mathbf{S})}{\partial S_i} \frac{\partial S_i}{\partial L_i}, \quad \forall i \in \Psi, \text{ since } C(\mathbf{S}) \text{ is separable in } S_i, i \in \Psi, \text{ by (C2)}.$$

Therefore, we have $\frac{\partial^2 C(\mathbf{S})}{\partial L_i \partial L_j} = 0, \forall i, j \in \Psi, i \neq j$, and

$$\frac{\partial^2 C(\mathbf{S})}{\partial L_i^2} = \frac{\partial^2 C(\mathbf{S})}{\partial S_i^2} \left(\frac{\partial S_i}{\partial L_i} \right)^2 + \frac{\partial^2 S_i}{\partial L_i^2} \frac{\partial C(\mathbf{S})}{\partial S_i} = \frac{\partial^2 C(\mathbf{S})}{\partial S_i^2} (\ln(10) S_i)^2 + (\ln(10))^2 S_i \frac{\partial C(\mathbf{S})}{\partial S_i}, \quad \forall i \in \Psi.$$

Noting that Condition (C2) is equivalent to $\frac{\partial^2 C(\mathbf{S})}{\partial L_i^2} > 0, \forall i \in \Psi$, the Hessian of $C(\mathbf{S})$ is positive-definite, and hence $C(\mathbf{S})$ is strictly, jointly convex in $\log(\mathbf{S})$, completing the proof. ■

We are ready to provide an equivalent formulation for the chance constraint $(CC(\alpha))$.

Lemma 9. *For a non-universal testing scheme with pool size vectors \mathbf{S}^F and \mathbf{S}^R , which respectively apply to first-time donors and repeat donors, the chance constraint $(CC(\alpha))$ can be equivalently written as the following set of constraints, for any $\alpha \geq 0.5$:*

$$\begin{cases} F_{\Gamma}^{-1}(\alpha) C(\mathbf{S}^F) + (1 - F_{\Gamma}^{-1}(\alpha)) C(\mathbf{S}^R) \leq B, \\ F_{\Gamma}^{-1}(1 - \alpha) C(\mathbf{S}^F) + (1 - F_{\Gamma}^{-1}(1 - \alpha)) C(\mathbf{S}^R) \leq B. \end{cases} \quad (D(\alpha))$$

Proof. For the case where $C(\mathbf{S}^F) = C(\mathbf{S}^R)$, Constraint $(D(\alpha))$ reduces to $\{C(\mathbf{S}^F) = C(\mathbf{S}^R) \leq B\}$, which always satisfies Constraint $(CC(\alpha))$, since $\Pr(C(\mathbf{S}^R) \leq B) = 1 \geq \alpha, \forall \alpha \in [0, 1]$. For the

case where $C(\mathbf{S}^F) > C(\mathbf{S}^R)$, we have the following:

$$\begin{aligned} & \Pr \left(\Gamma C(\mathbf{S}^F) + (1 - \Gamma)C(\mathbf{S}^R) \leq B \right) \geq \alpha \\ \Leftrightarrow & \Pr \left(\Gamma \leq \frac{B - C(\mathbf{S}^R)}{C(\mathbf{S}^F) - C(\mathbf{S}^R)} \right) \geq \alpha \Leftrightarrow F_{\Gamma}^{-1}(\alpha)C(\mathbf{S}^F) + (1 - F_{\Gamma}^{-1}(\alpha))C(\mathbf{S}^R) \leq B. \end{aligned} \quad (4.10)$$

Similarly, for the case where $C(\mathbf{S}^F) < C(\mathbf{S}^R)$, we can write:

$$\Pr \left(\Gamma C(\mathbf{S}^F) + (1 - \Gamma)C(\mathbf{S}^R) \leq B \right) \geq \alpha \Leftrightarrow F_{\Gamma}^{-1}(1 - \alpha)C(\mathbf{S}^F) + (1 - F_{\Gamma}^{-1}(1 - \alpha))C(\mathbf{S}^R) \leq B. \quad (4.11)$$

For $\alpha \geq 0.5$, we have $F_{\Gamma}^{-1}(\alpha) \geq F_{\Gamma}^{-1}(1 - \alpha)$. Then, for $C(\mathbf{S}^F) > C(\mathbf{S}^R)$, we have that:

$$F_{\Gamma}^{-1}(1 - \alpha)C(\mathbf{S}^F) + (1 - F_{\Gamma}^{-1}(1 - \alpha))C(\mathbf{S}^R) \leq F_{\Gamma}^{-1}(\alpha)C(\mathbf{S}^F) + (1 - F_{\Gamma}^{-1}(\alpha))C(\mathbf{S}^R),$$

implying that in the feasible region where all $(\mathbf{S}^F, \mathbf{S}^R)$ satisfy $C(\mathbf{S}^F) > C(\mathbf{S}^R)$, Constraint (4.11) is redundant. Similarly, in the feasible region where $C(\mathbf{S}^F) < C(\mathbf{S}^R)$, Constraint (4.10) is redundant. Therefore, for $\alpha \geq 0.5$, $(\text{CC}(\alpha))$ is equivalent to $(D(\alpha))$. ■

Note that since α refers to the probability of satisfying the budget constraint, cases of interest to us are those with $\alpha \geq 0.5$, as stated in the lemma. Lemma 9 allows us to replace the chance constraint $(\text{CC}(\alpha))$ with constraint set $(D(\alpha))$ in order to obtain an equivalent formulation for Problem NC^b , as formally stated below.

Theorem 7. *An equivalent formulation for Problem NC^b , $b \in \{LB, UB\}$, follows:*

Equivalent Chance-constrained Non-universal Testing Problem (E-NC^{UB}):

$$\underset{\mathbf{L}^F, \mathbf{L}^R}{\text{minimize}} \quad E \left[RR_N^{UB} \left(10^{\mathbf{L}^F}, 10^{\mathbf{L}^R} \right) \right] = \mu_{\Gamma} \sum_{i \in \Psi} p_i^F \beta_i(10^{L_i^F}) \delta_i^F(10^{\mathbf{L}^F}) + (1 - \mu_{\Gamma}) \sum_{i \in \Psi} p_i^R \beta_i(10^{L_i^R}) \delta_i^R(10^{\mathbf{L}^R})$$

$$\text{subject to} \quad F_{\Gamma}^{-1}(\alpha) C \left(10^{\mathbf{L}^F} \right) + (1 - F_{\Gamma}^{-1}(\alpha)) C \left(10^{\mathbf{L}^R} \right) \leq B \quad (4.12)$$

$$F_{\Gamma}^{-1}(1 - \alpha) C \left(10^{\mathbf{L}^F} \right) + (1 - F_{\Gamma}^{-1}(1 - \alpha)) C \left(10^{\mathbf{L}^R} \right) \leq B \quad (4.13)$$

$$\mathbf{0} \leq \mathbf{L}^F, \mathbf{L}^R \leq \log(\mathbf{S}^{max}) \quad (4.14)$$

$$10^{\mathbf{L}^F}, 10^{\mathbf{L}^R} \text{ integer.} \quad (4.15)$$

The equivalent formulation for E-NC^{LB} is similar, with the objective function replaced by $RR_N^{LB} \left(10^{\mathbf{L}^F}, 10^{\mathbf{L}^R} \right)$. Further, relaxing Constraint (4.15) in E-NC^b , $b \in \{LB, UB\}$, results in a convex programming problem.

Proof. Consider $b \in \{LB, UB\}$. The proof follows from Lemma 9 and by noting that $RR_N^b(10^{\mathbf{L}^F}, 10^{\mathbf{L}^R}) =$

$RR_N^b(\mathbf{S}^F, \mathbf{S}^R)$, and that Constraint (4.14) can be obtained by taking the logarithm of each side of Constraint (4.7). Further, from Lemma 8, the objective function of $\mathbf{E-NC}^b$ is strictly, jointly convex in $(\mathbf{L}^F, \mathbf{L}^R)$, and the left hand side of each of Constraints (4.12) and (4.13), which are the sum of strictly convex functions, is strictly convex in $(\mathbf{L}^F, \mathbf{L}^R)$. Therefore $\mathbf{E-NC}^b$ is a convex integer programming problem; and if Constraint (4.15) is relaxed, then $\mathbf{E-NC}^b$ becomes a convex programming problem. ■

Theorem 7 provides an equivalent formulation for \mathbf{NC}^b , $b \in \{LB, UB\}$, by replacing decision variables $(\mathbf{S}^F, \mathbf{S}^R)$ with $(\mathbf{L}^F, \mathbf{L}^R) = \log(\mathbf{S}^F, \mathbf{S}^R)$. This change of variable leads to convex integer programming problems for both upper and lower bound problems, which can be solved to optimality using an efficient algorithm, such as branch and bound. Similarly, using the same change of variable, \mathbf{UT}^b and \mathbf{NE}^b can be converted into convex integer programming problems.

The following result provides a linear cut for Problem \mathbf{UT}^b , $b \in \{LB, UB\}$, which leads to a substantial reduction in its solution space, as we discuss in Section 4.4.

Lemma 10. *Let $\mathbf{V}_i \equiv (S_1^{max}, \dots, S_i^{min}, \dots, S_n^{max})$, where $S_i^{min} \equiv \inf \{S_i \geq 1 : C(S_1^{max}, \dots, S_i, \dots, S_n^{max}) = B\}$, $i \in \Psi$, and let \mathbf{a} denote a solution to the following system of linear equations:*

$$\{\mathbf{a}^T \mathbf{V}_i = B, i \in \Psi\}.$$

Then, the following cut is valid for \mathbf{UT}^b , $b \in \{LB, UB\}$, for any given \mathbf{S} :

$$\mathbf{a}^T \mathbf{S} \leq B + \sqrt{n} \|\mathbf{a}\|_2, \tag{Cut}$$

where $\|\mathbf{a}\|_2 \equiv \sqrt{\sum_{i=1}^n a_i^2}$.

Proof. See Appendix C. ■

4.4 Numerical Results

We calibrate our model using clinical data on viral load growth rates, prevalence rates, and test sensitivity data published in the literature. We then perform a case study of the United States considering NAT screening for HBV, HCV, and HIV infections and NAT pool sizes of up to 24. We do not consider WNV screening, as WNV is an acute, seasonal infection and its disease progression does not follow the viral load growth models considered in this study. In Section 4.4.1, we discuss model calibration, and in Section 4.4.2, we discuss our findings.

4.4.1 Model Calibration and Data Sources

Table 4.2 reports, for each of HBV, HCV, and HIV, prevalence rates for first-time donors and repeat donors based on data from around 6 million donations collected by the American Red Cross in the year 2008 [125]. Table 4.2 also reports an average life-time treatment cost, which includes estimated average hospitalization and medication cost in the United States over the life-time of the infected individual (adjusted for inflation to 2015 US dollars).

Table 4.2: Prevalence rates for first-time and repeat donors (in %) and life-time treatment cost per TTI (in \$) in the United States.

<i>Infection (i)</i>	<i>Prevalence Rates [125]</i>		<i>Life-time Treatment Cost (w_i) (\$)</i>
	<i>First-time Donor (p_i^F) (%)</i>	<i>Repeat Donor (p_i^R) (%)</i>	
HBV	0.0413	0.0004	59,112 [77]
HCV	0.1634	0.0046	68,118 [91]
HIV	0.0095	0.0013	413,838 [37]

The literature suggests that the average proportion of first-time donor in the US in a given year (Γ) is around 20%, with a range of [10%, 30%] [42, 65, 125]. Therefore, we model Γ as truncated normal distribution with mean $\mu_\Gamma = 0.2$, standard deviation $\sigma_\Gamma = 0.2\mu_\Gamma$, and range [0.1, 0.3]. The minimum allowable inter-donation time for whole blood, τ , is 56 days in the US[48]. For the NAT testing cost function, we consider $C(\mathbf{S}) = \sum_{i \in \Psi} \frac{c_i}{S_i}$, where c_i ($= \14 [65]) represents the cost of individual NAT for infection i , and $\frac{c_i}{S_i}$ is the per-unit testing cost for a pool size of S_i , $i \in \Psi$. Table 4.3 presents the parameters for NAT sensitivity and viral load growth functions used in the case study.

Table 4.3: Parameters for viral load growth models and test sensitivity functions.

<i>Infection (i)</i>	<i>NAT Sensitivity Parameters [114]</i>		<i>Viral Load Growth Parameters (in days)</i>	
	x_i^1	x_i^2	λ_i [32]	t_i^w [12]
HBV	2.5	26.7	2.600	30.0
HCV	2.3	20.2	0.621	7.4
HIV	2.7	18.4	0.854	9.1

Model Calibration

For each infection $i \in \Psi$, we calibrate the sensitivity function for pooled NAT (see Lemma 5)

using the data reported in the literature. Specifically, based on studies of 48, 460, and 69 blood samples from window period donors respectively screened for HBV, HCV, and HIV, Stramer et al. [102] provides the window period sensitivity for pool sizes of 1, 6, 8, and 16; see Table 4.4. In order to calibrate the test sensitivity function given in Lemma 5 so that it applies to all pool sizes in [1 – 24], we use the following expression for window period sensitivity of NAT for infection i , $i \in \Psi$:

$$\begin{aligned} \Pr(T_i + (S_i) | A_i + (S_i), TD_i \leq t_i^w) &= \frac{1}{\Pr(TD_i \leq t_i^w)} \int_0^{t_i^w} \Pr(T_i + (S_i) | A_i + (S_i), TD_i = t) \frac{1}{\tau} dt \\ &= \frac{\lambda_i}{t_i^w b_i \log 2} \left[H\left(g_i(S_i) + t_i^w \frac{b_i}{\lambda_i} \log 2\right) - H(g_i(S_i)) \right]. \end{aligned} \quad (4.16)$$

Table 4.4: NAT sensitivity (in %) for HBV-, HCV-, and HIV-infected window period donors for various pool sizes (from [102]).

<i>Pool size</i>	HBV	HCV	HIV
1	93.75	99.57	100.00
6	89.58	99.14	100.00
8	83.33	N/A	N/A
16	75.00	98.93	88.40

N/A: Not studied in [102].

For each infection $i \in \Psi$, we then calibrate the test’s window period sensitivity function in Eq. (4.16) through parameter c_i^0 so that the function in (4.16) provides the best fit to the data in Table 4.4. This is done by minimizing the root mean square error (RMSE)⁵. The fitted c_i^0 values and the corresponding RMSE values are provided in Table 4.5, which reports an RMSE value of at most 2.47%.

Table 4.5: Calibrated values of c_i^0 , $i \in \Psi$, and the corresponding RMSE values.

<i>Infection (i)</i>	HBV	HCV	HIV
c_i^0 (viral copies per mL)	6.5	146.5	27.5
RMSE (%)	2.47	0.44	2.19

⁵ $RMSE = \sqrt{\frac{\sum_{i=1}^N (\hat{y}_i - y_i)^2}{N}}$, where y_i and \hat{y}_i , $i = 1, \dots, N$, respectively correspond to the actual data and fitted values.

4.4.2 Case Study

In our case study, we consider three types of pooling strategies:

1. The *current practice* in use by most US blood centers, which is a universal strategy having an NAT pool size of 16 for each of HBV, HCV, and HIV [6].
2. The *universal* strategy (the solution to Problem \mathbf{UT}^{UB}), which allows different pool sizes for the different infections, but does not differentiate based on donor group.
3. The *non-universal* strategy, which has the flexibility to screen first-time and repeat donors using different pool sizes for each infection. We study two variations of this strategy: (i) the solution to the chance-constrained formulation, \mathbf{NC}^{UB} , with a budget violation probability of at most 0.05 ($=1 - \alpha$), and (ii) the solution to the expectation-based formulation, \mathbf{NE}^{UB} , which ensures compliance with the testing budget only on average, i.e., with no probabilistic guarantee.

Using our cost data, the corresponding per unit testing budget for the *current practice* is $B_{current} = C(16, 16, 16) = \frac{14}{16} + \frac{14}{16} + \frac{14}{16} = \2.625 , and we use this budget level in our study of the universal and non-universal strategies.

Using Theorem 6, for the data used in the case study, the worst-case performance ratio of the Upper Bound Heuristic, \mathbf{UBH} , is bounded from above by $1/\delta^{min} = 4.71\%$ and 2.38% , respectively, for the *non-universal* and *universal* strategies. In addition, using the cut in Lemma 10 results in around a 16.67% reduction in the solution space for Problem \mathbf{UT}^{UB} .

Table 4.6 reports the pool sizes and the expected number of TTIs per 1,000,000 transfusions for *current practice*, *universal*, and *non-universal* strategies. We also report, for each strategy, the ratio of the expected number of TTIs generated by first-time donors to that generated by repeat donors. First, notice that among all strategies considered, the *current practice* leads to the highest expected number of TTIs, in the order of 11.85 TTIs per 1,000,000 transfusions. Further, since the highest dilution effect occurs for HBV NAT (e.g., a sensitivity of 75% for HBV NAT vs. 88.40% for HIV NAT for a pool size of 16; see Table 4.4), our *universal* strategy screens for HBV with a smaller pool size of 10 (vs. 16 in the *current practice*), leading to a reduction of 1.82 TTIs per 1,000,000 transfusions.

Also, with the flexibility of screening first-time and repeat donors with different pool sizes, *non-universal* strategies outperform the *universal* strategy, by further decreasing (by more than 1.6-

fold) the expected number of TTIs per 1,000,000 transfusions by 3.96 (\mathbf{NC}^{UB}) and 4.76 (\mathbf{NE}^{UB}). Finally, among *non-universal* strategies, not surprisingly, \mathbf{NE}^{UB} outperforms \mathbf{NC}^{UB} with a difference of 0.77 expected TTIs per 1,000,000 transfusions, but with a significantly higher probability of budget violation (0.5 for \mathbf{NE}^{UB} vs. 0.05 for \mathbf{NC}^{UB}).

Since the infection prevalence rates of first-time donors are higher than those of repeat donors (see Table 4.2), the *non-universal* strategies screen first-time donors more extensively. This leads to a significant reduction in the ratio of TTIs from first-time donors to that from repeat donors in 1,000,000 transfusions, which decreases from 17.9:1 and 14.7:1 (respectively for the *current practice* and *universal* strategy) to 6.4:1 and 5.4:1 (for the *non-universal* strategies, \mathbf{NC}^{UB} and \mathbf{NE}^{UB} , respectively). Note also that among all the strategies, the highest worst-case ratio for UBH is 3.404% for \mathbf{NC}^{UB} , which translates into 0.21 expected TTIs per 1,000,000 transfusions, implying that the solutions for the upper bound problems are close to optimality.

In order to estimate the distribution of the number of TTIs that occur in each strategy, we next perform a Monte Carlo simulation by generating 10,000 realizations of the random variable Γ , the proportion of first-time donors. Figure 4.2 plots the histogram of the difference in the expected number of TTI cases per 1,000,000 transfusions between the chance-constrained *non-universal* strategy and the *current practice* (Figure 4.2(a)) and the *universal* strategy (Figure 4.2(b)). Note that the *non-universal* strategy outperforms both the *universal* strategy and the *current practice* in all scenarios, with maximum deviations of 6.05 and 10.29 TTIs per 1,000,000 transfusions, respectively.

Table 4.6: Pool size solutions, the resulting expected number of TTIs per 1,000,000 transfusions (with ratio of TTIs coming from first-time donors to those coming from repeat transfusions) for all strategies considered, and the worst-case ratio (\mathcal{R}).

Strategy	Pool Sizes for First-time Donors			Pool Sizes for Repeat Donors			Expected Number of TTIs per 1,000,000 Transfusions	
	HBV	HCV	HIV	HBV	HCV	HIV	$E[RR] \times 1,000,000$ (First-time : Repeat)	\mathcal{R} (%)
<i>Current practice</i>	16	16	16	16	16	16	11.8494 (17.9:1)	—
<i>Universal</i> (\mathbf{UT}^{UB})	10	22	24	10	22	24	10.0282 (14.7:1)	1.962
<i>Non-universal</i> <i>Chance-constrained</i> (\mathbf{NC}^{UB})	4	13	23	24	24	24	6.0332 (6.4:1)	3.404
<i>Non-universal</i> <i>Expectation-based</i> (\mathbf{NE}^{UB})	3	16	24	24	24	24	5.2679 (5.4:1)	3.222

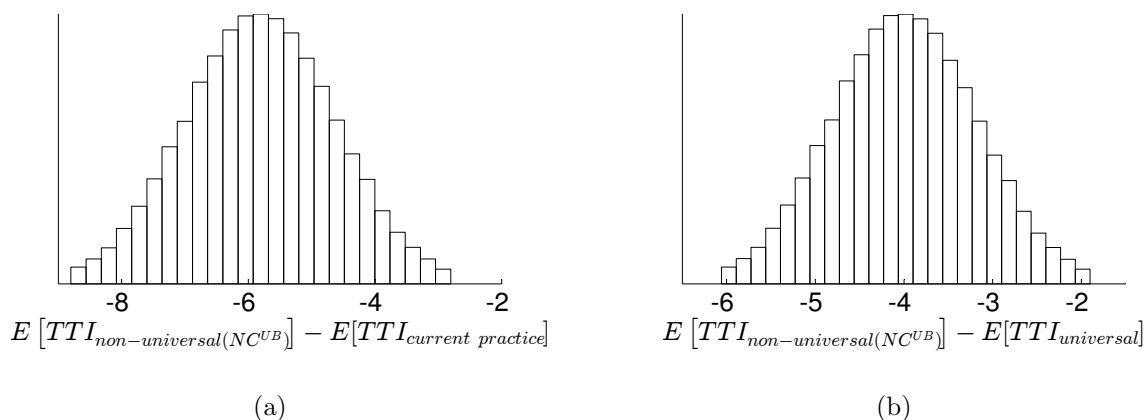


Figure 4.2: Histogram of the difference in expected number of TTI cases per 1,000,000 transfusions between the chance-constrained *non-universal* strategy (\mathbf{NC}^{UB}) and (a) *current practice* (\mathbf{UT}^{UB}), (b) *universal* strategy.

Next, we incorporate the life-time treatment cost of TTIs (see the data Table 4.2) in our formulations; see Table 4.7, which indicates that the pool size solutions vary substantially from those of Table 4.6. Both *universal* and *non-universal* strategies now screen for HIV with smaller pool sizes due to the high treatment cost of HIV compared to HBV and HCV (see Table 4.2). The *non-universal* strategies significantly reduce the life-time treatment cost by almost 1.6- to 1.8-fold compared to the *current practice* and *universal* strategy. Interestingly, among the two *non-universal strategies*, the chance-constrained strategy remains within the testing budget with probability 0.95

(vs. 0.5 for \mathbf{NE}^{UB}) at the expense of a relatively small increase, of 11.7%, in the expected TTI treatment cost. Similar to Table 4.6, the *non-universal* strategies screen first-time donors more extensively, leading to a significant reduction in the ratio of TTI treatment cost coming from first-time donors to those from repeat donors, that is, from 8.1:1 and 7.5:1 (for the *current practice* and *universal* strategy, respectively) to 3.1:1 and 2.7:1 (for the *non-universal* strategies, \mathbf{NC}^{UB} and \mathbf{NE}^{UB} , respectively). In addition, the solutions to the upper bound problem are near-optimal in terms of the expected life-time treatment cost, where the highest worst-case ratio, \mathcal{R} , is 2.993%, translating into a cost \$16,333 per 1,000,000 transfusions.

Table 4.7: Pool size solutions, the resulting expected life-time treatment cost per 1,000,000 transfusions for all strategies considered, and the worst-case ratio (\mathcal{R}).

Strategy	Pool Sizes for First-time Donors			Pool Sizes for Repeat Donors			Expected Life-time Treatment Cost per 1,000,000 transfusions (\$)	
	HBV	HCV	HIV	HBV	HCV	HIV	$\frac{E[C-RR] \times 1,000,000}{(\text{First-time} : \text{Repeat})}$	\mathcal{R} (%)
<i>Current practice</i>	16	16	16	16	16	16	841,508 (8.1:1)	—
<i>Universal</i> (\mathbf{UT}^{UB})	12	24	16	12	24	16	814,378 (7.5:1)	2.021
<i>Non-universal</i> <i>Chance-constrained</i> (\mathbf{NC}^{UB})	5	17	9	24	24	24	545,715 (3.1:1)	2.993
<i>Non-universal</i> <i>Expectation-based</i> (\mathbf{NE}^{UB})	4	16	8	24	24	24	488,421 (2.7:1)	2.871

Figure 4.3 plots the histogram of the difference in the expected life-time treatment cost per 1,000,000 transfusions between the chance-constrained *non-universal* strategy and the *current practice* (Figure 4.3(a)) and the *universal* strategy (Figure 4.3(b)). The *non-universal* strategy outperforms both the *universal* strategy and the *current practice* in all scenarios, with maximum expected cost deviations of \$415,000 and \$501,000 per 1,000,000 transfusions, respectively.

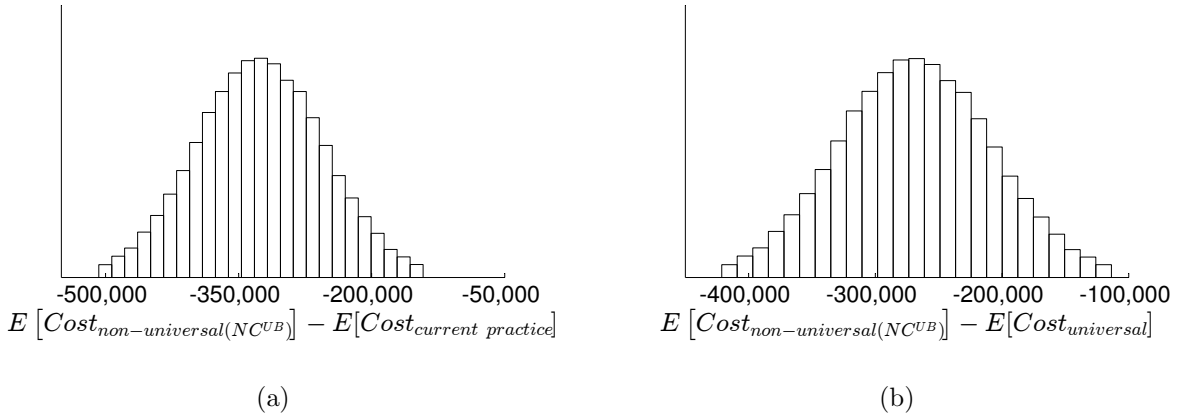


Figure 4.3: Histogram of the difference in expected TTI cost per 1,000,000 transfusions between the chance-constrained *non-universal* strategy (\mathbf{NC}^{UB}) and (a) *current practice* (\mathbf{UT}^{UB}), (b) *universal* strategy.

4.5 Conclusions and Suggestions for Future Research

In this study, we propose a methodology for determining optimal pooling strategies under uncertainty, while taking into account the viral load growth, the dilution effect, and the stochasticity in test outcomes. We study the value of non-universal pooling strategies, which provide the blood center with the flexibility to screen first-time and repeat donors with different pool sizes. Our case study of the United States indicates that non-universal screening schemes result in lower *Residual Risk* and TTI treatment cost. This is important, as all the infections considered in this study may lead to severe health outcomes, including fatality, reduction in quality of life, and high cost to society. In addition, our treatment of the non-universal screening scheme ensures that the blood center’s testing budget remains feasible with a high probability, which is specified by the decision-maker. This is important, since blood centers cannot afford to change their testing scheme frequently. Non-universal testing strategies are likely to increase the complexity of post-donation blood screening, and may require additional training and set up. However, non-universal testing strategies are not uncommon in US blood centers, but are currently limited to Chagas testing. We show in this paper that the benefits of such strategies, in terms of *Residual Risk* and cost reduction, may justify the additional complexity.

Various extensions of this work are worthy of future investigation. The viral load growth may vary from one infected individual to another (e.g., [27, 49, 52]), and hence, it is important to model NAT screening sensitivity with this additional stochasticity. Another important research direction

is to expand our models to the case where prevalence rates need to be estimated, and the blood center needs to allocate its budget among surveillance and screening activities. We hope that our study, which indicates that flexible non-universal screening strategies can benefit the society, motivates further studies of such strategies by the transfusion community and practitioners.

Chapter 5

Conclusions and Future Research Directions

The decision of how to allocate the testing budget to each TTI is of utmost importance for blood collection centers, and in turn, for the society, as poorly designed post-donation testing schemes may lead to a high number of TTIs. All infections considered in this study can lead to serious health outcomes, resulting in high healthcare costs and significant reduction in quality of life and even fatality in patients.

In Chapter 2, we consider the assay selection problem for a single infection, babesiosis, which can be fatal and is the leading cause of TTIs in the US. We perform a cost-effectiveness analysis that takes into consideration uncertainty in prevalence rates and variations in transmission probabilities in order to determine the optimal screening strategy for babesiosis. We suggest that universal PCR in four endemic states is an effective blood donation screening strategy, as it offers the dual benefits of identifying and removing the most infectious blood products from the blood supply, as well as mitigating donor loss due to resolved *B. microti* infections.

In Chapter 3, we study a robust screening scheme for multiple infections under limited information on prevalence rates. We formulate the blood screening problem using a robust formulation as well as an expectation-based formulation, and obtain structural properties of their optimal solutions. Further, we analytically characterize the *price of robustness* and the *price of expectation-based optimization*, which respectively represent the deviation, from the minimum possible expected *Risk*, of the robust solution and the expectation-based solution under forecast error. We show that the expected *Risk* minimizing testing solution that is based only on point prevalence rate estimates

can lead to sub-optimal testing schemes that may introduce significant, and unintended, *Risk* to the blood pool. Further, under forecast error, the robust testing solution outperforms the expected *Risk* minimizing solution not only in terms of *Regret*, but also in terms of the expected *Risk*. Our case study of the United States suggests that robust testing solutions can significantly reduce the maximum *Regret* values at a very low price of robustness. We also find that following the FDA guidelines is no guarantee of an optimal testing regime - sometimes it is better to deviate from the FDA recommendations. Indeed, our robust testing solution outperforms several policies that follow the FDA guidelines.

In Chapter 4, we propose a methodology for determining optimal pooling strategies under uncertainty, while taking into account the viral load growth, the dilution effect, and the stochasticity in test outcomes. We study the value of non-universal pooling strategies, which provide the blood center with the flexibility to screen first-time and repeat donors with different pool sizes. Our case study of the United States indicates that non-universal screening schemes result in lower *Risk* and TTI treatment cost. This is important, as all the infections considered in this study may lead to severe health outcomes, including fatality, reduction in quality of life, and high cost to society. In addition, our treatment of the non-universal screening scheme ensures that the blood center's testing budget remains feasible with a high probability, which is specified by the decision-maker. Non-universal testing strategies are likely to increase the complexity of post-donation blood screening, but we show in this paper that the benefits of such strategies, in terms of *Risk* and cost reduction, may justify the additional complexity.

Various extensions of this work are worthy of future research. It is important to expand our models to the case where prevalence rates need to be estimated, and the blood center needs to allocate its budget among surveillance and screening activities. It is also important to consider a dynamic, multi-period version of this problem, where infection dynamics change stochastically over time, and optimal screening strategies under this additional stochasticity need to be determined. Further, this work can be extended to customized screening, where donors are classified into different categories based on various characteristics (e.g., age, gender, racial group, first-time/repeat donors), and each category is screened with a customized strategy. In addition to blood screening, this work can be extended to organ and tissue screening, a significantly more constrained setting in which resources are more scarce, organs need to be transplanted much quicker, and organs from a single donor are transplanted to multiple recipients.

An important extension of this work is concerned with public health screening (e.g., screening

of newborns) and genetic testing, where screening for (potential) diseases is performed by searching for specific DNA sequences and mutations that match the profile of known conditions. Since the detection of possible future conditions has the potential to impact the lifestyle of individuals, this research could have important public policy implications.

Bibliography

- [1] Agapova, M., Busch, M.P., and Custer, B. (2010). “Cost-effectiveness of screening the US blood supply for *Trypanosoma cruzi*.” *Transfusion*, **50** (10), pp. 2220–2232.
- [2] AHRQ (2010). “Healthcare cost and utilization project (HCUP).” <http://www.ahrq.gov/data/hcup/>. Accessed in July, 2014.
- [3] Aissi, H., Bazgan, C., and Vanderpooten, D. (2006). “Approximating min-max (regret) versions of some polynomial problems.” In *Computing and Combinatorics*. Springer, pp. 428–438.
- [4] Amemiya, C., Alegria-Hartman, M., Aslanidis, C., Chen, C., Nikolic, J., Gingrich, J., and De Jong, P. (1992). “A two-dimensional YAC pooling strategy for library screening via STS and Alu-PCR methods.” *Nucleic Acids Research*, **20** (10), pp. 2559–2563.
- [5] American Association of Blood Banks (2002). *AABB Technical Manual*, chapter in “Noninfectious complications of blood transfusion”. 14th ed. Bethesda, MD, pp. 586–587.
- [6] American Red Cross (2014). “Blood testing.” <http://www.redcrossblood.org/learn-about-blood/what-happens-donated-blood/blood-testing>. Accessed in October 2014.
- [7] American Red Cross (2014). “Infectious disease testing.” <http://www.redcrossblood.org/learn-about-blood>. Accessed in October 2014.
- [8] Angus, D.C., Musthafa, A.A., Clermont, G., Griffin, M.F., Linde-Zwirble, W.T., Dremsizov, T.T., and Pinsky, M.R. (2001). “Quality-adjusted survival in the first year after the acute respiratory distress syndrome.” *American J. of respiratory and critical care medicine*, **163** (6), pp. 1389–1394.
- [9] Aprahamian, H., Bish, D.R., and Bish, E.K. (2015). “Modeling of residual risk and waste in donated blood with pooled nucleic acid testing.” *Working paper, Department of Industrial and Systems Engineering, Virginia Tech*.
- [10] Armstrong, G.L., Wasley, A., Simard, E.P., McQuillan, G.M., Kuhnert, W.L., and Alter, M.J. (2006). “The prevalence of hepatitis C virus infection in the United States, 1999 through 2002.” *Annals of Internal Medicine*, **144** (10), pp. 705–714.
- [11] Arora, D., Arora, B., and Khetarpal, A. (2010). “Seroprevalence of HIV, HBV, HCV and syphilis in blood donors in Southern Haryana.” *Indian J. of Pathology and Microbiology*, **53** (2), p. 308.
- [12] Atreya, C., Nakhasi, H., Mied, P., Epstein, J., Hughes, J., Gwinn, M., Kleinman, S., Dodd, R., Stramer, S., Walderhaug, M., Ganz, P., Goodrich, R., Tibbetts, C., and Asher, D. (2011). “FDA workshop on emerging infectious diseases: evaluating emerging infectious diseases (EIDs) for transfusion safety.” *Transfusion*, **51** (8), pp. 1855–1871.
- [13] Averbakh, I. (2004). “Minmax regret linear resource allocation problems.” *Operations Research Letters*, **32** (2), pp. 174–180.
- [14] Averbakh, I. and Lebedev, V. (2005). “On the complexity of minmax regret linear programming.” *European J. of Operational Research*, **160** (1), pp. 227–231.

- [15] Bazaraa, M.S., Jarvis, J.J., and Sherali, H.D. (2011). *Linear Programming and Network Flows, 4th ed.* John Wiley & Sons, Hoboken, NJ.
- [16] Behets, F., Bertozzi, S., Kasali, M., Kashamuka, M., Atikala, L., Brown, C., Ryder, R.W., and Quinn, T.C. (1990). “Successful use of pooled sera to determine HIV-1 seroprevalence in Zaire with development of cost-efficiency models.” *AIDS*, **4** (8), pp. 737–742.
- [17] Ben-Tal, A., Den Hertog, D., and Vial, J.P. (2015). “Deriving robust counterparts of nonlinear uncertain inequalities.” *Mathematical Programming*, **149** (1-2), pp. 265–299.
- [18] Ben-Tal, A., El Ghaoui, L., and Nemirovski, A. (2009). *Robust Optimization*. Princeton University Press, Princeton, NJ.
- [19] Ben-Tal, A. and Nemirovski, A. (1999). “Robust solutions of uncertain linear programs.” *Operations Research Letters*, **25** (1), pp. 1–13.
- [20] Ben-Tal, A. and Nemirovski, A. (2000). “Robust solutions of linear programming problems contaminated with uncertain data.” *Mathematical Programming*, **88** (3), pp. 411–424.
- [21] Ben-Tal, A. and Nemirovski, A. (2001). *Lectures on modern convex optimization: analysis, algorithms, and engineering applications*, volume 2. Society for Industrial and Applied Mathematics, Philadelphia, PA.
- [22] Bertsimas, D., Brown, D.B., and Caramanis, C. (2011). “Theory and applications of robust optimization.” *Society for Industrial and Applied Mathematics Review*, **53** (3), pp. 464–501.
- [23] Bish, D.R., Bish, E.K., Xie, S.R., and Stramer, S.L. (2014). “Going beyond “same-for-all” testing of infectious agents in donated blood.” *IIE Transactions*, **46** (11), pp. 1147–1168.
- [24] Bish, D.R., Bish, E.K., Xie, S.R., and Slonim, A.D. (2011). “Optimal selection of screening assays for infectious agents in donated blood.” *IIE Transactions on Healthcare Systems Engineering*, **1** (2), pp. 67–90.
- [25] Bish, E.K., Moritz, M.K., El-Amine, H., Bish, D.R., and Stramer, S.L. (2015). “Cost effectiveness of *Babesia microti* antibody and nucleic acid blood donation screening using results from prospective investigational studies.” *Transfusion*, **55** (9), pp. 2256–2271.
- [26] Bish, E.K., Ragavan, P.K., Bish, D.R., Slonim, A.D., and Stramer, S.L. (2014). “A probabilistic method for the estimation of residual risk in donated blood.” *Biostatistics*, **15** (4), pp. 620–635.
- [27] Biswas, R., Tabor, E., Hsia, C.C., Wright, D.J., Laycock, M.E., Fiebig, E.W., Peddada, L., Smith, R., Schreiber, G.B., Epstein, J.S., et al. (2003). “Comparative sensitivity of HBV NATs and HBsAg assays for detection of acute HBV infection.” *Transfusion*, **43** (6), pp. 788–798.
- [28] Bonacini, M., Lin, H.J., and Hollinger, F.B. (2001). “Effect of coexisting HIV-1 infection on the diagnosis and evaluation of hepatitis C virus.” *J. of AIDS*, **26** (4), pp. 340–344.
- [29] Boyd, S. and Vandenberghe, L. (2004). *Convex Optimization*. Cambridge University Press, Cambridge, United Kingdom.
- [30] Brandeau, M.L. (2004). *Allocating resources to control infectious diseases*, chapter in “Operations Research and Health Care: A Handbook of Methods and Applications”. Kluwer’s International Series, Boston, MA, pp. 443–464.
- [31] Busch, M.P. (2000). “HIV, HBV and HCV: new developments related to transfusion safety.” *Vox Sanguinis*, **78**, pp. 253–256.
- [32] Busch, M.P. (2006). “Transfusion-transmitted viral infections: building bridges to transfusion medicine to reduce risks and understand epidemiology and pathogenesis.” *Transfusion*, **46** (9), pp. 1624–1640.

- [33] Busch, M.P., Caglioti, S., Robertson, E.F., McAuley, J.D., Tobler, L.H., Kamel, H., Linnen, J.M., Shyamala, V., Tomasulo, P., and Kleinman, S.H. (2005). “Screening the blood supply for West Nile virus RNA by nucleic acid amplification testing.” *New England J. of Medicine*, **353** (5), pp. 460–467.
- [34] Busch, M.P., Glynn, S.A., Stramer, S.L., Strong, D.M., Caglioti, S., Wright, D.J., Pappalardo, B., and Kleinman, S.H. (2005). “A new strategy for estimating risks of transfusion-transmitted viral infections based on rates of detection of recently infected donors.” *Transfusion*, **45** (2), pp. 254–264.
- [35] Casella, G. and Berger, R.L. (2002). *Statistical Inference*, volume 2. Duxbury Pacific Grove, CA.
- [36] CDC (2012). “Babesiosis surveillance-18 states, 2011.” *MMWR. Morbidity and mortality weekly report*, **61** (27), p. 505.
- [37] CDC (2013). “HIV cost-effectiveness.” <http://www.cdc.gov/hiv/prevention/ongoing/costeffectiveness/>. Accessed in November, 2015.
- [38] CDC (2014). “Hepatitis B information for health professionals.” <http://www.cdc.gov/hepatitis/HBV/HBVfaq.htm>. Accessed in May 2014.
- [39] Chak, E., Talal, A.H., Sherman, K.E., Schiff, E.R., and Saab, S. (2011). “Hepatitis C virus infection in the USA: An estimate of true prevalence.” *Liver International*, **31** (8), pp. 1090–1101.
- [40] Custer, B., Busch, M.P., Marfin, A.A., and Petersen, L.R. (2005). “The cost-effectiveness of screening the US blood supply for West Nile virus.” *Annals of Internal Medicine*, **143** (7), pp. 486–492.
- [41] Delage, E. and Ye, Y. (2010). “Distributionally robust optimization under moment uncertainty with application to data-driven problems.” *Operations Research*, **58** (3), pp. 595–612.
- [42] Dodd, R., Notari, E., and Stramer, S. (2002). “Current prevalence and incidence of infectious disease markers and estimated window-period risk in the American Red Cross blood donor population.” *Transfusion*, **42** (8), pp. 975–979.
- [43] Dorfman, R. (1943). “The detection of defective members of large populations.” *The Annals of Mathematical Statistics*, **14** (4), pp. 436–440.
- [44] El-Amine, H., Bish, E.K., and Bish, D.R. (2014). “Robust post-donation screening under limited information on prevalence rates.” *Working paper, Department of Industrial and Systems Engineering, Virginia Tech.*
- [45] FDA (2008). “Cobas TaqScreen West Nile virus test for use on the Cobas S201 system.” <http://www.fda.gov/BiologicsBloodVaccines/BloodBloodProducts/ApprovedProducts/LicensedProductsBLAs/BloodDonorScreening/InfectiousDisease/ucm091785.htm>. Accessed in May 2014.
- [46] FDA (2010). “Blood products advisory committee.” <http://www.fda.gov/AdvisoryCommittees/CommitteesMeetingMaterials/BloodVaccinesandOtherBiologics/BloodProductsAdvisoryCommittee/ucm221857.htm>. Accessed in July, 2014.
- [47] FDA (2015). “Complete list of donor screening assays for infectious agents and HIV diagnostic assays.” <http://www.fda.gov/BiologicsBloodVaccines/BloodBloodProducts/ApprovedProducts/LicensedProductsBLAs/BloodDonorScreening/InfectiousDisease/default.htm>. Accessed in September 2015.
- [48] FDA (2015). “Have you given blood lately?” <http://www.fda.gov/ForConsumers/ConsumerUpdates/ucm048368.htm>. Accessed in September 2015.

- [49] Fiebig, E.W., Wright, D.J., Rawal, B.D., Garrett, P.E., Schumacher, R.T., Peddada, L., Heldebrant, C., Smith, R., Conrad, A., Kleinman, S.H., et al. (2003). “Dynamics of HIV viremia and antibody seroconversion in plasma donors: implications for diagnosis and staging of primary HIV infection.” *AIDS*, **17** (13), pp. 1871–1879.
- [50] Furini, F., Iori, M., Martello, S., and Yagiura, M. (2015). “Heuristic and exact algorithms for the interval min–max regret knapsack problem.” *INFORMS J. on Computing*, **27** (2), pp. 392–405.
- [51] Glynn, S.A., Kleinman, S.H., Wright, D.J., and Busch, M.P. (2002). “International application of the incidence rate/window period model.” *Transfusion*, **42** (8), pp. 966–972.
- [52] Glynn, S.A., Wright, D.J., Kleinman, S.H., Hirschhorn, D., Tu, Y., Heldebrant, C., Smith, R., Giachetti, C., Gallarda, J., and Busch, M.P. (2005). “Dynamics of viremia in early hepatitis C virus infection.” *Transfusion*, **45** (6), pp. 994–1002.
- [53] Goodell, A.J., Bloch, E.M., Krause, P.J., and Custer, B. (2014). “Costs, consequences, and cost-effectiveness of strategies for Babesia microti donor screening of the US blood supply.” *Transfusion*, **54** (9), pp. 2245–2257.
- [54] Gorenflot, A., Moubri, K., Precigout, E., Carcy, B., and Schetters, T. (1998). “Human babesiosis.” *Annals of tropical medicine and parasitology*, **92** (4), pp. 489–501.
- [55] Grassly, N., Morgan, M., Walker, N., Garnett, G., Stanecki, K., Stover, J., Brown, T., and Ghys, P. (2004). “Uncertainty in estimates of HIV/AIDS: The estimation and application of plausibility bounds.” *Sexually Transmitted Infections*, **80** (suppl 1), pp. i31–i38.
- [56] Habteslassie, Y., Haines, L.M., Mwambi, H., and Odhiambo, J. (2015). “Array-based schemes for group screening with test errors which incorporate a concentration effect.” *J. of Statistical Planning and Inference*, **167**, pp. 41–57.
- [57] Hatcher, J.C., Greenberg, P.D., Antique, J., and Jimenez-Lucho, V.E. (2001). “Severe babesiosis in Long Island: review of 34 cases and their complications.” *Clinical infectious diseases*, **32** (8), pp. 1117–1125.
- [58] Hay, S.N., Scanga, L., and Brecher, M.E. (2006). “Life, death, and the risk of transfusion: A university hospital experience.” *Transfusion*, **46** (9), pp. 1491–1493.
- [59] Hayes, E.B., Komar, N., Nasci, R.S., Montgomery, S.P., OLeary, D.R., and Campbell, G.L. (2005). “Epidemiology and transmission dynamics of West Nile virus disease.” *Emerg Infect Dis*, **11** (8), pp. 1167–1173.
- [60] Hecht, F.M., Busch, M.P., Rawal, B., Webb, M., Rosenberg, E., Swanson, M., Chesney, M., Anderson, J., Levy, J., and Kahn, J.O. (2002). “Use of laboratory tests and clinical symptoms for identification of primary HIV infection.” *AIDS*, **16** (8), pp. 1119–1129.
- [61] Herwaldt, B.L., Linden, J.V., Bosserman, E., Young, C., Olkowska, D., and Wilson, M. (2011). “Transfusion-associated babesiosis in the United States: a description of cases.” *Annals of internal medicine*, **155** (8), pp. 509–519.
- [62] Homer, M.J., Aguilar-Delfin, I., Telford, S.R., Krause, P.J., and Persing, D.H. (2000). “Babesiosis.” *Clinical microbiology reviews*, **13** (3), pp. 451–469.
- [63] Hunfeld, K.P., Hildebrandt, A., and Gray, J. (2008). “Babesiosis: recent insights into an ancient disease.” *International Journal for Parasitology*, **38** (11), pp. 1219–1237.
- [64] Icardi, G., Ansaldi, F., Marisa, B., Durando, P., Lee, S., de Luigi, C., and Crovari, P. (2001). “Novel approach to reduce the Hepatitis C Virus (HCV) window period: Clinical evaluation of a new enzyme-linked immunosorbent assay for HCV core antigen.” <http://www.jcm.asm.org/content/39/9/311.full>. Accessed in May 2014.

- [65] Jackson, B., Busch, M., Stramer, S., and AuBuchon, J. (2003). “The cost-effectiveness of NAT for HIV, HCV, and HBV in whole-blood donations.” *Transfusion*, **43** (6), pp. 721–729.
- [66] Johnson, S.T., Cable, R.G., and Leiby, D.A. (2012). “Lookback investigations of Babesia microti-seropositive blood donors: seven-year experience in a Babesia-endemic area.” *Transfusion*, **52** (7), pp. 1509–1516.
- [67] Joseph, J.T., Roy, S.S., Shams, N., Visintainer, P., Nadelman, R.B., Hosur, S., Nelson, J., and Wormser, G.P. (2011). “Babesiosis in Lower Hudson Valley, New York, USA.” *Emerging infectious diseases*, **17** (5), p. 843.
- [68] Katz, L.M. (2010). “Joint statement before the Blood Products Advisory Committee - risk of Dengue virus infection in blood donors.” *From the Joint Statement of the AABB, American Red Cross, and America’s Blood Centers*. <http://www.aabb.org/advocacy/statements/Pages/jstatment121410.aspx>. Accessed in December 2012.
- [69] Kessler, D., Erwin, J., Busch, M., Levin, A., and Shaz, B. (2012). “Serological findings in donors who are deferred for a history of Babesiosis.” *Transfusion*, **52**, pp. 211A–211A.
- [70] Kim, H.Y., Hudgens, M.G., Dreyfuss, J.M., Westreich, D.J., and Pilcher, C.D. (2007). “Comparison of group testing algorithms for case identification in the presence of test error.” *Biometrics*, **63** (4), pp. 1152–1163.
- [71] Kleinman, S., Busch, M.P., Korelitz, J.J., and Schreiber, G.B. (1997). “The incidence/window period model and its use to assess the risk of transfusion-transmitted human immunodeficiency virus and hepatitis C virus infection.” *Transfusion Medicine Reviews*, **11** (3), pp. 155–172.
- [72] Kleinman, S., Marshall, D., AuBuchon, J., and Patton, M. (2004). “Survival after transfusion as assessed in a large multistate US cohort.” *Transfusion*, **44** (3), pp. 386–390.
- [73] Korves, C.T., Goldie, S.J., and Murray, M.B. (2006). “Cost-effectiveness of alternative blood-screening strategies for West Nile virus in the United States.” *PLoS Medicine*, **3** (2), p. e21.
- [74] Krause, P.J., Gewurz, B.E., Hill, D., Marty, F.M., Vannier, E., Foppa, I.M., Furman, R.R., Neuhaus, E., Skowron, G., Gupta, S., et al. (2008). “Persistent and relapsing babesiosis in immunocompromised patients.” *Clinical Infectious Diseases*, **46** (3), pp. 370–376.
- [75] Lackritz, E.M., Satten, G.A., Aberle-Grasse, J., Dodd, R.Y., Raimondi, V.P., Janssen, R.S., Lewis, W.F., Notari, E.P., and Petersen, L.R. (1995). “Estimated risk of transmission of the human immunodeficiency virus by screened blood in the United States.” *New England J. of Medicine*, **333** (26), pp. 1721–1725.
- [76] Lancet Editorial (2005). “Blood supply and demand.” **365**, p. 2151. <http://www.thelancet.com/pdfs/journals/lancet/PIIS0140-6736%2805%2966749-9.pdf>. Accessed in May 2015.
- [77] Lavanchy, D. (2004). “Hepatitis B virus epidemiology, disease burden, treatment, and current and emerging prevention and control measures.” *J. of Viral Hepatitis*, **11** (2), pp. 97–107.
- [78] Lavelle, T.A., Meltzer, M.I., Gebremariam, A., Lamarand, K., Fiore, A.E., and Prosser, L.A. (2011). “Community-based values for 2009 pandemic influenza A H1N1 illnesses and vaccination-related adverse events.” *PloS one*, **6** (12), p. e27,777.
- [79] Marshall, D.A., Kleinman, S.H., Wong, J.B., AuBuchon, J.P., Grima, D.T., Kulin, N.A., and Weinstein, M.C. (2004). “Cost-effectiveness of Nucleic Acid Test screening of volunteer blood donations for hepatitis B, hepatitis C and human immunodeficiency virus in the United States.” *Vox Sanguinis*, **86**, pp. 28–40.

- [80] Mastin, A., Jaillet, P., and Chin, S. (2015). *Randomized minmax regret for combinatorial optimization under uncertainty*, chapter in “Algorithms and Computation”. Springer-Verlag, Berlin, Germany, pp. 491–501.
- [81] Moritz, E.D., Johnson, S., Winton, C., Townsend, R., Tonnetti, L., Foster, G., Brissette, E., Berardi, V., and Stramer, S. (2013). “Prospective investigational blood donation screening for *Babesia microti* (Bm).” *Transfusion*, **53**, pp. 13A–13A.
- [82] Moritz, E.D., Winton, C., Townsend, R., Tonnetti, L., Berardi, V., and Stramer, S. (2014). “Extended *Babesia microti* investigational screening studies: implications for transfusion-transmitted babesiosis (TTB).” **54**, pp. 26A–27A.
- [83] Moritz, E.D. and Stramer, S.L. (2015). “Blood donation screening for *Babesia microti*: feasibility and results.” *ISBT Science Series*, **10 (S1)**, pp. 169–172.
- [84] Moritz, E.D., Winton, C.S., Johnson, S.T., Krysztof, D.E., Townsend, R.L., Foster, G.A., Devine, P., Molloy, P., Brissette, E., Berardi, V.P., and Stramer, S.L. (2014). “Investigational screening for *Babesia microti* in a large repository of blood donor samples from nonendemic and endemic areas of the United States.” *Transfusion*, **54 (9)**, pp. 2226–2236.
- [85] Ness, P., Braine, H., and King, K. (2001). “Single-donor platelets reduce the risk of septic platelet transfusions.” *Transfusion*, **41**, pp. 857–861.
- [86] Parikh, R., Mathai, A., Parikh, S., Sekhar, G.C., and Thomas, R. (2008). “Understanding and using sensitivity, specificity and predictive values.” *Indian J. of Ophthalmology*, **56 (1)**, pp. 45–50.
- [87] Patriksson, M. (2008). “A survey on the continuous nonlinear resource allocation problem.” *European Journal of Operational Research*, **185 (1)**, pp. 1–46.
- [88] Perakis, G. and Roels, G. (2008). “Regret in the newsvendor model with partial information.” *Operations Research*, **56 (1)**, pp. 188–203.
- [89] Platonov, A.E., Fedorova, M.V., Karan, L.S., Shopenskaya, T.A., Platonova, O.V., and Zhuravlev, V.I. (2008). “Epidemiology of West Nile infection in Volgograd, Russia, in relation to climate change and mosquito (Diptera: Culicidae) bionomics.” *Parasitology Research*, **103 (1)**, pp. 45–53.
- [90] Poorsepahy-Samian, H., Kerachian, R., and Nikoo, M.R. (2012). “Water and pollution discharge permit allocation to agricultural zones: application of game theory and min-max regret analysis.” *Water Resources Management*, **26 (14)**, pp. 4241–4257.
- [91] Razavi, H., ElKhoury, A.C., Elbasha, E., Estes, C., Pasini, K., Poynard, T., and Kumar, R. (2013). “Chronic hepatitis C virus (HCV) disease burden and cost in the United States.” *Hepatology*, **57 (6)**, pp. 2164–2170.
- [92] Richard, L., Pellegrin, J., Barbeau, P., Brossard, G., Leng, B., and Fleury, H. (1993). “HIV-1 and HCV co-infected patients: detection of active viral expression using a nested polymerase chain reaction.” *Molecular and Cellular Probes*, **7 (5)**, pp. 405–410.
- [93] Ruebush 2nd, T., Juranek, D.D., Chisholm, E.S., Snow, P.C., Healy, G.R., and Sulzer, A.J. (1977). “Human babesiosis on Nantucket Island. Evidence for self-limited and subclinical infections.” *The New England J. of medicine*, **297 (15)**, pp. 825–827.
- [94] Savage, L.J. (1951). “The theory of statistical decision.” *J. of the American Statistical Association*, **46 (253)**, pp. 55–67.
- [95] Schreiber, G.B., Busch, M.P., Kleinman, S.H., and Korelitz, J.J. (1996). “The risk of transfusion-transmitted viral infections.” *New England J. of Medicine*, **334 (26)**, pp. 1685–1690.

- [96] Sendi, P., Al, M.J., Gafni, A., and Birch, S. (2003). “Optimizing a portfolio of health care programs in the presence of uncertainty and constrained resources.” *Social Science & Medicine*, **57** (11), pp. 2207–2215.
- [97] Shapiro, A. (2016). “Rectangular sets of probability measures.” *Forthcoming in Operations Research*. URL <http://dx.doi.org/10.1287/opre.2015.1466>
- [98] Shapiro, A., Dentcheva, D., and Ruszczyński, A. (2014). *Lectures on Stochastic Programming: Modeling and Theory*, volume 16. SIAM, Philadelphia, PA.
- [99] Simon, M.S., Leff, J.A., Pandya, A., Cushing, M., Shaz, B.H., Calfee, D.P., Schackman, B.R., and Mushlin, A.I. (2014). “Cost-effectiveness of blood donor screening for *Babesia microti* in endemic regions of the United States.” *Transfusion*, **54** (3pt2), pp. 889–899.
- [100] Stramer, S.L., Fang, C.T., Foster, G.A., Wagner, A.G., Brodsky, J.P., and Dodd, R.Y. (2005). “West Nile virus among blood donors in the United States, 2003 and 2004.” *New England J. of Medicine*, **353** (5), pp. 451–459.
- [101] Stramer, S.L., Glynn, S.A., Kleinman, S.H., Strong, D.M., Caglioti, S., Wright, D.J., Dodd, R.Y., and Busch, M.P. (2004). “Detection of HIV-1 and HCV infections among antibody-negative blood donors by nucleic acid–amplification testing.” *New England J. of Medicine*, **351** (8), pp. 760–768.
- [102] Stramer, S.L., Krysztof, D.E., Brodsky, J.P., Fickett, T.A., Reynolds, B., Dodd, R.Y., and Kleinman, S.H. (2013). “Comparative analysis of triplex nucleic acid test assays in United States blood donors.” *Transfusion*, **53** (10pt2), pp. 2525–2537.
- [103] Teal, A.E., Habura, A., Ennis, J., Keithly, J.S., and Madison-Antenucci, S. (2012). “A new real-time PCR assay for improved detection of the parasite *Babesia microti*.” *J. of Clinical Microbiology*, **50** (3), pp. 903–908.
- [104] Tonnetti, L., Eder, A.F., Dy, B., Kennedy, J., Pisciotto, P., Benjamin, R.J., and Leiby, D.A. (2009). “Transfusion complications: Transfusion-transmitted *Babesia microti* identified through hemovigilance.” *Transfusion*, **49** (12), pp. 2557–2563.
- [105] Truven Health Analytics (2011). “Red Book.” <http://www.redbook.com/redbook/online>. Accessed in July, 2014.
- [106] UNAIDS (2012). *Global Report: UNAIDS Report on the Global AIDS Epidemic: 2012*. http://www.unaids.org/sites/default/files/media_asset/20121120_UNAIDS_Global_Report_2012_with_annexes_en_1.pdf. Accessed in May 2015.
- [107] Vairaktarakis, G.L. (2000). “Robust multi-item newsboy models with a budget constraint.” *International J. of Production Economics*, **66** (3), pp. 213–226.
- [108] Van Hulst, M., Hubben, G., Sagoe, K., Promwong, C., Permpikul, P., Fongsatitkul, L., Glynn, D.M., Sibinga, C.T.S., and Postma, M.J. (2009). “Web interface–supported transmission risk assessment and cost-effectiveness analysis of postdonation screening: A global model applied to Ghana, Thailand, and the Netherlands.” *Transfusion*, **49** (12), pp. 2729–2742.
- [109] Van Hulst, M., Smit Sibinga, C.T., and Postma, M.J. (2010). “Health economics of blood transfusion safety–focus on sub-Saharan Africa.” *Biologicals*, **38** (1), pp. 53–58.
- [110] Vannier, E., Gewurz, B.E., and Krause, P.J. (2008). “Human babesiosis.” *Infectious disease clinics of North America*, **22** (3), pp. 469–488.
- [111] Walker, N., Garcia-Calleja, J.M., Heaton, L., Asamoah-Odei, E., Pומרol, G., Lazzari, S., Ghys, P.D., Schwartländer, B., and Stanek, K.A. (2001). “Epidemiological analysis of the quality of HIV sero-surveillance in the world: how well do we track the epidemic?” *AIDS*, **15** (12), pp. 1545–1554.

- [112] Wein, L.M. and Zenios, S.A. (1996). “Pooled Testing for HIV Screening: Capturing the Dilution Effect.” *Operations Research*, **44** (4), pp. 543–569.
- [113] Western, K.A., Benson, G.D., Gleason, N.N., Healy, GeorgeDanand Schultz, M.G., et al. (1970). “Babesiosis in a Massachusetts resident.” *New England J. of Medicine*, **283**, pp. 854–856.
- [114] Weusten, J., Vermeulen, M., Drimmelen, H.V., and Lelie, N. (2011). “Refinement of a viral transmission risk model for blood donations in seroconversion window phase screened by nucleic acid testing in different pool sizes and repeat test algorithms.” *Transfusion*, **51**, pp. 203–215.
- [115] Weusten, J.J., Van Drimmelen, H.A., and Lelie, P.N. (2002). “Mathematic modeling of the risk of HBV, HCV, and HIV transmission by window-phase donations not detected by NAT.” *Transfusion*, **42** (5), pp. 537–548.
- [116] White, D.J., Talarico, J., Chang, H.G., Birkhead, G.S., Heimberger, T., and Morse, D.L. (1998). “Human babesiosis in New York State: review of 139 hospitalized cases and analysis of prognostic factors.” *Archives of internal medicine*, **158** (19), pp. 2149–2154.
- [117] WHO (2015). “Malaria, other vectorborne and parasitic diseases.” http://www.wpro.who.int/mvp/climate_change/en/. Accessed in May 2015.
- [118] Xie, S.R., Bish, D.R., Bish, E.K., Slonim, A.D., and Stramer, S.L. (2012). “Safety and waste considerations in donated blood screening.” *European J. of Oper. Research*, **217** (3), pp. 619–632.
- [119] Yasui, Y., Yanai, H., Sawanpanyalert, P., and Tanaka, H. (2002). “A statistical method for the estimation of window-period risk of transfusion-transmitted HIV in donor screening under non-steady state.” *Biostatistics*, **3** (1), pp. 133–143.
- [120] Young, C., Chawla, A., Berardi, V., Padbury, J., Skowron, G., and Krause, P.J. (2012). “Preventing transfusion-transmitted babesiosis: preliminary experience of the first laboratory-based blood donor screening program.” *Transfusion*, **52** (7), pp. 1523–1529.
- [121] Yue, J., Chen, B., and Wang, M.C. (2006). “Expected value of distribution information for the newsvendor problem.” *Operations Research*, **54** (6), pp. 1128–1136.
- [122] Zacharias, N.M., Athanassaki, I.D., Sangi-Haghpeykar, H., and Gardner, M.O. (2004). “High false-positive rate of human immunodeficiency virus rapid serum screening in a predominantly hispanic prenatal population.” *J. of Perinatology*, **24** (12), pp. 743–747.
- [123] Zenios, S.A. and Wein, L.M. (1998). “Pooled testing for HIV prevalence estimation: exploiting the dilution effect.” *Statistics in Medicine*, **17** (13), pp. 1447–1467.
- [124] Zhang, M. (2011). “Two-stage minimax regret robust uncapacitated lot-sizing problems with demand uncertainty.” *Operations Research Letters*, **39** (5), pp. 342–345.
- [125] Zou, S., Stramer, S.L., and Dodd, R.Y. (2012). “Donor testing and risk: current prevalence, incidence, and residual risk of transfusion-transmissible agents in US allogeneic donations.” *Transfusion Medicine Reviews*, **26** (2), pp. 119–128.

Appendix A

Appendix for Chapter 2

Performance of the Questionnaire

1. From Rhode Island Blood Centers data [120], 0.03% of donors answered “yes” to the question on babesiosis history in the questionnaire.
2. Using IFA as the gold standard, the prevalence of babesiosis in Rhode Island was estimated as 1.4% [120].
3. Using data from New York Blood Center [69], it can be deduced that 94.2% of donors who previously answered “yes” to the question of babesiosis history in the questionnaire were actually not infected with babesiosis (i.e., not IFA/ELISA reactive). Equivalently, only 5.8% of donors who previously answered “yes” to the question of babesiosis history in the questionnaire were IFA/ELISA reactive.

Therefore, applying the Bayes rule, we get the following probabilities:

Questionnaire sensitivity = Probability of positive result given donor is actually infected

$$\begin{aligned} &= \frac{\textit{Probability of positive result and actual infection}}{\textit{Prevalence}} \\ &= \frac{\textit{Probability of actual infection given a positive result} \times \textit{Probability of positive result}}{\textit{Prevalence}} \\ &= \frac{0.058 \times 0.0003}{0.014} \approx 0.00125 = 0.125\%. \end{aligned}$$

Questionnaire specificity = Probability of negative result given donor is actually not infected

$$\begin{aligned}
 &= 100\% - \text{Probability of positive result given no infection} \\
 &= 1 - \frac{\text{Probability of no infection given a positive result} \times \text{Probability of positive result}}{1 - \text{Prevalence}} \\
 &= 1 - \frac{0.942 \times 0.0003}{1 - 0.014} \approx 0.9997 = 99.97\%.
 \end{aligned}$$

***Babesia microti* prevalence rates**

All prevalence rates were based on ongoing investigational studies conducted by the ARC [83]. Donors were categorized into three categories: window-period donors, actively infected donors, and donors with resolved infection. The prevalence values were calculated based on a population of 83,330 donors with 8, 52, and 261 donors in each respective category. The population considered was in endemic regions of the US (Connecticut, Massachusetts, Minnesota, and Wisconsin). The ranges used in the sensitivity analysis were chosen so that they cover the 95% binomial confidence interval.

Cost parameters

The total unit cost (\$ per transfusion) of each screening strategy is composed of three components: The unit cost of administering the test(s), the cost of a positive test result (i.e., donor notification, counseling and follow-up, product quarantine/withdrawal and recipient tracing), and the treatment cost of a symptomatic TTB case (cost of hospitalization, medication, etc.). We used the following formula to calculate the total cost of each screening strategy:

$$\begin{aligned}
 \text{Total unit cost of screening strategy (per transfusion)} &= \text{Unit test administering cost} + \\
 &\text{cost of positive test result} \times (\text{proportion of donors who test positive under this strategy}) + \\
 &\text{treatment cost of a positive TTB case} \times (\text{probability of a TTB case when using this strategy}).
 \end{aligned}$$

Deriving the QALY for each strategy

In QALY calculations, we used a time horizon of 40 years after transfusion, based on life table statistics in the US and in accordance with Simon et al. [99].

Supplementary material for one-way deterministic sensitivity analysis on the transmission probability for actively infected donors

Figures A.1 and A.2 present the results for the deterministic sensitivity analysis on the transmission probability from actively infected donors for Scenario 2-Low (donor-recipient scenario when the transmission probability from donors with resolved infections to low-risk recipients is 0.3% and to high-risk recipients is 0.6%) and scenario 2-high (donor-recipient scenario when the transmission probability from donors with resolved infections to low-risk recipients is 2.9% and to high-risk recipients is 5.8%). The figures demonstrate that when donors with resolved infections present a transmission probability of 0.3% to low-risk recipients and 0.6% to high-risk recipients, universal-Ab screening is the most cost-effective only when transmission probability from actively infected donors to low-risk recipients is $\leq 3\%$ and to high-risk recipients is $\leq 6\%$, at which point universal-Ab and universal-PCR achieve the same cost-effectiveness. At higher transmission probabilities, the ICER (\$/QALY) drops dramatically and universal-PCR is the most cost-effective option (Figure A.1). When donors with resolved infection present a transmission probability of 2.9% to low-risk recipients and 5.8% to high-risk recipients, universal Ab screening is the most cost-effective until transmission probability from actively infected donors reaches $\sim 30\%$ for low-risk recipients and $\sim 60\%$ to high-risk recipients, at which point universal-Ab and universal-PCR achieve the same cost-effectiveness (Figure 2.2).

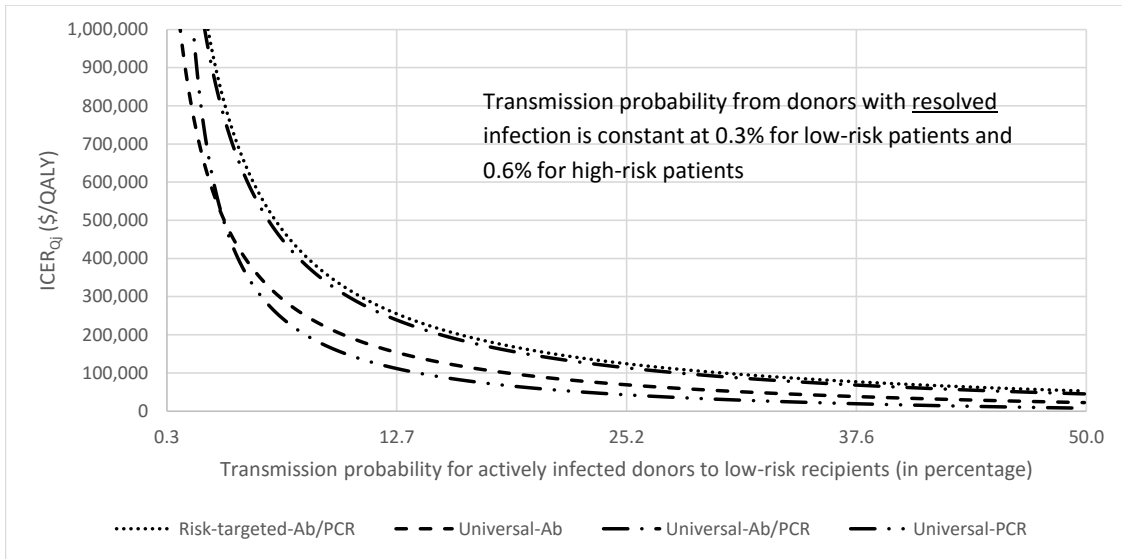


Figure A.1: ICER_{Qj} as a function of transmission probability from actively infected donors to low-risk recipients for Scenario 2-Low (donor-recipient scenario) in which blood units from donors with resolved infection present a transmission probability of 0.3% to low-risk recipients and 0.6% to high-risk recipients.

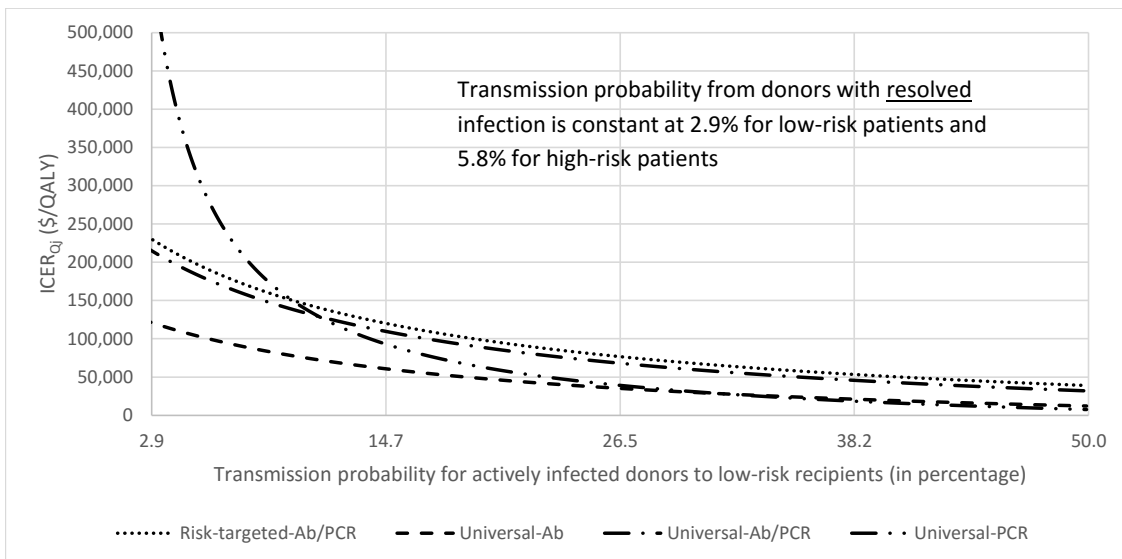


Figure A.2: ICER_{Qj} as a function of transmission probability from actively infected donors to low-risk recipients for Scenario 2-High (donor-recipient scenario) in which blood units from donors with resolved infection present a transmission probability of 2.9% to low-risk patients and 5.8% to high-risk recipients.

Results of one-way deterministic sensitivity analysis on prevalence rates

The sensitivity analysis on the prevalence rates of window-period donors, actively infected donors, and donors with resolved infections indicate that the universal-PCR strategy is the most cost-effective under all scenarios.

Results of probabilistic sensitivity analysis

Table A.1: Probabilistic sensitivity analysis results for Scenarios 1 (donor-only scenario) and 2 (donor-recipient scenario).

Testing Strategy	TTB cases averted pht	Total unit cost (per transfusion) (\$)	QALY per transfusion recipient	CER (\$/QALY)	ICER (\$/QALY)	ICER over questionnaire (\$/QALY)
Results for Scenario 1						
No Screening questionnaire (status quo)	0.00	7.69	5.91417946	1.30		
Risk-targeted Ab/PCR	0.58	7.59	5.91418341	1.28	-17,444	
Universal PCR	9.21	20.78	5.91425882	3.51	187,935	187,935
Universal Ab	22.24	14.93	5.91435017	2.52	-60,075	46,454
Universal Ab/PCR	26.00	16.30	5.91436231	2.76	105,129	51,171
Universal Ab/PCR	31.44	27.61	5.91439975	4.67	341,171	97,026
Results for Scenario 2						
No Screening questionnaire (status quo)	0.00	9.94	5.91410001	1.68		
Risk-targeted Ab/PCR	0.74	9.80	5.91410534	1.66	-20,423	
Universal PCR	18.43	20.86	5.91425616	3.53	78,839	78,839
Universal Ab	31.34	15.50	5.91433023	2.62	-69,448	26,678
Universal Ab/PCR	33.61	16.74	5.91434660	2.83	70,529	30,159
Universal Ab/PCR	40.66	27.69	5.91439708	4.68	243,918	63,970

CER = cost-effectiveness ratio.

Table A.2: Probabilistic sensitivity analysis detailed TTB, waste, and cost values for Scenarios 1 (donor-only scenario) and 2 (donor-recipient scenario).

Testing Strategy	TTB cases pht	Complicated TTB cases pht	Waste (number of blood units wasted) pht	Waste index (ratio of the number of wasted blood units to the number of true positives)	Testing cost per transfusion (\$)	Cost of positive test results per transfusion (\$)	Treatment cost of TTB per transfusion (\$)
Results for Scenario 1							
No Screening questionnaire (status quo)	33.13	12.25	0.00	0.00	0.00	0.00	7.69
Risk-targeted Ab/PCR	32.55	12.04	332.21	1098.71	0.00	0.03	7.56
Universal PCR	23.34	7.22	4301.32	50.88	14.65	0.71	5.42
Universal Ab	8.31	3.08	334.11	4.40	12.50	0.50	1.93
Universal Ab/PCR	6.55	2.42	6588.87	21.40	12.50	2.28	1.52
Universal Ab/PCR	1.11	0.41	6587.53	19.21	25.00	2.35	0.26
Results for Scenario 2							
No Screening questionnaire (status quo)	42.83	17.33	0.00	0.00	0.00	0.00	9.94
Risk-targeted Ab/PCR	42.09	17.03	3332.21	1098.71	0.00	0.03	9.77
Universal PCR	23.66	7.39	4301.32	50.88	14.65	0.71	5.49
Universal Ab	10.75	4.35	334.11	4.40	12.50	0.50	2.49
Universal Ab/PCR	8.47	3.43	6588.87	21.40	12.50	2.28	1.97
Universal Ab/PCR	1.43	0.58	6587.53	19.21	25.00	2.35	0.33

Appendix B

Appendix for Chapter 3

B.1 Summary of Notation

Table B.1: The notation.

Parameters	
$\Psi = \{1, 2, \dots, n\}$	Set of infections that require (or are recommended for) screening
B^T	Total testing budget per donation
Under Assumption (A3) , i.e., $f_i(B_i) = e^{-k_i B_i}$, $i \in \Psi$:	
k_i	Testing effectiveness parameter for infection $i \in \Psi$
S	$= \sum_{i \in \Psi} \frac{1}{k_i}$
c_i	$= \frac{1/k_i}{S}$, $i \in \Psi$
Random variables and related parameters	
$\mathbf{P} = (P_i)_{i \in \Psi}$	Prevalence vector, with mean $\boldsymbol{\mu}$ and uncertainty set (support) $\boldsymbol{\Omega} = ([l_i, u_i])_{i \in \Psi}$
$\boldsymbol{\Omega}^b$	$= \{\mathbf{p} \in \boldsymbol{\Omega} : p_i = l_i \text{ or } p_i = u_i, \forall i \in \Psi\}$, set of boundary vectors
$\boldsymbol{\Omega}^h$	$\subseteq \{\mathbf{p} \in \boldsymbol{\Omega}^b : \lceil n/2 \rceil - 1 \leq \sum_{i \in \Psi} \mathcal{I}_{(p_i=u_i)} \leq \lceil n/2 \rceil + 1\}$, set of “balanced” vectors
$\hat{\boldsymbol{\mu}}$	Mean prevalence estimate
\mathcal{Z}	$= \{1, \dots, \boldsymbol{\Omega}^b \}$, index set of all vectors in $\boldsymbol{\Omega}^b$
$U_i \subseteq \mathcal{Z}$	Index set of vectors in $\boldsymbol{\Omega}^b$ for which the i^{th} component is at its upper bound, $i \in \Psi$
Decision variables	
\mathbf{B}^{*X}	The optimal budget allocation vector, with $X = E$ denoting the ERM optimal solution and $X = R$ denoting the RMM optimal solution
I^{*X}	The optimal allocation set, with $X = E$ denoting the ERM optimal solution and $X = R$ denoting the RMM optimal solution
Dual variables:	
$\alpha_{\mathbf{p}}, \mathbf{p} \in \boldsymbol{\Omega}, \theta, \delta_i, i \in \Psi$	Dual variables for RMM
$\lambda, \gamma_i, i \in \Psi$	Dual variables for ERM
A_i	$= 1 + a_i^u \sum_{z \in U_i} \alpha_z - a_i^l \sum_{z \in \mathcal{Z} \setminus U_i} \alpha_z, i \in \Psi$

B.2 Comparative Statics Analysis

Theorem 8. *As the estimated mean prevalence vector ($\hat{\boldsymbol{\mu}}$), support multiplier vectors (\mathbf{a}^l and \mathbf{a}^u), and the testing budget (B^T) vary, optimal **ERM** and **RMM** solutions change as in Table B.2.*

Next, Example 1 illustrates that the ordering of **ERM** and **RMM** budget allocations does not necessarily follow the ordering with which infections enter the corresponding allocation set as B^T increases (see Theorem 1).

Table B.2: Comparative statics results for **ERM** and **RMM**

(—: remains the same, \nearrow : increases, \searrow : decreases).

Parameter [†]	ERM	RMM
$\hat{\mu}_i \nearrow^\ddagger$	(a) TH^j : $\begin{cases} \text{—}, & j = 1, \dots, i-1 \\ \searrow, & j = i \\ \nearrow, & j = i+1, \dots, n \end{cases}$ (b) $B_i^{*E}(\hat{\boldsymbol{\mu}})$: $\begin{cases} \nearrow, & \text{if } i \in I^{*E}(\hat{\boldsymbol{\mu}}) \\ \text{— or } \nearrow, & \text{o/w} \end{cases}$ $B_j^{*E}(\hat{\boldsymbol{\mu}}) \searrow, \quad j \in I^{*E}(\hat{\boldsymbol{\mu}}) \setminus \{i\}$	— [§]
$(1 - a_i^l)$ or $(1 + a_i^u) \nearrow$	—	(c) $B_i^{*R} \nearrow$
$B^T \nearrow$	(d) $B_i^{*E}(\hat{\boldsymbol{\mu}})$: $\begin{cases} \nearrow, & \text{if } i \in I^{*E}(\hat{\boldsymbol{\mu}}) \\ \text{— or } \nearrow, & \text{o/w} \end{cases}$	(e) B_i^{*R} : $\begin{cases} \nearrow, & \text{if } i \in I^{*R} \\ \text{— or } \nearrow, & \text{o/w} \end{cases}$

[†] When all other parameter values remain the same.

[‡] In a way that the ranking in (3.9) does not change.

[§] As long as $[l_i, u_i]$ remains the same.

Example 1. *Consider $n = 4$, with $\boldsymbol{\mu} = (0.40\%, 0.15\%, 0.10\%, 0.05\%)$ (with no forecast error), respective uncertainty sets $[0.20\%, 0.45\%]$, $[0.10\%, 0.20\%]$, $[0.05\%, 0.15\%]$, and $[0.02\%, 0.20\%]$, and $f_i(B_i) = e^{-0.1B_i}$, for $i = 1, 3, 4$, and $f_2(B_2) = e^{-0.2B_2}$.*

For **ERM**, from the ordering of infections according to (3.9), we have that $\mu_1 > \mu_2 > \mu_3 > \mu_4$, with budget thresholds $(TH^1, TH^2, TH^3, TH^4) = (0.000, 2.175, 19.575, 36.975)$, that is, as B^T increases, infections enter set I^{*E} in this order at their corresponding thresholds. Figure B.1(a) shows that the ordering of budget allocations need not follow the ordering in (3.9). (A similar result holds for the optimal **RMM** solution, see Figure B.1(b).) For example, at $B^T = \$60$, $B_2^{*E} < B_3^{*E}$ despite the fact that infection 2 enters set I^{*E} before infection 3. This happens because $f_2(\cdot)$, the test effectiveness function for infection 2, brings in a larger marginal return at any budget allocation

than that for the other three infections. Once the total budget reaches a certain level, infection 2 does not require as much budget.

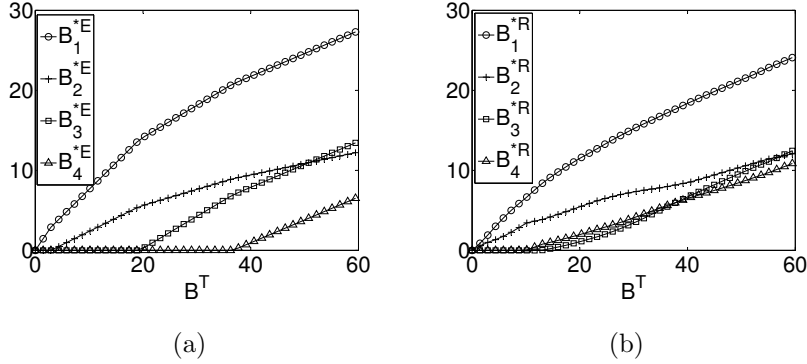


Figure B.1: The optimal budget allocation for (a) **ERM** and (b) **RMM** vs. B^T .

B.3 Discussion on Condition (C1)

Under Assumption **(A3)**, Condition **(C1)** can be equivalently expressed as:

$$(k_i p_i)^{S - \frac{1}{k_i}} \geq e^{-B^T} \prod_{j \in \Psi \setminus \{i\}} (k_j p_j)^{\frac{1}{k_j}}, \forall i \in \Psi, \forall \mathbf{p} \in \Omega^b.$$

As an example, Figure B.2 depicts the \mathbf{p} -space that satisfies Condition **(C1)** for $n = 2$ and realistic parameter values; see Section 3.5 and Appendix B.5. (Similar results hold for $n \geq 3$.)

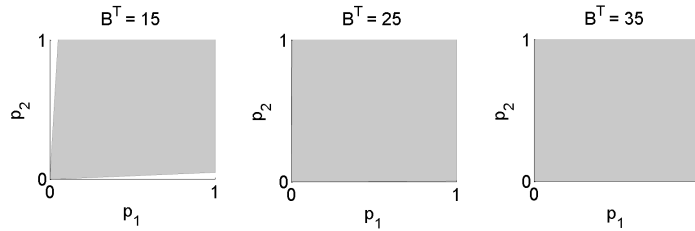


Figure B.2: Regions that satisfy Condition **(C1)** (shaded) for $n = 2$, $\mathbf{k} = (0.2, 0.2)$, and $B^T = 15, 25, 35$.

B.4 Proofs

Recall that for $\mathbf{p} \in \Omega^b$, function $h_i(\mathbf{p})$ is defined as:

$$h_i(\mathbf{p}) = \begin{cases} 1 - a_i^l, & \text{if } p_i = l_i \\ 1 + a_i^u, & \text{if } p_i = u_i \end{cases}, \quad \forall i \in \Psi.$$

Also, recall that $S(I) = \sum_{i \in I} \frac{1}{k_i}$, for $I \subseteq \Psi$, with S denoting $S(\Psi)$. We denote the inverse of a function by the superscript -1 .

Proof of Lemma 1: The proof trivially follows by Assumption **(A1)** since the function $E[R(\mathbf{B}, \hat{\boldsymbol{\mu}})] = \sum_{i \in \Psi} \hat{\mu}_i f_i(B_i)$ is strictly jointly convex in \mathbf{B} . Then, the first-order KKT conditions are necessary and sufficient for optimality and Eqn.s (3.7)-(3.8) follow. Finally, since Constraint (3.5) is tight in an optimal solution (because $f_i(\cdot)$ is strictly decreasing in B_i and vector \mathbf{B} is continuous), the complementary slackness condition, $\lambda(\sum_{i \in \Psi} B_i - B^T) = 0$, is redundant. ■

Proof of Theorem 1: For ease of notation, we write $\mathbf{B}^{*E}(\hat{\boldsymbol{\mu}})$ and $I^{*E}(\hat{\boldsymbol{\mu}})$ as \mathbf{B}^{*E} and I^{*E} , respectively. Consider any $i \in I^{*E}$ and $j \in \Psi \setminus I^{*E}$. By definition, we have that $B_i^{*E} > 0$ and $B_j^{*E} = 0$, which, along with (3.8), imply that $\gamma_i = 0$ and $\gamma_j \geq 0$. From (3.7), we can write:

$$\begin{aligned} \lambda &= \gamma_j - \hat{\mu}_j f_j'(0) = -\hat{\mu}_i f_i'(B_i) \\ \Rightarrow \gamma_j &= \hat{\mu}_j f_j'(0) - \hat{\mu}_i f_i'(B_i) \quad (\text{since } f_j(0) = 1 \text{ by definition}) \\ \Rightarrow \hat{\mu}_i [-f_i'(B_i)] &\geq \hat{\mu}_j [-f_j'(0)] \quad (\text{since } \gamma_j \geq 0) \\ \Rightarrow \hat{\mu}_i [-f_i'(0)] &\geq \hat{\mu}_j [-f_j'(0)] \quad (\text{since } f_i(\cdot) \text{ is strictly decreasing}). \end{aligned}$$

We can therefore deduce that the ranking in (3.9) implies that infections enter set I^{*E} in this order.

By definition, TH^i is the total budget level, B^T , at which infection i enters set I^{*E} . In other words, for $B^T \leq TH^i$, $B_i^{*E} = 0$; and for $B^T > TH^i$, $B_i^{*E} > 0$. Obviously $TH^1 = 0$ because Constraint (3.5) is tight in an optimal solution and therefore for any $B^T < TH^2$, we must have $\sum_{i \in I^{*E}} B_i^{*E} = B_1^{*E} = B^T$. The expressions for all other thresholds, $TH^i, i = 2, \dots, n$, directly follow from the first-order KKT conditions in Eqn.s (3.7)-(3.8) at $B^T = TH^i$. Note that the

solution to $\hat{\mu}_j f'_j(\tilde{B}_j^i) = \hat{\mu}_i f'_i(0)$ is unique since $f'_j(\cdot)$ is strictly increasing.

To prove the optimality condition in (3.11), consider any $i, j \in I^{*E}, i \neq j$. Since, by definition, $B_i^{*E} > 0$ and $B_j^{*E} > 0$, the complementary slackness conditions in (3.8) imply that $\gamma_i = 0$ and $\gamma_j = 0$, and the result follows from (3.7). ■

The Optimal ERM Solution and Threshold Values: For exponential test-effectiveness functions of the form $f_i(B_i) = e^{-k_i B_i}, k_i > 0, B_i \geq 0, i \in \Psi$, from Eq. (3.11), we have:

$$B_i^{*E}(\hat{\boldsymbol{\mu}}) = \frac{1}{k_i S(I^{*E}(\hat{\boldsymbol{\mu}}))} B^T + \frac{1}{k_i} \left[\ln(k_i \hat{\mu}_i) - \ln \left(\prod_{j \in I^{*E}(\hat{\boldsymbol{\mu}})} (k_j \hat{\mu}_j)^{\frac{1}{k_j S(I^{*E}(\hat{\boldsymbol{\mu}}))}} \right) \right], \quad \forall i \in I^{*E}(\hat{\boldsymbol{\mu}}) \quad (\text{B.1})$$

$$TH^i = \ln \left(\prod_{j \in I^{*E}(\hat{\boldsymbol{\mu}})} (k_j \hat{\mu}_j)^{\frac{1}{k_j}} \right) - S(I^{*E}(\hat{\boldsymbol{\mu}})) \ln(k_i \hat{\mu}_i), \quad \text{for } i = 2, \dots, n. \quad (\text{B.2})$$

Similarly, the optimal solution ($\mathbf{B}^*(\mathbf{p})$) and threshold values for the deterministic *Risk* minimization problem with a given \mathbf{p} can be derived by replacing $\hat{\boldsymbol{\mu}}$ with \mathbf{p} in Eqn.s (B.1) and (B.2).

Proof of Theorem 2: We have:

$$\begin{aligned} \min_{\mathbf{B} \in \mathcal{F}} \max_{\mathbf{p} \in \Omega} \left\{ \text{Regret}(\mathbf{B}, \mathbf{p}) \right\} &= \min_{\mathbf{B} \in \mathcal{F}} \max_{\mathbf{p} \in \Omega} \left\{ R(\mathbf{B}, \mathbf{p}) - \min_{\mathbf{Z} \in \mathcal{F}} R(\mathbf{Z}, \mathbf{p}) \right\} = \min_{\mathbf{B} \in \mathcal{F}} \max_{\mathbf{p} \in \Omega} \max_{\mathbf{Z} \in \mathcal{F}} \left\{ R(\mathbf{B}, \mathbf{p}) - R(\mathbf{Z}, \mathbf{p}) \right\} \\ &= \min_{\mathbf{B} \in \mathcal{F}} \max_{\mathbf{Z} \in \mathcal{F}} \max_{\mathbf{p} \in \Omega} \left\{ R(\mathbf{B}, \mathbf{p}) - R(\mathbf{Z}, \mathbf{p}) \right\} = \min_{\mathbf{B} \in \mathcal{F}} \max_{\mathbf{Z} \in \mathcal{F}} \max_{\mathbf{p} \in \Omega} \left\{ \sum_{i \in \Psi} p_i f_i(B_i) - \sum_{i \in \Psi} p_i f_i(Z_i) \right\} \\ &= \min_{\mathbf{B} \in \mathcal{F}} \max_{\mathbf{Z} \in \mathcal{F}} \max_{\mathbf{p} \in \Omega} \left\{ \sum_{i \in \Psi} p_i (f_i(B_i) - f_i(Z_i)) \right\} \end{aligned}$$

Let $\mathbf{p}^* \equiv \operatorname{argmax}_{\mathbf{p} \in \Omega} \left\{ \sum_{i \in \Psi} p_i (f_i(B_i) - f_i(Z_i)) \right\}$. By noting that the maximization is of a linear function in \mathbf{p} , we have:

$$p_i^* = \begin{cases} u_i, & \text{if } f_i(B_i) \geq f_i(Z_i) \\ l_i, & \text{if } f_i(B_i) < f_i(Z_i) \end{cases}, \quad i \in \Psi.$$

Therefore, we have:

$$\max_{\mathbf{p} \in \Omega} \left\{ \sum_{i \in \Psi} p_i (f_i(B_i) - f_i(Z_i)) \right\} = \max_{\mathbf{p} \in \Omega^b} \left\{ \sum_{i \in \Psi} p_i (f_i(B_i) - f_i(Z_i)) \right\}. \quad \blacksquare$$

The following result will be used in the proof of Lemma 2.

Lemma 11. *For any $\mathbf{p} \in \Omega$, $\text{Regret}(\mathbf{B}, \mathbf{p})$ is strictly jointly convex in \mathbf{B} .*

Proof: By definition, $\text{Regret}(\mathbf{B}, \mathbf{p}) = \sum_{i \in \Psi} p_i f_i(B_i) - R(\mathbf{B}^*(\mathbf{p}), \mathbf{p})$. By Assumption (A1), the first term is strictly jointly convex in \mathbf{B} , and the second term is a constant, and the result follows. ■

Proof of Lemma 2: RMM minimizes a linear objective function over a convex set (see Lemma 11). Hence, the first-order KKT conditions are necessary and sufficient for optimality. Finally, since Constraint (3.5) is tight in an optimal solution (because $f_i(\cdot)$ is strictly decreasing in B_i and vector \mathbf{B} is continuous), the complementary slackness condition, $\theta(\sum_{i \in \Psi} B_i - B^T) = 0$, is redundant. ■

The next result allows us to characterize how *Regret* functions, and hence the maximum *Regret* value, shift as parameters $\boldsymbol{\mu}$ and B^T are perturbed, greatly facilitating sensitivity analyses.

Theorem 9. *Consider a family of problem instances. When B^T and $\boldsymbol{\mu}$ are perturbed to some B'^T and $\boldsymbol{\mu}'$, the following holds:*

$$\frac{\text{Regret}(\mathbf{B}^{*R}(\boldsymbol{\mu}', B'^T), \mathbf{p}')}{\text{Regret}(\mathbf{B}^{*R}(\boldsymbol{\mu}, B^T), \mathbf{p})} = e^{\left(\frac{B^T - B'^T}{S}\right)} \prod_{i \in \Psi} \left(\frac{\mu'_i}{\mu_i}\right)^{\frac{1}{k_i S}}, \quad \forall \mathbf{p} \in \Omega^b,$$

where for each $\mathbf{p} \in \Omega^b$, the corresponding $\mathbf{p}' \in \Omega'^b$ is constructed such that if $p_i = \mu_i(1 + a_i^u)$, then $p'_i = \mu'_i(1 + a_i^u)$, and if $p_i = \mu_i(1 - a_i^l)$, then $p'_i = \mu'_i(1 - a_i^l)$, $\forall i \in \Psi$.

Proofs of Lemma 3, Theorem 3, and Theorem 9: Assume that $\mathbf{B}^{*R} (> \mathbf{0})$ denotes the optimal solution to RMM for a problem instance with some $\boldsymbol{\mu}$ and B^T . In what follows, we perturb $\boldsymbol{\mu}$ and B^T , and construct a new RMM solution in which \mathbf{A} remains the same. We first prove Theorems 3 and 9 under the assumption that the constructed solution is optimal for RMM, and then show that this new solution satisfies the first-order KKT conditions with the perturbed $(\boldsymbol{\mu}, B^T)$ values, and hence, must indeed be the optimal solution under the perturbed $(\boldsymbol{\mu}, B^T)$ values.

Assume that \mathbf{A} does not change when $\boldsymbol{\mu}$ and B^T are perturbed, that is, \mathbf{A} is not a function of $\boldsymbol{\mu}$ and B^T . We first show that this assumption implies that Δ_b^* is independent of $\boldsymbol{\mu}$ and B^T . By

Lemma 2, we can write:

$$\mu_i A_i f'_i(B_i^{*R}) = -\mu_i k_i A_i e^{-k_i B_i^{*R}} = -\mu_i k_i A_i e^{-k_i B_i^{*E}(\boldsymbol{\mu})} e^{-k_i \Delta_{bi}^*} = -\theta, \quad \forall i \in \Psi. \quad (\text{B.3})$$

Note that by Condition (C1), $I^{*E}(\boldsymbol{\mu}) = \Psi$. Therefore, by Theorem 1, it follows that $\mu_i k_i e^{-k_i B_i^{*E}(\boldsymbol{\mu})} = \mu_j k_j e^{-k_j B_j^{*E}(\boldsymbol{\mu})}$, $\forall i, j \in \Psi$. Hence, from (B.3), we can write:

$$A_i e^{-k_i \Delta_{bi}^*} = A_j e^{-k_j \Delta_{bj}^*}, \quad \forall i, j \in \Psi. \quad (\text{B.4})$$

Note that (B.4) implies that $\boldsymbol{\Delta}_b^*$ is the optimal solution to (3.18). Since \mathbf{A} is independent of $\boldsymbol{\mu}$ and B^T , it follows that $\boldsymbol{\Delta}_b^*$ is also independent of $\boldsymbol{\mu}$ and B^T . Then Theorem 3 holds.

Next, we show that under the assumption that \mathbf{A} is independent of $\boldsymbol{\mu}$ and B^T , Theorem 9 holds. Consider two problem instances with parameters $(\boldsymbol{\mu}, B^T)$ and $(\boldsymbol{\mu}', B'^T)$, and respectively denote their optimal solutions to **ERM** (**RMM**) as $B^{*E}(\boldsymbol{\mu})$ (B^{*R}) and $B^{*E}(\boldsymbol{\mu}')$ (B^{*R}). From (B.1), we have:

$$B_i^{*E}(\boldsymbol{\mu}') = B_i^{*E}(\boldsymbol{\mu}) + \frac{1}{k_i} \left[\ln \left(\frac{\mu_i}{\mu'_i} \right) - \ln \left(\prod_{j \in \Psi} \left(\frac{\mu'_j}{\mu_j} \right)^{\frac{1}{S k_j}} \right) \right] + \frac{1}{S k_i} (B'^T - B^T), \quad \forall i \in \Psi. \quad (\text{B.5})$$

Then, by definition of $\boldsymbol{\Delta}_b^*$, we have:

$$B_i^{*R} = B_i^{*E}(\boldsymbol{\mu}') + \Delta_{bi}^* = B_i^{*E}(\boldsymbol{\mu}) + \frac{1}{k_i} \left[\ln \left(\frac{\mu_i}{\mu'_i} \right) - \ln \left(\prod_{j \in \Psi} \left(\frac{\mu'_j}{\mu_j} \right)^{\frac{1}{S k_j}} \right) \right] + \frac{1}{S k_i} (B'^T - B^T) + \Delta_{bi}^*, \quad \forall i \in \Psi. \quad (\text{B.6})$$

Then, for a given $\mathbf{p} \in \Omega^b$:

$$\begin{aligned} \text{Regret}(\boldsymbol{\mu}', B'^T) &= \sum_{i \in \Psi} \mu'_i (h_i(\mathbf{p})) e^{-k_i B_i^{*R}} - \sum_{i \in \Psi} \mu'_i (h_i(\mathbf{p})) e^{-k_i B_i^*(\mathbf{p})} \\ &= \sum_{i \in \Psi} \mu'_i (h_i(\mathbf{p})) e^{-k_i B_i^{*E}(\boldsymbol{\mu}') e^{-k_i \Delta_{bi}^*}} - \sum_{i \in \Psi} \mu'_i (h_i(\mathbf{p})) e^{-k_i B_i^*(\mathbf{p})} \\ &= \left(\sum_{i \in \Psi} \mu_i (h_i(\mathbf{p})) e^{-k_i B_i^{*E}(\boldsymbol{\mu}) e^{-k_i \Delta_{bi}^*}} - \sum_{i \in \Psi} \mu_i (h_i(\mathbf{p})) e^{-k_i B_i^*(\mathbf{p})} \right) e^{\left(\frac{B^T - B'^T}{S} \right)} \prod_{i \in \Psi} \left(\frac{\mu'_i}{\mu_i} \right)^{\frac{1}{k_i S}} \\ &= \text{Regret}(\boldsymbol{\mu}, B^T) e^{\left(\frac{B^T - B'^T}{S} \right)} \prod_{i \in \Psi} \left(\frac{\mu'_i}{\mu_i} \right)^{\frac{1}{k_i S}}, \end{aligned}$$

which proves Theorem 9.

To complete the proof, it suffices to show that the constructed solution satisfies the first-order KKT conditions in (3.13)-(3.16). Note that all *Regret* functions are scaled by the same factor when the parameters change from $(\boldsymbol{\mu}, B^T)$ to $(\boldsymbol{\mu}', B'^T)$. This implies that as $(\boldsymbol{\mu}, B^T)$ varies, the binding *Regret* functions will remain the same. Therefore, under the assumption that \mathbf{A} does not change as B^T and $\boldsymbol{\mu}$ change, $\alpha_z, z \in \mathcal{Z}$, remains constant, implying that Lemma 3 holds. This also implies that the complementary slackness conditions in (3.14) are satisfied. Finally note that by changing $\boldsymbol{\mu}$ and B^T and keeping \mathbf{A} the same, we have found a solution $B_i^{*R} = B_i^{*E}(\boldsymbol{\mu}') + \Delta_{bi}^*$, with $\Delta_{bi}^* = B_i^R - B_i^E(\boldsymbol{\mu})$, that satisfies (3.13) in the first-order KKT conditions, and hence, this solution must be optimal for **RMM** under $(\boldsymbol{\mu}', B'^T)$. This completes the proof. ■

Proof of Theorem 4: We first derive the price of robustness ratio, Π^R :

$$\begin{aligned}
\Pi^R &= \frac{E[R(\mathbf{B}^{*R}, \boldsymbol{\mu})]}{E[R(\mathbf{B}^{*E}(\boldsymbol{\mu}), \boldsymbol{\mu})]} \\
&= \frac{\sum_{i \in \Psi} \mu_i e^{-k_i B_i^{*R}}}{\sum_{i \in \Psi} \mu_i e^{-k_i B_i^{*E}}} = \frac{\sum_{i \in \Psi} \mu_i e^{-k_i B_i^{*E}} e^{-k_i \Delta_{bi}^*}}{\sum_{i \in \Psi} \mu_i e^{-k_i B_i^{*E}}} \quad (\text{by Theorem 3}) \\
&= \frac{\sum_{i \in \Psi} \frac{1}{k_i} k_i \mu_i e^{-k_i B_i^{*E}} e^{-k_i \Delta_{bi}^*}}{\sum_{i \in \Psi} \frac{1}{k_i} k_i \mu_i e^{-k_i B_i^{*E}}} = \frac{k_1 \mu_1 e^{-k_1 B_1^{*E}} \sum_{i \in \Psi} \frac{1}{k_i} e^{-k_i \Delta_{bi}^*}}{k_1 \mu_1 e^{-k_1 B_1^{*E}} \sum_{i \in \Psi} \frac{1}{k_i}} \quad (\text{by Theorem 1}) \\
&= \frac{\sum_{i \in \Psi} \frac{1}{k_i} e^{-k_i \Delta_{bi}^*}}{S}. \tag{B.7}
\end{aligned}$$

Since Δ_b^* is a solution to (3.18), we can write (using (B.1)):

$$\Delta_{bi}^* = \frac{1}{k_i} \left(\ln(A_i) - \ln \left(\prod_{j \in \Psi} A_j^{c_j} \right) \right), \quad i \in \Psi, \tag{B.8}$$

and substituting (B.8) into (B.7), we obtain:

$$\Pi^R = \frac{\sum_{i \in \Psi} c_i / A_i}{\prod_{i \in \Psi} (1/A_i)^{c_i}}.$$

Next, we derive the price of expectation-based optimization ratio, $\Pi^E(\hat{\boldsymbol{\mu}})$:

$$\begin{aligned}\Pi^E(\hat{\boldsymbol{\mu}}) &= \frac{E[R(\mathbf{B}^{*E}(\hat{\boldsymbol{\mu}}), \boldsymbol{\mu})]}{E[R(\mathbf{B}^{*E}(\boldsymbol{\mu}), \boldsymbol{\mu})]} = \frac{\sum_{i \in \Psi} \mu_i e^{-k_i B_i^{*E}(\hat{\boldsymbol{\mu}})}}{\sum_{i \in \Psi} \mu_i e^{-k_i B_i^{*E}(\boldsymbol{\mu})}} \\ &= \frac{\sum_{i \in \Psi} \mu_i \frac{\prod_{j \in \Psi} (k_j \hat{\mu}_j)^{c_j}}{k_i \hat{\mu}_i}}{\sum_{i \in \Psi} \mu_i \frac{\prod_{j \in \Psi} (k_j \mu_j)^{c_j}}{k_i \mu_i}} = \frac{\sum_{i \in \Psi} \frac{(\mu_i / \hat{\mu}_i)}{k_i}}{\prod_{i \in \Psi} (\mu_i / \hat{\mu}_i)^{c_i} \sum_{i \in \Psi} \frac{1}{k_i}} = \frac{\sum_{i \in \Psi} c_i (\mu_i / \hat{\mu}_i)}{\prod_{i \in \Psi} (\mu_i / \hat{\mu}_i)^{c_i}} \quad (\text{by (B.1)}).\end{aligned}$$

Finally, we derive the lower bound, \mathcal{R}^L , on the **ERM** *Regret* deviation, \mathcal{R} :

$$\begin{aligned}\mathcal{R} &= \max_{\mathbf{p} \in \Omega} \frac{\text{Regret}(\mathbf{B}^{*E}(\boldsymbol{\mu}), \mathbf{p})}{\text{Regret}(\mathbf{B}^{*R}, \mathbf{p})} \\ &= \max_{\mathbf{p} \in \Omega} \frac{\sum_{i \in \Psi} p_i e^{-k_i B_i^{*E}} - \sum_{i \in \Psi} p_i e^{-k_i B_i^*(\mathbf{p})}}{\sum_{i \in \Psi} p_i e^{-k_i B_i^{*E}} e^{-k_i \Delta_{bi}^*} - \sum_{i \in \Psi} p_i e^{-k_i B_i^*(\mathbf{p})}} \quad (\text{by Theorem 3}) \\ &= \max_{\mathbf{p} \in \Omega} \frac{e^{-\frac{B^T}{S}} \sum_{i \in \Psi} \frac{p_i}{k_i \mu_i} \times \prod_{i \in \Psi} (k_i \mu_i)^{\frac{1}{k_i S}} - e^{-\frac{B^T}{S}} S \times \prod_{i \in \Psi} (k_i p_i)^{\frac{1}{k_i S}}}{e^{-\frac{B^T}{S}} \sum_{i \in \Psi} \frac{p_i}{k_i \mu_i} e^{-k_i \Delta_{bi}^*} \times \prod_{i \in \Psi} (k_i \mu_i)^{\frac{1}{k_i S}} - e^{-\frac{B^T}{S}} S \times \prod_{i \in \Psi} (k_i p_i)^{\frac{1}{k_i S}}} \quad (\text{by Eq. (B.2)}) \\ &\geq \max_{\mathbf{p} \in \Omega^b} \frac{\sum_{i \in \Psi} \frac{p_i}{k_i \mu_i} \times \prod_{i \in \Psi} (k_i \mu_i)^{\frac{1}{k_i S}} - S \times \prod_{i \in \Psi} (k_i p_i)^{\frac{1}{k_i S}}}{\sum_{i \in \Psi} \frac{p_i}{k_i \mu_i} e^{-k_i \Delta_{bi}^*} \times \prod_{i \in \Psi} (k_i \mu_i)^{\frac{1}{k_i S}} - S \times \prod_{i \in \Psi} (k_i p_i)^{\frac{1}{k_i S}}} \quad (\text{since } \Omega^b \subseteq \Omega) \\ &= \max_{\mathbf{p} \in \Omega^b} \frac{\sum_{i \in \Psi} \frac{p_i / \mu_i}{k_i} - S \prod_{i \in \Psi} (p_i / \mu_i)^{\frac{1}{k_i S}}}{\sum_{i \in \Psi} \frac{p_i / \mu_i}{k_i} e^{-k_i \Delta_{bi}^*} - S \prod_{i \in \Psi} (p_i / \mu_i)^{\frac{1}{k_i S}}} \\ &= \max_{\mathbf{p} \in \Omega^b} \frac{\sum_{i \in \Psi} \frac{h_i(\mathbf{p})}{k_i} - S \prod_{i \in \Psi} (h_i(\mathbf{p}))^{\frac{1}{k_i S}}}{\sum_{i \in \Psi} \frac{h_i(\mathbf{p})}{k_i} e^{-k_i \Delta_{bi}^*} - S \prod_{i \in \Psi} (h_i(\mathbf{p}))^{\frac{1}{k_i S}}} \quad (\text{since } p_i / \mu_i = h_i(\mathbf{p}), \quad \forall \mathbf{p} \in \Omega^b). \blacksquare\end{aligned}$$

Proof of Lemma 4: We have $\ln \Pi^E(\hat{\boldsymbol{\mu}}) = \ln(\sum_{i \in \Psi} c_i q_i) - \sum_{i \in \Psi} c_i \ln q_i$, where $q_i \equiv \mu_i / \hat{\mu}_i$. Using the change of variable $q_i = e^{y_i}$, we get $\ln \Pi^E(\hat{\boldsymbol{\mu}}) = \ln(\sum_{i \in \Psi} c_i e^{y_i}) - \sum_{i \in \Psi} c_i y_i$. Hence $\ln \Pi^E(\hat{\boldsymbol{\mu}})$ is the sum of the weighted log-sum-exp function [29] and a linear function, and hence is jointly convex in $y_i = \ln(\mu_i / \hat{\mu}_i)$, $i \in \Psi$. Since the $\ln(\cdot)$ function is strictly increasing, $\Pi^E(\hat{\boldsymbol{\mu}})$ is maximized on the boundary, i.e., when $\hat{\mu}_i = \mu_i(1 + r_i)$ or $\hat{\mu}_i = \mu_i(1 - r_i)$, which completes the proof. \blacksquare

Proof of Corollary 2: From (B.1), *Regret* incurred by the optimal **ERM** solution, $\mathbf{B}^{*E}(\boldsymbol{\mu})$, at prevalence vector $\mathbf{p} \in \Omega^b$ can be written as:

$$\text{Regret}(\mathbf{B}^{*E}(\boldsymbol{\mu}), \mathbf{p}) = \sum_{i \in \Psi} \mu_i (h_i(\mathbf{p})) e^{-B^T/n} \frac{\sqrt[n]{\mu_1 \dots \mu_n}}{\mu_i} - n e^{-B^T/n} \sqrt[n]{\mu_1 (h_1(\mathbf{p})) \dots \mu_n (h_n(\mathbf{p}))}. \quad (\text{B.9})$$

Denote by x the number of infections whose prevalence realizations are at their upper bounds (i.e.,

$p_i = u_i$). Then, (B.9) can be rewritten as follows:

$$Regret(\mathbf{B}^{*E}(\boldsymbol{\mu}), \mathbf{p}) = Regret(x) = e^{-B^T/n} \sqrt[n]{\mu_1 \dots \mu_n} \left(n + a(2x - n) - \left(\frac{1+a}{1-a} \right)^{x/n} (1-a) \right). \quad (\text{B.10})$$

Clearly, (B.10) is strictly concave in x with a maximizer:

$$x_{max} = \frac{n}{\ln\left(\frac{1+a}{1-a}\right)} \ln\left(\frac{2an}{(1-a)\ln\left(\frac{1+a}{1-a}\right)}\right). \quad (\text{B.11})$$

Note also the following:

1. Prevalence vectors with the same value of x exhibit the same value of $Regret$, and
2. The value of x that maximizes $Regret$ is independent of the mean prevalence vector $\boldsymbol{\mu}$.

Hence, $Regret(x)$ is maximized at either $\lfloor x_{max} \rfloor$ or $\lceil x_{max} \rceil$. Denote by $\mathcal{X} \subset \mathcal{Z}$ the index set of prevalence vectors (scenarios) that maximize $Regret$ (i.e., that have $x = \lfloor x_{max} \rfloor$ or $x = \lceil x_{max} \rceil$). For $\mathbf{B}^{*E}(\boldsymbol{\mu})$ to be the optimal solution for **RMM**, there must exist a set of KKT multipliers α_z , $z \in \mathcal{Z}$, and γ_i , $i \in \Psi$, that, along with $\mathbf{B}^{*E}(\boldsymbol{\mu})$, satisfy the first-order KKT conditions in Lemma 2. Since $Regret$ is maximized for all scenarios in \mathcal{X} , setting $\alpha_z = 0$, $\forall z \notin \mathcal{X}$, satisfies the the first-order KKT condition in (3.14). Also, under Condition **(C1)**, KKT condition in (3.15) will hold by setting $\gamma_i = 0$, $\forall i \in \Psi$. Note that by (3.11), we have $\hat{\mu}_1 f'_1(B_1^{*E}) = \dots = \hat{\mu}_n f'_n(B_n^{*E})$. Therefore, from the first-order KKT condition in (3.13), we need:

$$a \left(\sum_{z \in U_i \cap \mathcal{X}} \alpha_z - \sum_{z \in (\mathcal{Z} \setminus U_i) \cap \mathcal{X}} \alpha_z \right) = a \left(\sum_{z \in U_j \cap \mathcal{X}} \alpha_z - \sum_{z \in (\mathcal{Z} \setminus U_j) \cap \mathcal{X}} \alpha_z \right), \quad \forall i, j \in \Psi. \quad (\text{B.12})$$

Note that by symmetry, for all scenarios in \mathcal{X} , each infection is at its upper bound in an equal number of scenarios. Hence $|U_i \cap \mathcal{X}| = |U_j \cap \mathcal{X}|$, $\forall i, j \in \Psi$. Similarly, $|(\mathcal{Z} \setminus U_i) \cap \mathcal{X}| = |(\mathcal{Z} \setminus U_j) \cap \mathcal{X}|$, $\forall i, j \in \Psi$. Therefore, $\alpha_{z_1} = \alpha_{z_2}$, $\forall z_1, z_2 \in \mathcal{X}$ is a solution to (B.12), which implies that $\mathbf{B}^{*E}(\boldsymbol{\mu})$ satisfies the first-order KKT conditions in Lemma 2 and must be optimal for **RMM**. ■

Proof of Theorem 5: We can write:

$$Regret(\mathbf{B}^{*R}, \boldsymbol{\mu}) \leq \max_{\mathbf{p} \in \Omega^b} \left\{ Regret(\mathbf{B}^{*R}, \mathbf{p}) \right\} \leq \max_{\mathbf{p} \in \Omega^b} \left\{ Regret(\mathbf{B}, \mathbf{p}) \right\}, \quad \forall \mathbf{B} \in \mathcal{F},$$

where the upper bound follows by the optimality of \mathbf{B}^{*R} for **RMM**, and the lower bound follows

by Theorem 2, as $\boldsymbol{\mu} \in \Omega \setminus \Omega^b$. Hence, we can write:

$$R(\mathbf{B}^{*R}, \boldsymbol{\mu}) - R(\mathbf{B}^{*E}(\boldsymbol{\mu}), \boldsymbol{\mu}) \leq \max_{\mathbf{p} \in \Omega^b} \left\{ R(\mathbf{B}, \mathbf{p}) - R(\mathbf{B}^*(\mathbf{p}), \mathbf{p}) \right\}, \quad \forall \mathbf{B} \in \mathcal{F}. \quad (\text{B.13})$$

By dividing both sides of (B.13) by $R(\mathbf{B}^{*E}(\boldsymbol{\mu}), \boldsymbol{\mu})$ and rearranging the terms, the proof follows. ■

Proof of Theorem 8:

Part (a): For $j = 1, \dots, i-1$, the expression for TH^j does not depend on the parameters of infection i . Then, if $\hat{\mu}_i$ changes in such a way that the ranking of infections (according to (3.9)) is preserved, then TH^j , $j = 1, \dots, i-1$, does not change. On the other hand, we have that $TH^i = \sum_{j=1}^{i-1} \tilde{B}_j^i$, where \tilde{B}_j^i is the solution to:

$$\hat{\mu}_j f'_j(\tilde{B}_j^i) = \hat{\mu}_i f'_i(0). \quad (\text{B.14})$$

(Note that Eq. (B.14) has a unique solution since $f'_j(\cdot)$ is strictly increasing.) Notice that when $\hat{\mu}_i$ increases, the RHS of (B.14) decreases since $f'_i(0) < 0$. Now assume that \tilde{B}_j^i increases, which implies that $f'_j(\tilde{B}_j^i)$ increases. Since $f'_j(\tilde{B}_j^i) < 0$, the LHS of (B.14) increases, which is a contradiction. Hence we conclude that \tilde{B}_j^i decreases as $\hat{\mu}_i$ increases. This implies that $TH^i = \sum_{j=1}^{i-1} \tilde{B}_j^i$ decreases as $\hat{\mu}_i$ increases. For $j \notin I^{*E}$, we can write:

$$TH^j = \sum_{k=1}^{i-1} \tilde{B}_k^j + \tilde{B}_i^j + \sum_{k=i+1}^{j-1} \tilde{B}_k^j, \quad (\text{B.15})$$

where \tilde{B}_i^j is the solution to:

$$\hat{\mu}_i f'_i(\tilde{B}_i^j) = \hat{\mu}_j f'_j(0). \quad (\text{B.16})$$

Notice that the RHS of (B.16) does not depend on $\hat{\mu}_i$. Therefore, as $\hat{\mu}_i$ increases, \tilde{B}_i^j must vary in a way that the LHS of (B.16) remains constant. Since If \tilde{B}_i^j decreases, then $f'_i(\tilde{B}_i^j)$ decreases, which implies that the LHS of (B.16) decreases since $f'_i(\tilde{B}_i^j) < 0$, which is a contradiction. Therefore, we conclude that \tilde{B}_i^j must increase as $\hat{\mu}_i$ increases and hence, from (B.15), TH^j increases as $\hat{\mu}_i$ increases.

Part (b): For ease of notation, we write $\mathbf{B}^{*E}(\hat{\boldsymbol{\mu}})$ and $I^{*E}(\hat{\boldsymbol{\mu}})$ as \mathbf{B}^{*E} and I^{*E} , respectively. If $i \notin I^{*E}$, then $B_i^{*E} = 0$ and the result trivially holds. Next consider the case where $i \in I^{*E}$. As proven in part (a), if $\hat{\mu}_i$ increases, then TH^i decreases, which implies that i remains in set I^{*E} as

$\hat{\mu}_i$ increases. From the first-order KKT conditions in (3.7), we can write $\lambda = \hat{\mu}_i(-f'_i(B_i^{*E}))$. To simplify the notation, we let $L_i \equiv \hat{\mu}_i f'_i(B_i^{*E})$, $\forall i \in I^{*E}$. Thus, we can write $\lambda = L_i(-f'_i(B_i^{*E}))$, $\forall i \in I^{*E}$. We first prove, by contradiction, that B_i^{*E} increases in $\hat{\mu}_i$. Assume, to the contrary, that B_i^{*E} decreases as $\hat{\mu}_i$ increases. This implies that L_i and $-f'_i(B_i^{*E})$ both increase, which in turn imply that λ increases. Assume that B_j^{*E} , $j \in I^{*E} \setminus \{i\}$, increases. Hence L_j and $-f'_j(B_j^{*E})$ both decrease, which imply that λ decreases, which is a contradiction. Hence B_j^{*E} decreases, and since $B^T = \sum_{k \in I^{*E}} B_k^{*E}$ is a constant, B_j^{*E} cannot decrease. We therefore conclude that B_i^{*E} must increase. Next, we will prove that as $\hat{\mu}_i$ increases, λ increases. Assume, to the contrary, that λ decreases. If B_j^{*E} , $j \in I^{*E} \setminus \{i\}$, decreases, then L_j and $-f'_j(B_j^{*E})$ both decrease, which imply that λ increases. This contradicts with the assumption that λ is decreasing. Hence, B_j^{*E} must increase. Since $B^T = \sum_{k \in I^{*E}} B_k^{*E}$ is a constant, this is a contradiction and λ must increase with $\hat{\mu}_i$. Finally, using a similar argument, we can show that if λ increases, then B_j^{*E} , $\forall j \in I^{*E} \setminus \{i\}$, decreases. This completes the proof. ■

Part (c): By definition, $Regret(\mathbf{B}, \mathbf{p}) = \sum_{i \in \Psi} p_i f_i(B_i) - \sum_{i \in \Psi} p_i f_i(B_i^*(\mathbf{p}))$, for $\mathbf{p} \in \Omega^b$. Assume that for some $i \in \Psi$, p_i increases to $p'_i = p_i + \epsilon$, for some $\epsilon > 0$, while p_j , $j \neq i$, remain the same. Let \mathbf{p}' represent the new prevalence vector. Assume that $Regret$ at \mathbf{p} is binding, i.e., $Regret_{max}^* = Regret(\mathbf{B}^{*R}, \mathbf{p})$. Also assume that $Regret(\mathbf{B}^{*R}, \mathbf{p})$ increases as \mathbf{p} changes to \mathbf{p}' , i.e., $Regret(\mathbf{B}^{*R}, \mathbf{p}) < Regret(\mathbf{B}^{*R}, \mathbf{p}')$ (the case where $Regret(\mathbf{B}^{*R}, \mathbf{p}) \geq Regret(\mathbf{B}^{*R}, \mathbf{p}')$ is not of interest since it implies that \mathbf{p}' is not binding). Hence, we can write:

$$Regret(\mathbf{B}^{*R}, \mathbf{p}') - Regret(\mathbf{B}^{*R}, \mathbf{p}) = f_i(B_i^{*R})(p'_i - p_i) - \sum_{j \in \Psi \setminus \{i\}} p_j [f_j(B_j^*(\mathbf{p}')) - f_j(B_j^*(\mathbf{p}))] > 0. \quad (\text{B.17})$$

Note that the summation term in (B.17) does not depend on \mathbf{B}^{*R} . Also, since \mathbf{B}^{*R} is no longer optimal for the new problem with \mathbf{p}' , it needs to change in a way to decrease the LHS in (B.17). Noting that $p'_i - p_i > 0$ and $f_i(\cdot)$ is strictly decreasing, \mathbf{B}'^{*R} , the optimal solution for the problem with \mathbf{p}' satisfies $B_i'^{*R} \geq B_i^{*R}$. This completes the proof. ■

Part (d): For ease of notation, we write $\mathbf{B}^{*E}(\hat{\mu})$ and $I^{*E}(\hat{\mu})$ as \mathbf{B}^{*E} and I^{*E} , respectively. First assume that B^T increases in such a way that set I^{*E} does not change, that is, the increase in B^T does not change the threshold interval it belongs to (see Theorem 1). Since for $i \in I^{*E}$, $\gamma_i = 0$,

from (3.7) with $w = 0$, we can write:

$$B_i^{*E} = f_i'^{-1} \left(-\frac{\lambda}{\widehat{\mu}_i} \right), \quad i \in I^{*E}. \quad (\text{B.18})$$

Since $\sum_{i \in I^{*E}} B_i^{*E} = B^T$ in an optimal solution, we have:

$$\sum_{i \in I^{*E}} f_i'^{-1} \left(-\frac{\lambda}{\widehat{\mu}_i} \right) = B^T. \quad (\text{B.19})$$

Note that since $f_i(\cdot)$ is strictly decreasing and convex, $f_i'(\cdot)$ is strictly increasing, which also implies that $f_i'^{-1}(\cdot)$ is strictly increasing. In what follows, we will first prove that λ is decreasing in B^T . Assume, to the contrary, that λ increases as B^T increases. Then $\left(-\frac{\lambda}{\widehat{\mu}_i}\right)$ decreases, which in turn implies that $f_i'^{-1}\left(-\frac{\lambda}{\widehat{\mu}_i}\right)$ decreases, $\forall i \in I^{*E}$. Hence, the LHS of (B.19) decreases, which is a contradiction. Therefore λ must decrease in B^T . Then, from (B.18), it follows that B_i^{*E} increases, $\forall i \in I^{*E}$, when B^T increases in such a way that set I^{*E} does not change.

Next assume that B^T increases in such a way that a new infection, say infection k , enters set I^{*E} . Hence, it is sufficient to show that B_i^{*E} is continuous in B^T at the threshold points, $TH^j, j = 2, 3, \dots, n$, that is, at points where set I^{*E} is incremented by one new infection. Consider, without loss of generality, that $B^T = TH^k$ and define $TH^{k-} \equiv \lim_{\epsilon \rightarrow 0} (TH^k - \epsilon)$. To simplify the notation, let $B_i^{*E}(TH^{k-}) = B_i^{*-}$ and $B_i^{*E}(TH^k) = B_i^*$, and similarly, let $\lambda(TH^{k-}) = \lambda^-$ and $\lambda(TH^k) = \lambda$, that is, from (B.18), we have that $f_i'^{-1}\left(-\frac{\lambda^-}{\widehat{\mu}_i}\right) = B_i^{*-}$ and $f_i'^{-1}\left(-\frac{\lambda}{\widehat{\mu}_i}\right) = B_i^*$, where $f_i'^{-1}\left(-\frac{\lambda}{\widehat{\mu}_i}\right)$ is continuous and strictly decreasing in λ . Define function $g_{k-1}(\lambda) \equiv \sum_{j=1}^{k-1} f_j'^{-1}\left(-\frac{\lambda}{\widehat{\mu}_j}\right)$. Clearly $g(\cdot)$ is continuous and strictly decreasing in λ . By definition of a threshold, we have that $B_k^*(TH^k) = B_k^*(TH^{k-}) = 0$. Hence, we can write:

$$g_{k-1}(\lambda^-) = \sum_{j=1}^{k-1} f_j'^{-1} \left(-\frac{\lambda^-}{\widehat{\mu}_j} \right) = TH^{k-} \quad (\text{B.20})$$

$$g_{k-1}(\lambda) = \sum_{j=1}^{k-1} f_j'^{-1} \left(-\frac{\lambda}{\widehat{\mu}_j} \right) = TH^k. \quad (\text{B.21})$$

Hence, from the monotonicity and continuity of $g(\cdot)$, we have that $\lambda^- = \lambda$. Hence, we deduce that $B_i^{*-} = B_i^*$, and consequently B_i^* is continuous in B^T . Therefore, we conclude that B_i^{*E} is strictly increasing in $B^T, \forall i \in I^{*E}$, and is non-decreasing in $B^T, \forall i \in \Psi \setminus I^{*E}$.

Part (e): This result trivially follows from Theorems 3 and 8 part (d), which imply that for any $i \in \Psi$, $B_i^{*R} = B_i^{*E}(\boldsymbol{\mu}) + \Delta_{bi}^*$, where Δ_{bi}^* is independent of B^T , and $B_i^{*E}(\boldsymbol{\mu})$ is increasing in B^T . ■

B.5 Prevalence Data and Fitting of Test Effectiveness Functions

B.5.1 Prevalence Data

All prevalence estimates are specifically for the United States. [106] and [38] respectively estimate HIV and HBV prevalence based on data for the United States in 2012, provided by the Center for Disease Control and Prevention. Sample size information has not been provided. [10] estimates HCV prevalence as 1.6% (95% CI, 1.3% to 1.9%), based on a sample size of 17,548 from 1999 to 2002. [84] estimates the babesiosis prevalence using data from an ongoing investigational study by the American Red Cross in four endemic states (CT, WI, MN, MA) using a sample size of 83,330 from 2012 to 2015. Finally, [33] and [100] estimate the WNV prevalence based on a sample size of 5,370,499 from 2002 to 2004.

B.5.2 Fitting Test Effectiveness Functions

Let Ω^i denote the set of all FDA-licensed tests for infection i , $i \in \Psi$. For each test-set $S_t \subseteq \Omega^i$, let $C(S_t)$ denote the unit cost of administering all tests in set S_t . Let $T^i - (S_t)$ denote the event that the blood unit is classified as free of infection i when test-set S_t is administered. Decision variables for infection i 's problem include $Prop_t^i$, $t = 1, \dots, 2^{|\Omega^i|}$, the proportion of blood units screened by test-set S_t , $\forall S_t \subseteq \Omega^i$, $i \in \Psi$.

For each infection i , $i \in \Psi$, we vary B_i , its possible budget allocation, within the range $[0 - 19]$ (\$19 corresponds to the cost of the most sensitive paired test), in step sizes of 0.5, and solve the following LP to determine $f_i(B_i)$, $i \in \Psi$:

$$f_i(B_i) = \underset{(Prop_t^i)_{t=1, \dots, 2^{|\Omega^i|}}}{\text{minimize}} \sum_{S_t \subseteq \Omega^i} Pr(T^i - (B_i) | A_i +) Prop_t^i$$

subject to

$$\sum_{S_t \subseteq \Omega^i} Prop_t^i C(S_t) \leq B_i \tag{B.22}$$

$$\sum_{S_t \subseteq \Omega^i} Prop_t^i = 1 \tag{B.23}$$

$$Prop_t^i \geq 0, \quad t = 1, \dots, 2^{|\Omega^i|}. \tag{B.24}$$

Thus, function $f_i(B_i)$, $\forall B_i \geq 0$, $i \in \Psi$, is derived considering non-universal testing schemes (i.e., fractional values of $Prop_t^i$ variables are allowed). Observe that an optimal non-universal testing scheme uses all the allocated budget, B_i , for all $B_i \geq 0$, $i \in \Psi$. From LP theory, as B_i , the RHS of Constraint (B.22), increases, the objective function value, $f_i(B_i)$, decreases in a piece-wise convex manner (e.g., [15], p. 273-275).

For each infection $i \in \Psi$, given the values of the function $f_i(B_i)$, $\forall B_i \in [0 - 19]$, $i \in \Psi$, we fit an exponential function of the form $f_i(B_i) = e^{-k_i B_i}$, where parameter k_i is the value that provides the best fit, i.e., the minimum coefficient of determination (R_i^2).¹ Table B.3 reports the values of k_i and R_i^2 for each infection i considered in Section 3.5. As an example, Figure B.3 depicts the curve fitted for HBV.

¹ $R^2 = 1 - \frac{\sum_k (Y_k - F_k)^2}{\sum_k (Y_k - \bar{Y})^2}$, where Y_k are the actual test data points, F_k are the fitted curve data points, and \bar{Y} is the mean of Y_k ; see [35], p. 556.

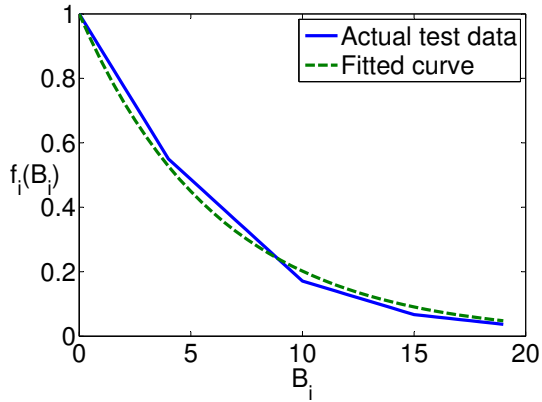


Figure B.3: Fitted exponential test effectiveness function ($k_i = 0.16$) vs. the actual test data for HBV.

Table B.3: Fitted parameters, k_i , and coefficients of determination (R_i^2), for $f_i(B_i) = e^{-k_i B_i}$ for HIV, HBV, HCV, babesiosis, and WNV.

<i>Infection (i)</i>	k_i	R_i^2
HIV	0.28	99%
HBV	0.16	99%
HCV	0.14	95%
Babesiosis	0.38	97%
WNV	0.185	94%

Appendix C

Appendix for Chapter 4

Proof of Lemma 10: First, we show that any vector \mathbf{S} that satisfies $\{\mathbf{a}^T \mathbf{S} \geq B \text{ and } \mathbf{S} \leq \mathbf{S}^{max}\}$ also satisfies the budget constraint, $\{C(\mathbf{S}) \leq B\}$. We first write \mathbf{S} as a convex combination of \mathbf{V}_i , $i \in \Psi$, and \mathbf{S}^{max} as follows: $\mathbf{S} = \sum_{i=1}^n \alpha_i \mathbf{V}_i + \alpha_{n+1} \mathbf{S}^{max}$, with $\sum_{i=1}^{n+1} \alpha_i = 1$. By convexity of $C(\cdot)$, and by noting that $C(\mathbf{V}_i) = B$, $i \in \Psi$, we get:

$$C(\mathbf{S}) = C\left(\sum_{i=1}^n \alpha_i \mathbf{V}_i + \alpha_{n+1} \mathbf{S}^{max}\right) \leq \sum_{i=1}^n \alpha_i C(\mathbf{V}_i) + \alpha_{n+1} C(\mathbf{S}^{max}) \leq \sum_{i=1}^{n+1} \alpha_i B = B.$$

In order to prove the validity of (Cut), given by $\mathbf{a}^T \mathbf{S} \leq B + \sqrt{n} \|a\|_2$, it is sufficient to show that for every integer vector \mathbf{S} that lies on the boundary of (Cut), i.e., $\mathbf{a}^T \mathbf{S} = B + \sqrt{n} \|a\|_2$, there exists an integer vector \mathbf{S}' that satisfies $\{\mathbf{a}^T \mathbf{S}' \geq B\}$, with $\mathbf{S}' = \mathbf{S} - \mathbf{e}_i$ for some $i \in \Psi$, where \mathbf{e}_i denotes the i^{th} unit vector in \mathbb{R}^n . In other words, \mathbf{S}' “dominates” \mathbf{S} since: (1) \mathbf{S}' is feasible (it satisfies $\mathbf{a}^T \mathbf{S}' \geq B$, hence $C(\mathbf{S}') \leq B$), and (2) \mathbf{S}' incurs less *Residual Risk*, since $S_j = S'_j$, $j \neq i$, and $S'_i < S_i$, for some $i \in \Psi$. We prove this by contradiction. Assume that $\mathbf{a}^T \mathbf{S}' < B$, $\forall i \in \Psi$. Hence:

$$\begin{aligned} \mathbf{a}^T (\mathbf{S} - \mathbf{e}_i) < B, \forall i \in \Psi & \Leftrightarrow \mathbf{a}^T \mathbf{S} - \mathbf{a}^T \mathbf{e}_i < B, \forall i \in \Psi \\ \Leftrightarrow B + \sqrt{n} \|a\|_2 - \mathbf{a}^T \mathbf{e}_i < B, \forall i \in \Psi & \Leftrightarrow \sqrt{n} \|a\|_2 < \mathbf{a}^T \mathbf{e}_i, \forall i \in \Psi \\ \Leftrightarrow n < \frac{a_i^2}{\|a\|_2^2} \forall i \in \Psi & \Leftrightarrow \sum_{i=1}^n n < \sum_{i=1}^n \frac{a_i^2}{\|a\|_2^2} \Leftrightarrow n^2 < 1, \end{aligned}$$

which is a contradiction. Hence (Cut) is valid. ■